



Nordisk kernesikkerhedsforskning  
Norrænar kjarnöryggisrannsóknir  
Pohjoismainen ydinturvallisuustutkimus  
Nordisk kjernesikkerhetsforskning  
Nordisk kärnsäkerhetsforskning  
Nordic nuclear safety research

NKS-225  
ISBN 978-87-7893-295-2

---

# Modeling of Condensation, Stratification, and Mixing Phenomena in a Pool of Water

H. Li  
P. Kudinov  
W. Villanueva

Division of Nuclear Power Safety, Royal Institute of Technology, KTH, Sweden

December 2010

---

## Abstract

This work pertains to the research program on Containment Thermal-Hydraulics at KTH. The objective is to evaluate and improve performance of methods, which are used to analyze thermal-hydraulics of steam suppression pools in a BWR plant under different abnormal transient and accident conditions. As a passive safety system, the function of steam pressure suppression pools is paramount to the containment performance. In the present work, the focus is on apparently-benign but intricate and potentially risk-significant scenarios in which thermal stratification could significantly impede the pool's pressure suppression capacity. For the case of small flow rates of steam influx, the steam condenses rapidly in the pool and the hot condensate rises in a narrow plume above the steam injection plane and spreads into a thin layer at the pool's free surface. When the steam flow rate increases significantly, momentum introduced by the steam injection and/or periodic expansion and shrink of large steam bubbles due to direct contact condensation can cause breakdown of the stratified layers and lead to mixing of the pool water. Accurate prediction of the pool thermal-hydraulics in such scenarios presents a computational challenge. Lumped-parameter models have no capability to predict temperature distribution of water pool during thermal stratification development. While high-order-accurate CFD (RANS, LES) methods are not practical due to excessive computing power needed to calculate 3D high-Rayleigh-number natural circulation flow in long transients. In the present work, a middle-ground approach is used, namely CFD-like model of the general purpose thermal-hydraulic code GOTHIC. Each cell of 3D GOTHIC grid uses lumped parameter volume type closures for modeling of various heat and mass transfer processes at subgrid scale. We use GOTHIC to simulate POOLEX/PPOOLEX experiment, in order to (a) quantify errors due to GOTHIC's physical models and numerical schemes, and (b) propose necessary improvements in GOTHIC sub-grid scale modeling. The study performed on thermal stratification in a water pool indicates that GOTHIC CFD-like model is fit for reactor applications in complex fluid-physics scenarios that avoids both over-simplification (as in single lumped-parameter model) and over-complication (as in CFD models). However, simulation of direct steam injection into a subcooled pool cannot be predicted reliably with the existing models. Thus we develop "effective heat source" and "effective momentum" approaches, and provide feasibility study for the prediction of thermal stratification and mixing in a BWR pressure suppression pool. The results are encouraging and further activity on the development and implementation of the proposed models in GOTHIC is currently underway.

## Key words

BWR pressure suppression pool, thermal stratification, mixing, effective models, GOTHIC

NKS-225

ISBN 978-87-7893-295-2

Electronic report, November 2010

NKS Secretariat

NKS-776

P.O. Box 49

DK - 4000 Roskilde, Denmark

Phone +45 4677 4045

Fax +45 4677 4046

[www.nks.org](http://www.nks.org)

e-mail [nks@nks.org](mailto:nks@nks.org)



**NKS-POOL**

## **Research report**

# **Modeling of Condensation, Stratification and Mixing Phenomena in a Pool of Water**

*Hua Li, Pavel Kudinov, Walter Villanueva*

Division of Nuclear Power Safety  
Department of Physics,  
School of Engineering Science  
Royal Institute of Technology (KTH)  
10691 Stockholm, Sweden

October 2010



# CONTENTS

|   |           |
|---|-----------|
| <b>EXECUTIVE SUMMARY .....</b>  | <b>5</b>  |
| <b>1. INTRODUCTION AND BACKGROUND.....</b>  | <b>7</b>  |
| 1.1. PROJECT GOALS .....  | 7         |
| 1.2. SUMMARY OF RESEARCH ON STRATIFICATION AND MIXING IN WATER POOLS AND FORMULATION OF APPROACH .....                        | 7         |
| <b>2. EFFECTIVE HEAT SOURCE APPROACH TO SIMULATION OF STRATIFICATION DEVELOPMENT.....</b>                                     | <b>16</b> |
| 2.1. LUMPED PARAMETER SIMULATION OF POOLEX TEST STB-20 .....  | 16        |
| 2.2. SIMULATION OF DIRECT STEAM INJECTION IN POOLEX TEST STB-20.....  | 21        |
| 2.3. EFFECTIVE HEAT SOURCE APPROACH TO SIMULATION OF STRATIFICATION DEVELOPMENT AT SMALL RATE OF STEAM INJECTION .....        | 23        |
| 2.4. VALIDATION OF EFFECTIVE HEAT SOURCE APPROACH FOR SIMULATION OF STRATIFICATION DEVELOPMENT .....                          | 25        |
| 2.4.1. Sensitivity to Boundary Conditions.....  | 25        |
| 2.4.2. Sensitivity to Grid Resolution Study .....   | 28        |
| 2.4.3. Sensitivity Study to Gas Space and Free Surface Modeling .....   | 33        |
| 2.5. APPLICATION OF EFFECTIVE HEAT SOURCE APPROACH TO PREDICTION OF STRATIFICATION DEVELOPMENT WITH CFD .....                 | 36        |
| 2.5.1. CFD Simulation of Heating Phase of the POOLEX STB-20 Experiment .....  | 36        |
| 2.5.2. CFD Simulation of Isothermal Layer Development during Cooling Phase .....  | 39        |
| 2.6. APPLICATION OF EFFECTIVE HEAT SOURCE APPROACH TO SIMULATION OF STRATIFICATION DEVELOPMENT IN A PROTOTYPIC SIZE POOL..... | 43        |
| 2.6.1. GOTHIC Model of a Prototypic Size Pool .....   | 43        |
| 2.6.2. Simulation of Direct Steam Injection into a Prototypic Size Subcooled Water Pool.....                                  | 44        |
| 2.6.3. Simulation of Stratification Development in a Prototypic Size Pool with Effective Heat Source Approach.....            | 45        |
| <b>3. EFFECTIVE MOMENTUM APPROACH TO PREDICTION OF MIXING IN A POOL</b>   | <b>47</b> |
| 3.1. DEVELOPMENT AND IMPLEMENTATION OF EFFECTIVE MOMENTUM APPROACH IN GOTHIC  | 47        |
| 3.2. FEASIBILITY STUDY OF EFFECTIVE MOMENTUM APPROACH IN GOTHIC BY COMPARISON WITH STB-21 TEST DATA FROM POOLEX.....          | 49        |
| <b>4. SIMULATION OF PPOOLEX TESTS WITH GOTHIC.....</b>  | <b>53</b> |
| 4.1. PRE-TEST SIMULATIONS WITH LUMPED PARAMETER MODEL .....   | 53        |
| 4.1.1. Simulation with pressure boundary.....   | 53        |
| 4.1.2. Analysis of Results .....  | 55        |
| 4.1.3. Simulation with flow boundary.....   | 58        |
| 4.1.4. Analysis of Results .....  | 59        |
| 4.2. POST-TEST LUMPED PARAMETER SIMULATION .....  | 61        |
| <b>5. SUMMARY AND OUTLOOK .....</b>   | <b>67</b> |
| <b>6. ACKNOWLEDGEMENT.....</b>  | <b>70</b> |
| <b>7. REFERENCES.....</b>   | <b>71</b> |
| <b>APPENDIX 1 .....</b>   | <b>75</b> |
| <b>APPENDIX 2 .....</b>   | <b>81</b> |
| <b>APPENDIX 3 .....</b>   | <b>84</b> |



## **Executive Summary**

This work pertains to the research program on Containment Thermal-Hydraulics at KTH. The objective is to evaluate and improve performance of methods, which are used to analyze thermal-hydraulics of steam suppression pools in a BWR plant under different abnormal transient and accident conditions. As a passive safety system, the function of steam pressure suppression pools is paramount to the containment performance. In the present work, the focus is on apparently-benign but intricate and potentially risk-significant scenarios in which thermal stratification could significantly impede the pool's pressure suppression capacity. For the case of small flow rates of steam influx, the steam condenses rapidly in the pool and the hot condensate rises in a narrow plume above the steam injection plane and spreads into a thin layer at the pool's free surface. When the steam flow rate increases significantly, momentum introduced by the steam injection and/or periodic expansion and shrink of large steam bubbles due to direct contact condensation can cause breakdown of the stratified layers and lead to mixing of the pool water. Accurate prediction of the pool thermal-hydraulics in such scenarios presents a computational challenge. Lumped-parameter models have no capability to predict temperature distribution of water pool during thermal stratification development. While high-order-accurate CFD (RANS, LES) methods are not practical due to excessive computing power needed to calculate 3D high-Rayleigh-number natural circulation flow in long transients. In the present work, a middle-ground approach is used, namely CFD-like model of the general purpose thermal-hydraulic code GOTHIC. Each cell of 3D GOTHIC grid uses lumped parameter volume type closures for modeling of various heat and mass transfer processes at subgrid scale. We use GOTHIC to simulate POOLEX/PPOOLEX experiment, in order to (a) quantify errors due to GOTHIC's physical models and numerical schemes, and (b) propose necessary improvements in GOTHIC sub-grid scale modeling. The study performed on thermal stratification in a water pool indicates that GOTHIC CFD-like model is fit for reactor applications in complex fluid-physics scenarios that avoids both over-simplification (as in single lumped-parameter model) and over-complication (as in CFD models). However, simulation of direct steam injection into a subcooled pool cannot be predicted reliably with the existing models. Thus we develop "effective heat source" and "effective momentum" approaches, and provide feasibility study for the prediction of thermal stratification and mixing in a BWR pressure suppression pool. The results are encouraging and further activity on the development and implementation of the proposed models in GOTHIC is currently underway.





# **1. INTRODUCTION AND BACKGROUND**

## ***1.1. Project Goals***

This work is a first step to implement the NORTHNET Roadmap 3 (Containment Thermal Hydraulics) at KTH. It contributes to development of capability and sustaining of expertise in area of containment thermal-hydraulics. Objectives of current project are:

- (i) to examine the state-of-the-art understanding of multiphase flow phenomena that govern pressure suppression pool dynamics;
- (ii) to assess capability of existing tools (codes and models) in predicting key behaviors and parameters of suppression pools;
- (iii) to provide an evaluation of, and analytical support for, the related experimental program conducted at Lappeenranta University of Technology (LUT) on condensation pools, namely POOLEX and PPOOLEX experiments.

As specific task, the work aims to validate the GOTHIC code for prediction of thermal stratification and mixing in a pressure suppression pool. In the present work we focus on validation of GOTHIC against data provided in POOLEX tests STB-20 and STB-21 [9].

The goal of validation activity is clarification of deficiencies in the present code simulation models for prediction of safety important phenomena:

- (a) development of thermal stratification at low mass flow rate of steam,
- (b) time scale for mixing of stratified pool.

The structure of this report is organized as follows. Goals of the project, review of state of the art in experimental and analytical research related to thermal stratification, mixing and steam condensation in water pool are presented in **Chapter 1**. Concept of “Effective heat source” (EHS) approach to modeling of stratification at small steam flow rate is introduced and validated against POOLEX data in **Chapter 2**. Concept and results of feasibility study for “Effective momentum source” (EMS) approach to simulation of mixing in a pool at high steam flow rate are discussed in **Chapter 3**. Pre- and post-test analysis of selected PPOOLEX experiments with lumped parameter models in GOTHIC are presented in **Chapter 4**. **Chapter 5** discusses summary of the present work and suggests further steps on development, implementation and validation of EHS and EMS approaches. Detailed description of GOTHIC models used in the analysis and some additional results are presented in the appendixes.

## ***1.2. Summary of Research on Stratification and Mixing in Water Pools and Formulation of Approach***

Thermal stratification in a large water pool is a well known physical phenomenon which is responsible for formation of horizontal liquid layers of differing densities at different depths. Stratification is important factor in environmental and biological

science (stratification in lakes and oceans) it is also widely applied in various kinds of sensible heat storage systems [57].

Configuration of the stratified layers generally depends on location of the heat source and history of transient heat transfer in the pool (heating and cooling phases). In the present work we consider scenarios of thermal stratification development caused by a heat source immersed into the pool at certain depth. Such configuration is motivated by the focus of the present work on BWR pressure suppression pool operation. Two typical transient stratification configurations presented in Figure 1 are considered. Specifically we are interested in (i) the rate of thermal stratification development with continuous increase of water temperature in the layer of the pool above the bottom of the heat source and constant temperature of cold water  $T_c$  below the heat source (Figure 1a), and in (ii) formation of the top isothermal layer at temperature  $T_h$  separated from the bottom layer of cold water by relatively thin thermocline layer where temperature is changing rapidly from  $T_c$  to  $T_h$  (Figure 1b).

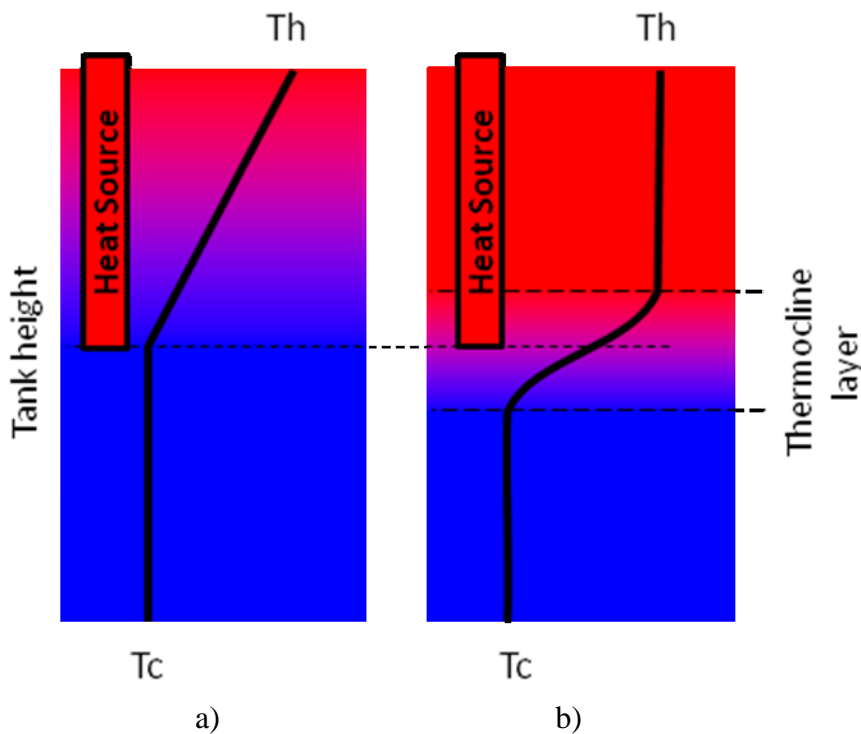


Figure 1: Typical configurations of thermal stratification in a tank:  
 a) developing stratification; b) thermocline layer.  
 $T_h$  – temperature of hot liquid;  $T_c$  – temperature of cold liquid.

Pressure suppression pool is a crucially important part of BWR reactor containment safety system. It serves as a heat sink and steam condenser to prevent containment pressure buildup during loss of coolant accident or during safety relief valve opening in normal operations. Steam flowing out of reactor vessel or out of main steam line is vented through blowdown pipes and condenses in the pressure suppression water pool. Weak mixing in the pool, in the case of small mass flow rate of steam, may be insufficient for prevention development of thermal stratification. As a result, the temperature of the pool surface can increase significantly. That will lead to reduction of pool's pressure suppression capacity. In the post accident long-term cooling

process, partial steam pressure in the wetwell gas space is defined by the pool surface temperature. Increase of the pool surface temperature due to stratification can lead to significant increase of containment pressure [14]. If water in the layer above the pipe outlet will reach saturation temperature the injected steam will not be condensed in this layer.

Breakdown of thermal stratification in the pool can be achieved by mixing. Increased steam flow rate or active pool mixing systems can provide sufficient momentum for mixing of water in the pool. Mixing of stratified pool takes certain time which generally depends on the momentum injected in the pool. The time which is necessary to achieve mixing determines how fast suppression pool capacity can be restored. Therefore characteristic mixing time scale is considered as important parameter of the pool operation. Condensation of steam in the subcooled pool plays an important role in determining of the resultant momentum of the steam jet and thus affects dynamics and characteristic time scales of mixing and thermal stratification development.

Reliable and computationally efficient methods for prediction of mixing and stratification phenomena are necessary for safety analysis of the pressure suppression pool operations.

State of the art in the suppression pool stratification and mixing research can be summarized as follows:

- (i) Numerous experimental studies were performed in the past on stratification and mixing in a pool, but only few are full or large scale tests. Westinghouse methodology for addressing pool stratification is based on a series of blowdown tests performed in the Nordic BWR suppression pools. However, not all experimental data is available and suitable for validation of codes and models.
- (ii) POOLEX/PPOOLEX [9, 10] is relatively large scale experiment which provides most complete set of data necessary for code validation.
- (iii) Lumped-parameter and 1D models based on scaling approaches [12-18] were developed and successfully utilized for prediction of a number of tests problems. Unfortunately, applicability of these methods is limited to stably stratified or well mixed conditions. In addition, time scale of stratified layer breakdown transient has not been addressed in these models.
- (iv) Direct application of high-order accurate CFD (RANS, LES, DNS) methods are not practical due to excessive computing power needed to calculate 3D high-Rayleigh-number natural convection flows [22], and direct contact condensation of the steam [47].
- (v) The need for development in GOTHIC code of effective subgrid models and approaches to prediction of thermal stratification development and mixing is identified in the present work (see also [19, 20, 21]). Validation and feasibility studies of proposed approaches are also discussed in the present work [19, 20, 21]. The key elements in the proposed approach are concepts of “Effective heat source” (EHS) and “Effective momentum source” (EMS) generated by steam injected into a subcooled water pool. The effective momentum defines time scale for mixing of initially stratified pool. In order to predict effective momentum one has to combine knowledge about (a) flow regimes of steam injection into a subcooled pool [45] and (b) models for analysis of heat and momentum transfer caused by

direct contact condensation [31-44] in each flow regime. New models are to be implemented in the codes to enable computationally efficient and sufficiently accurate prediction of stratification and mixing phenomena.

A more detailed discussion of previous works is presented below.

Intensive research has been done in the past on suppression pool behavior during the blowdown phase of a loss-of-coolant accident (LOCA). The tests were performed at the Pressure Suppression Test Facility (PSTF) at different scales [1, 2, 3]. Although PSTF experiments were focused on LOCA blowdown conditions characterized by violent pool mixing, some tests have shown that a significant stratification can exist in the pool at the end of the transient [1, 2, 3].

Stratification and mixing phenomena in a large water pool with a heat source have been studied experimentally and analytically [4-20].

Strong stratification above a heat source submerged in a water pool was observed in different tests [4, 5, 6, 7, 8, 9, 10, 11]. Kataoka et al. [5] found that heat transfer into layer below the heat and momentum source is limited by thermal conduction. Thus stratification limits the available heat sink capacity of the pool. The region below the source of momentum and heat remains inactive as a heat sink [4, 5, 6, 7, 8, 9, 10, 11].

Two most recent experimental efforts on study of thermal stratification and mixing in relatively large pools are worth mentioning. Namely, experiments performed in the PUMA facility [8] systematically addressed effects of vent opening submergence depth, pool initial pressure, steam injection rate, and volume fraction of non-condensable gases on thermal stratification in suppression pool. Unfortunately, information provided in [8] is not sufficient to perform independent validation of codes and models against PUMA data.

Another large experimental program that is partially motivated by investigation of thermal stratification development and mixing in a relatively large pool [9, 10] includes POOLEX (POOL EXperiment) and PPOOLEX (Pressurized POOLEX) experiments performed at Lappeenranta University of Technology (LUT, Finland). POOLEX/PPOOLEX experimental data generally confirms observations made in a smaller scale experiments. Breakdown of stratified layer by steam injection at large mass flow rate was also investigated [9]. Decrease of the steam flow rate leads to redevelopment of thermal stratification this time with higher temperature of the bottom layer below the blowdown pipe outlet [9].

The POOLEX facility is open to the lab atmosphere, cylindrical stainless steel tank with outer diameter 2.4 m and water pool depth 2.95 m. Three vertical trains of thermocouples (with 16 thermocouples in each train) were installed in the tank to monitor water temperature during the test. Heating by steam injection through the blowdown pipe and cooling (after stop of steam injection) phases were studied in the POOLEX tests. During the experiment STB-20 [9] the steam mass flow rate was kept in range of 25-55 g/s to make sure that steam condenses inside the blowdown pipe. Strong stratification above outlet of the blowdown tube was observed in the test.

The most important source of uncertainty in the POOLEX experiment is the immeasurable heat losses from the vessel walls and from the open pool free surface to the atmosphere of the lab. A method of combining experimental data and lumped parameter simulations was proposed in [19] for recovery of necessary data for providing of boundary conditions and validation of 2D/3D models.

The problem of uncontrolled heat and mass exchange with the lab atmosphere was partially solved in the next modification of POOLEX namely in PPOOLEX facility. Specifically, volume of the PPOOLEX facility is a leak tight vessel with a drywell compartment installed on top of the wetwell compartment. PPOOLEX is a scaled model of BWR containment and has possibility to install several blowdown tubes which connect the drywell and the wetwell sections [10]. Several tests were performed in PPOOLEX facility in 2009. Strong stratification both in liquid and in gas space of the wetwell were indicated in the tests STR-01 – 06 [10].

PPOOLEX is a leak tight vessel, and has no mass exchange with the lab atmosphere. Yet vessel outer surface is not insulated and heat flux to the lab is still significant and its spatial distribution over the vessel outer surface (necessary for 2D/3D models boundary conditions) is hardly measurable in the experiment. Present work provides some preliminary results for pre- and post-test analysis of the PPOOLEX data.

Scaling approaches for prediction of thermal stratification and mixing in pools and in large interconnected enclosures were developed and applied by Peterson and co workers at UC Berkeley [12-18]. Experimental study of gas mixing processes and heat transfer augmentation by a forced jet in a large cylindrical enclosure with an isothermal bottom heating/cooling surface was performed in [15]. Cold/hot air was injected at several positions with different pipe diameters and injection orientations, and was removed from the top of the enclosure. Criteria for a jet or plume not able to disturb the stable vertical stratification were proposed. Developed scaling methods for mixing processes under stratified conditions allow one to take into account effects of buoyant jets, plumes from heat sources, wall jets and heat transfer to structures. Criterion was introduced for prediction of onset of thermal stratification breakdown, but time necessary for breaking down of stratification was not addressed. 1D simulation code BMIX/BMIX++ was also developed at UC Berkeley to simulate stratification development [16]. It was validated against a number of experimental tests [15, 16, 17, 18]. However, BMIX++ is applicable only for the stably stratified conditions or well-mixed volumes. Details of transition from stratified to mixed conditions and specifically the time scale for such process are not addressed.

Gamble et al. [14] studied post-accident long-term containment performance in case of passive SBWR containment and found that surface temperature of the pressure suppression pool is an important factor in determining the overall long-term containment pressure. The mixing by jets from the main vents is identified as the key phenomena influencing the thermal response of the suppression pool. Effects of clearing and venting of non-condensable gases together with steam over a range of flow rates at various submerged depths were considered with respect to the thermal stratification and surface temperature in the pool. Analytical models were developed and implemented into a system simulation code, TRACG, and used to model thermal stratification behavior in a scaled test facility [14]. The main idea of the proposed model is based on analysis of the effect of injected momentum in each computational

cell. The analytical models were used to model thermal stratification behavior in a scaled test facility. Good agreement with scaled experimental test data is reported.

Condensation and mixing phenomena during loss of coolant accident in a scaled down pressure suppression pool of simplified boiling water reactor were also studied in [11]. Results of experiments [11] were compared with the TRACE code predictions and showed deficiency in the code capabilities to predict thermal stratification in the pool. Specifically uniform temperature distribution was predicted with TRACE while experiments performed at the same conditions showed significant stratification [11].

Experimental investigation of steam condensation and CFD analysis of thermal stratification and mixing in subcooled water of In-containment Refueling Water Storage Tank (IRWST) of the Advanced Power Reactor 1400 (APR1400) were performed by Song et al. [54], Kang and Song [55] and Moon et al. [48]. The IRWST is, in fact, a BWR SP technology adopted in a PWR designs to reduce the containment failure risk by condensing steam in a subcooled pool. Contemporary CFD codes don't have a standard model for direct contact condensation analysis. Therefore a lumped volume condensation region model [55] was used to provide boundary conditions for temperature and velocity of the condensed steam and the entrained water in the CFD simulations. Similar approach to modeling of steam injection was initially proposed by Austin and Baisley [56]. A comparison of the calculated and experimentally measured temperature profiles [48] shows some disagreement in the vicinity of the sparger. The main reason for this disagreement is claimed to be caused by the difference in the test and simulating conditions at the tank wall. However, moving away from the sparger, the rate of temperature increase becomes similar to that in the experiment [48]. Only stable flow condensation regime was addressed [48, 55].

Hydrodynamic flow regimes of steam injection into a subcooled water pool at different conditions were studied intensively in the past [45, 49, 51, 52, 53]. Figure 2 depicts a flow regime map.

Unlike condensation oscillations, chugging [46, 45] can result in large oscillations of the steam-liquid interface which can enhance mixing [14]. Apparent influence of chugging on mixing in the pool was observed in POOLEX experiment [9]. Steam flow rate in the POOLEX STB-20 and STB-21 was kept below certain limit to prevent mixing in the pool by steam flow pulsations.

Therefore important element in development of models for predicting stratification and mixing in the BWR pressure suppression pool is the problem of direct contact condensation of steam jet discharged into a subcooled pool. The problem of direct contact condensation has been addressed in a number of studies [31-44]. Different approaches have been developed to predict the distance required for complete condensation of the steam and pressure oscillations. Furthermore, different idealized shapes (conical, ellipsoidal and divergent) of the pure steam jet plume in a subcooled pool of water were considered based on experimental observations, where the plume shape and length were found to depend on the injection diameter, injection orientation and pool subcooling, and steam mass flux.

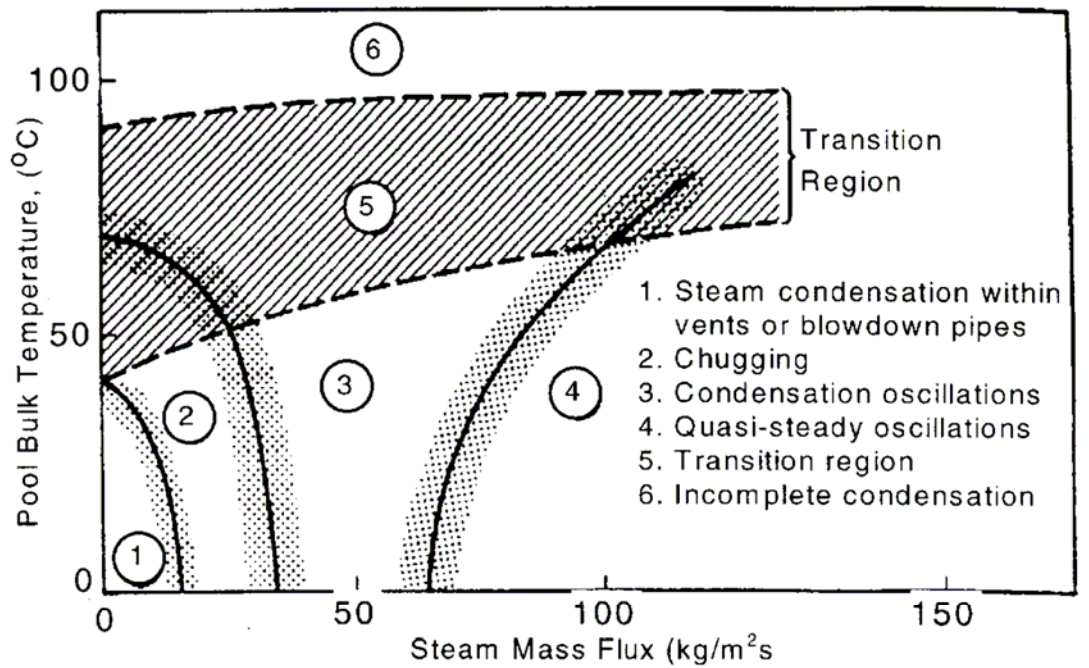


Figure 2: Regime map of steam condensation [45]

Direct application of high-order accurate CFD (RANS, LES, DNS) methods to plant scale analysis is usually impractical due to excessive computing power needed to calculate 3D high-Rayleigh-number natural convection flows [22], and direct contact condensation of the steam [47], especially in long transients and in real geometry of the BWR pressure suppression pool [19]. Therefore CFD-like model of the general purpose thermal-hydraulic code GOTHIC [23, 24] is selected as a computational vehicle in present study. GOTHIC provides a middle-ground approach between lumped parameter and pure CFD models. In each cell of a 3D grid GOTHIC uses lumped parameter type closures and correlations for simulation of heat, mass, and momentum transfer at subgrid scales. With such approach the computational efficiency can be dramatically improved in comparison with pure CFD methods due to much less strict demands for necessary grid resolution. For example, there is no need in GOTHIC to resolve near wall boundary layers, because heat and mass transfer is resolved by subgrid scale models based on boundary layer theories or experimental correlations. At the same time, 3D resolution of the flow field in GOTHIC is big advantage for study of phenomena such as mixing and stratification, and it provides much greater flexibility than 0D and 1D models can afford.

Extensive validation of the GOTHIC has been performed in the past [23] including simulation of Marviken tests, which are unique full scale experiments on the venting through a pressure suppression pool in the wetwell [26]. GOTHIC also has been validated against experiments performed in large scale PANDA facility on the mixing process in the drywells gas space, initially filled with air, during the start of steam purging transient [27, 28].

GOTHIC version 7.0 was used to model five tests that were conducted in the Nuclear Power Engineering Corporation facility in Japan [29]. The tests involved steam and helium injection into a scaled model of a pressurized water reactor dry containment. The focus of simulation is on gas and steam temperatures and concentrations distribution in the containment.

GOTHIC 3.4 was used to evaluate performance of passively cooled containment of integrated pressurized water reactor [30]. The focus was on development of thermal and concentration stratification in the gas space of the containment. Two experiments were carried out; one to test the performance of the external moat, and one to verify the code's ability to predict thermal-stratification inside the containment.

We did not find in the open literature any validation of GOTHIC against the problem of thermal stratification and mixing in case of steam injection into a large water pool.

In [19, 20] and in the present work the GOTHIC CFD-like option is used to simulate POOLEX [9] and PPOOLEX [10] experiments to validate GOTHIC's physical and numerical models, and to identify need for improvement of the models. One of the main reasons for selection of POOLEX/PPOOLEX data for the code validation is detailed description of experimental conditions and results provided in the research reports [9, 10].

The objective of the present work is to propose a method for reasonably-accurate and computationally affordable simulations of thermal stratification and mixing transients in BWR suppression pools.

As it has been discussed above, direct contact condensation (DCC) phenomena including different oscillatory flow regimes of steam injection into a subcooled pool are important for development of stratification or mixing in the pool.

Following ideas proposed by Austin and Baisley [56] and developed by Kang and Song [55] we propose (see also [19, 20]) instead of "direct" CFD-type simulations of DCC phenomena based on first principles to use subgrid models in GOTHIC to predict DCC **effect** on development of thermal stratification and mixing.

We realize that steam injection affects stratification and mixing by two main mechanisms:

- I) Localized heat source in the pool due to steam condensation.
- II) Localized momentum source induced by steam injection (by motion of steam water interface and by buoyancy plum of steam bubbles escaping the blowdown pipe).

Thus to resolve the effect of steam condensation on mixing and stratification in the pool one has to provide models for the heat source and for the momentum source induced by steam injection. Fortunately characteristic time and space scales of DCC phenomena are much smaller than characteristic time and space scales of development of thermal stratification and global circulation and mixing in the pool. Such scale separation suggests that computationally affordable "effective" models for assessment of the "net effects" of steam injection don't need to resolve details of DCC phenomena. We call such models "Effective heat source" (EHS) and "Effective momentum source" (EMS) approaches to emphasize that these modes are dealing with the **effect** of steam condensation on stratification and mixing.

Figure 3 shows the assumed configuration of the phases for a lumped parameter volume in GOTHIC. In the pool/drop regime, all the liquid is assumed to be in the



form of a pool at the bottom of the volume. Drops entering the volume through connecting junctions are assumed to settle towards the bottom of the cell at their terminal velocity. Bubbles of vapor that enter the volume below the pool surface will rise through the pool at the bubble terminal velocity. This conceptual picture is used to calculate interfacial heat transfer and drop deposition rates for lumped parameter volumes [25].

Direct contact condensation phenomena occurring in the vicinity of blowdown pipe outlet when steam is injected into a pool are not resolved in GOTHIC. On the other hand, these phenomena are driving mechanisms for the flow regimes [45, 49, 51, 52, 53]. Therefore, to predict effective momentum, one has to combine knowledge about (a) flow regimes of steam injection into a subcooled pool [45] and (b) models for analysis of heat and momentum transfer caused by direct contact condensation [31-44] in each flow regime. New models are to be implemented in the codes to enable computationally efficient and sufficiently accurate prediction of stratification and mixing phenomena.

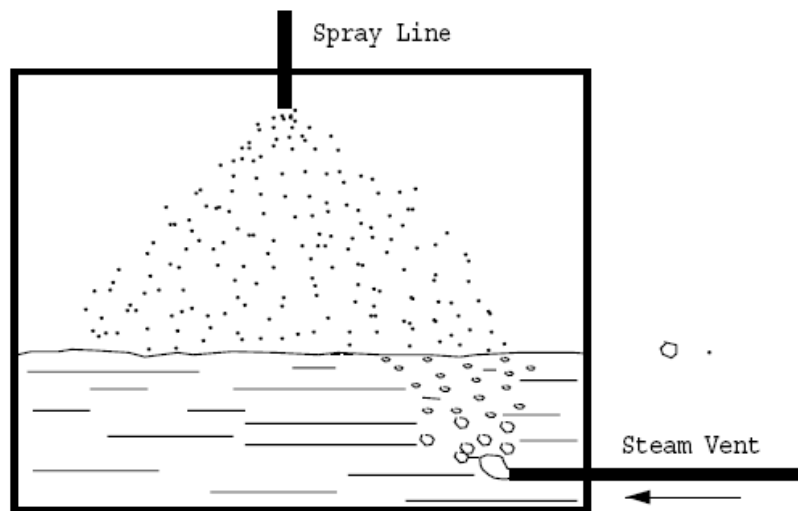


Figure 3: Phase Configuration for Lumped Parameter Volumes [25]

In the present work we focus on discussion of development and validation of the EHS model. Feasibility study for the EMS model also provides encouraging preliminary results.

## **2. EFFECTIVE HEAT SOURCE APPROACH TO SIMULATION OF STRATIFICATION DEVELOPMENT**

In this chapter we discuss “effective heat source” approach to simulation of thermal stratification development in a subcooled water pool under low steam flow rate conditions.

In Section 2.1 inherent uncertainties are discussed in the POOLEX experimental data used for code validation. We use GOTHIC lumped parameter model to recover missing information for providing boundary conditions for 2D/3D models.

Section 2.2 presents results of simulation obtained with GOTHIC in case of direct steam injection into a pool. We demonstrate that artificial mixing of the pool is observed and no development of thermal stratification is predicted. Moreover, direct injection of steam into a subcooled water pool imposes serious limitations on computational time step.

Effective heat source approach is proposed in Section 2.3 to solve the problem of adequate and robust prediction of thermal stratification development. Validation of proposed approach with GOTHIC code including study of sensitivity (i) to uncertainty in boundary conditions, and (ii) to grid resolution is presented in Section 2.4. Reasonable agreement between simulation results and experimental data on thermal stratification development in POOLEX STB-20 is reported. High computational efficiency is also achieved with effective heat source approach because of no severe limitations on computational time step.

Application of effective heat source approach with CFD code (Fluent) simulations of thermal stratification development is discussed in Section 2.5. Good agreement with experimental data is demonstrated. Basic mechanisms for development of top isothermal layer in cooling phase of the POOLEX experiment are also addressed in Section 2.5.

Results obtained with direct steam injection and with effective heat source approach to simulation of stratification development in a prototypic size pool are presented in Section 2.6. It is concluded that for reliable prediction of thermal stratification in large, prototypic scale pools effective heat source approach shall be used.

### ***2.1. Lumped Parameter Simulation of POOLEX Test STB-20***

POOLEX facility has an open tank and heat losses from the tank to ambient atmosphere are not directly measured in the POOLEX experiments. Thus, a lumped parameter model in GOTHIC is used to calculate the missing experimental data on heat fluxes through the vessel walls and on the pool free surface. Then we use these data as unsteady boundary conditions for the distributed parameter model (also in GOTHIC) in the simulations of thermal stratification.

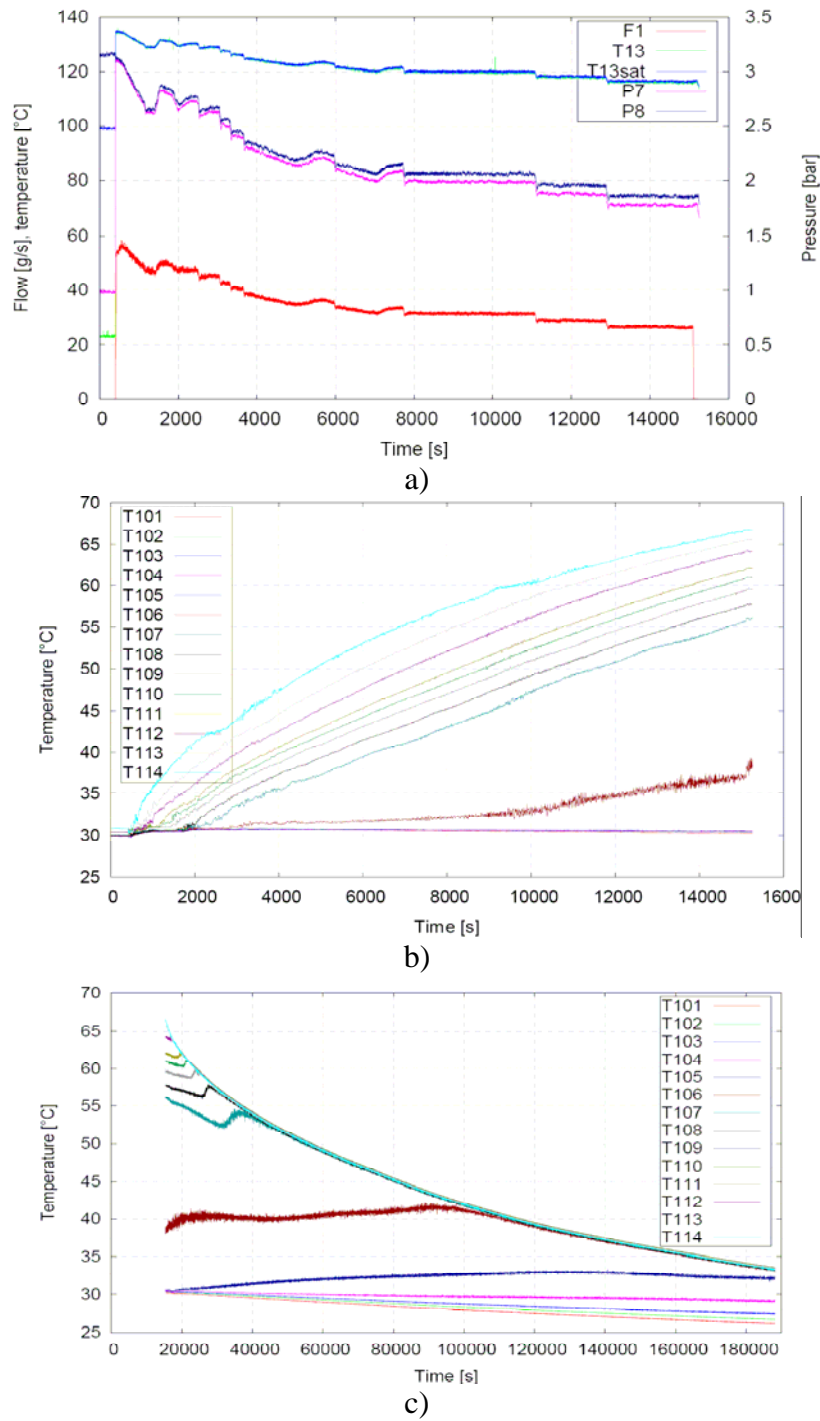


Figure 4: POOLEX STB-20 [9]: a) steam injection conditions, b) history of vertical temperature distribution in heating phase and in c) cooling phase

Conditions and main results of the POOLEX STB-20 test [9] are presented in (Figure 4). The total duration of the STB-20 experiment was approximately 52 hours. The initial pool water temperature was 30 °C. During the first four hours, the pool water was heated with steam flow. The initial steam mass flow rate of 55 g/s was slowly reduced to 25 g/s as the experiment progressed to make sure that steam condenses inside the blowdown pipe and that the steam-water interface remains close to the blowdown pipe outlet [9]. Steam blowdown was terminated when the water maximum

temperature in the upper part of the pool was 67 °C. After the heating phase, the pool water was cooled down for the next 48 hours [9].

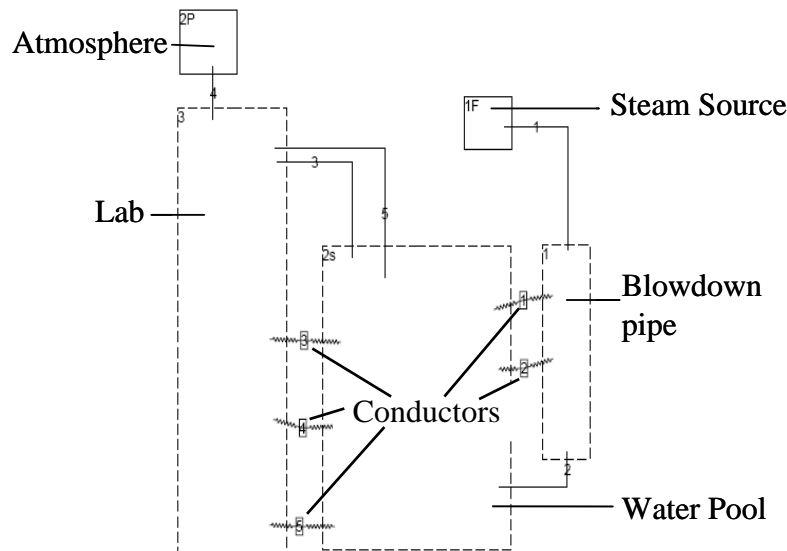


Figure 5: GOTHIC lumped parameter input model

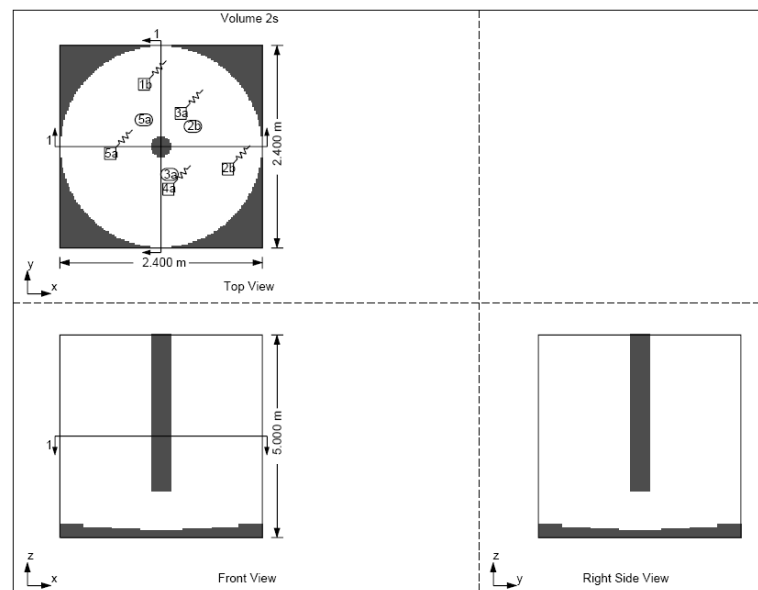


Figure 6: POOLEX tank geometry representation in GOTHIC model

The lumped parameter model developed for simulation of POOLEX experiment is shown in Figure 5. First, the steam source is represented by the flow boundary condition (marked 1F). The experimental data, i.e., steam temperature, pressure, and flow rate [9] are used as time dependent flow boundary condition for 1F. Next, the atmosphere is modeled by a pressure boundary condition (2P) with constant pressure (1 bar) and temperature (20°C). The blowdown pipe, water pool, and the lab, are represented by volumes 1, 2s, and 3, respectively. The heat transfer between the blowdown pipe and the vapor phase is simulated by thermal conductor 1 while the heat transfer between the blowdown pipe and the liquid phase is simulated by thermal conductor 2. Similarly, the heat transfer between the vessel walls and the lab atmosphere are represented by thermal conductors 3, 4 and 5. The vapor part of the vessel sidewall is represented by conductors 3 while the liquid part is represented by

conductor 4. Lastly, the bottom wall of the vessel is represented by conductor 5. The heat transfer coefficients for all heat conductors are calculated by default GOTHIC models for natural convection on vertical (conductors 1, 2, 3, 4) and horizontal (conductor 5) surfaces [23].

A blockage is used to represent the geometry of the pool in GOTHIC [24]. Analysis performed in Section 2.4.1 with the distributed parameter model suggests that shape of the vessel bottom has no significant effect on the result of simulation and can be approximated by a flat surface. An example of the tank geometry representation, obtained by partial blockage in GOTHIC rectangular cell is shown in Figure 6. Again, similar blockage is used to represent vessel geometry in distributed parameter model (see next section).

The POOLEX facility lab has a ventilation system but is not modeled in the present work because the parameters of this system are uncertain. Instead, an effect of ventilation system is introduced by a large ( $10^7 \text{ m}^3$ ) volume of the lab. The temperature of the lab atmosphere in the experiment and in the calculations is about  $24^\circ\text{C}$ . In addition, the natural circulation above the pool surface is taken into account (according to the recommendations of GOTHIC manual [24]) by two parallel flow paths (marked 3 and 5 in Figure 5). Intensity of natural circulation in such model depends on (i) the difference between the vertical positions of the parallel flow paths' outlets, and on (ii) the loss coefficients assumed for the flow paths [24]. The elevations of the flow paths' outlets and loss coefficients in the flow paths (see Appendix 1, Table A1-1) are adjusted to match the experimental data for the average temperature in the pool measured in the STB-20 test.

In the STB-20 experiment, steam injection was initiated at 400 s since the start of the data recording by the data acquisition system. This was done in order to provide measurements of initial conditions in the pool. In GOTHIC calculations we are not considering the first 400 s without steam injection. The simulation is started directly at the moment when steam injection starts in experiment, which means that heating (steam injection) phase lasts for 14 600 s. The whole transient physical time is 187 600 s (~52 hours).

Comparison of experimental and simulation results for averaged pool water temperature are shown in Figure 7a. Good agreement between experimental and simulation data for both heating and cooling phases of the STB-20 test are obtained.

As mentioned previously, the main goal of the lumped parameter model calculations is to obtain proper boundary conditions for the distributed parameter model simulation. In Figure 7b we show the heat losses from the tank to the lab through the side and bottom walls of the tank. It can be observed that the heat loss through the bottom wall of the tank is much smaller than that through the side walls.

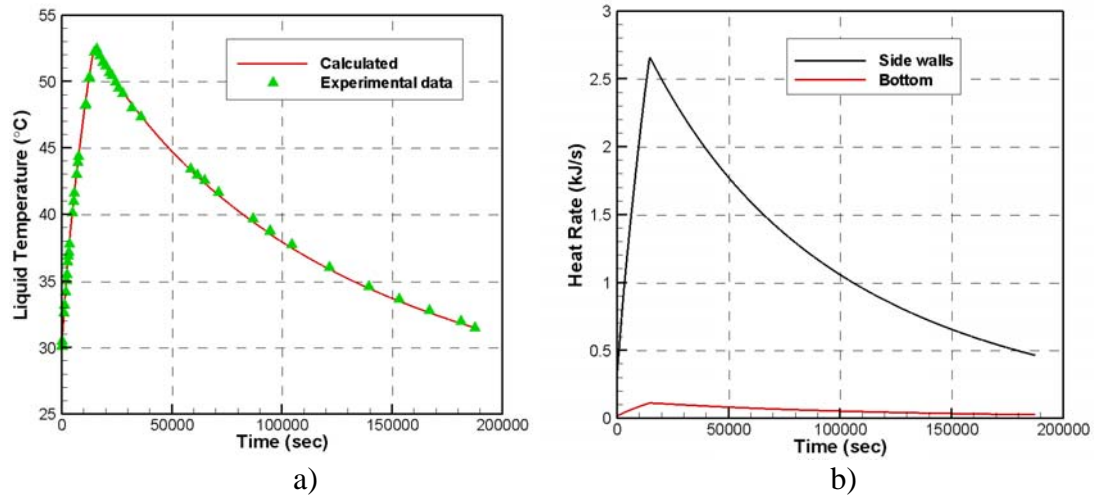


Figure 7: Lumped parameter model results:  
a) averaged water temperature in the tank; b) heat fluxes to the vessel walls

The CPU time for calculation of STB-20 whole transient, including heating and cooling phases (187 600 s of physical time), with lumped parameter model is about 250 seconds on a PC Pentium IV with 2.8 GHz processor.

## 2.2. Simulation of Direct Steam Injection in POOLEX Test STB-20

A simulation of direct steam injection into the water pool for STB-20 is also performed. The model and coarse grid configuration are shown in Figure 8. Volumes 1 and 2s model the blowdown pipe and tank, respectively. Flow boundary 1F, supplying steam at experimental conditions, is connected to blowdown pipe (volume 1) by flow path 1. The pressure boundary (marked 2P) connected to the tank by flow path 3 represents atmospheric conditions. Flow path 2 connects the blowdown pipe and open tank. Thermal conductors 1s and 2s models heat transfer from the pipe to vapor and liquid part of tank, respectively. Conductors 3s and 4s are spanned along tank sidewall and represent heat loss from vapor and liquid part respectively. Heat loss through the bottom wall is modeled by conductor 5s. Horizontal XY plane of is divided uniformly into 3 by 3 cells. For vertical Z direction, there are 11 grid layers for liquid part and 6 layers for vapor part. The geometry of tank bottom and space occupied by pipe are modeled with blockages.

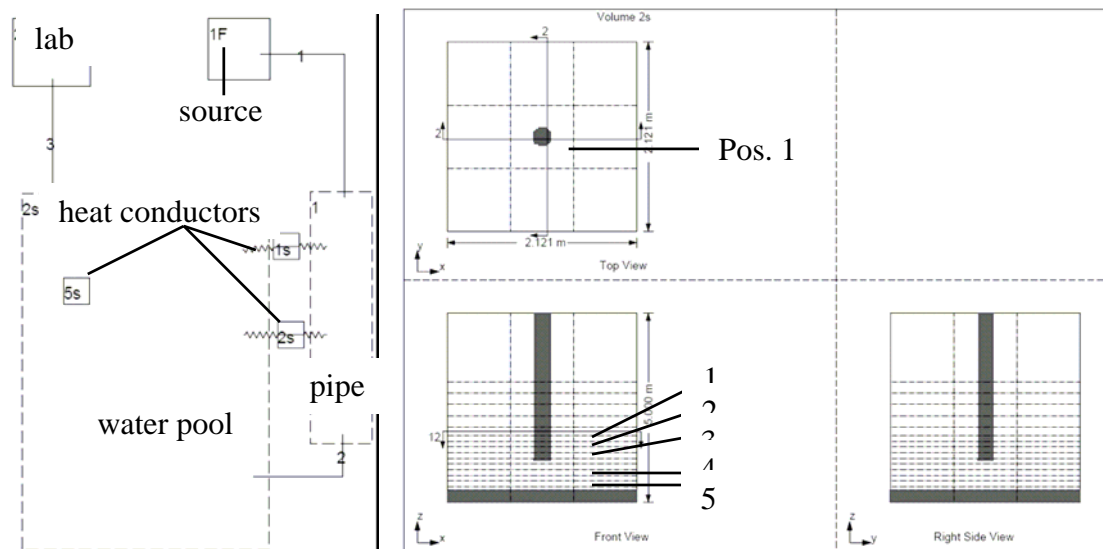


Figure 8: Prototype of POOLEX modeling and grid configuration of tank  
(1-1.615m, 2-1.465m, 3-1.165m, 4-0.715m, 5-0.415m)

Figure 9 shows temperature variation during 10000 seconds in layers at different elevation in Pos. 1 (Figure 8). As can be seen in Figure 9 no thermal stratification was predicted in the simulation. This and other cases calculated with modeling of direct steam injection (see also [21] and chapter 2.6.2) imply that GOTHIC model cannot reproduce experimentally observed development of thermal stratification when direct steam injection into pool is modeled. Mixing predicted with direct steam injection is caused by overestimation of large scale circulation in the pool [21]. Possible reasons for the overestimation of the circulation are (i) not completely condensed inside the pipe and (ii) strong oscillations of steam-water flow inside the pipe. Both buoyant plum of steam bubbles and flow oscillations are considerable sources of momentum in the pool and can cause large scale circulation and mixing.

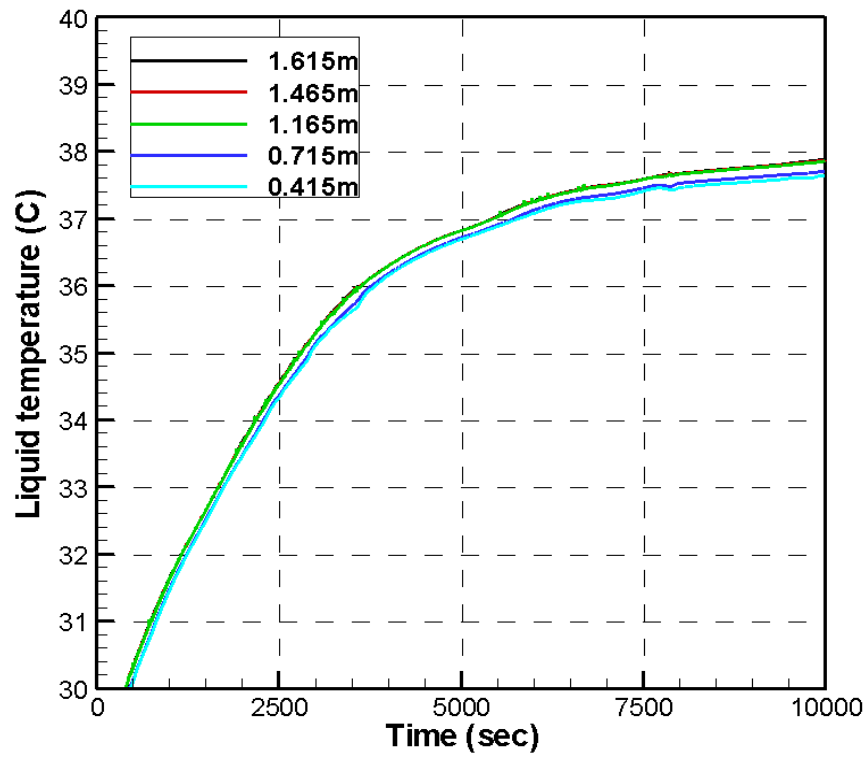


Figure 9: Temperature history in GOTHIC direct simulation with steam injection



### 2.3. Effective Heat Source Approach to Simulation of Stratification Development at Small Rate of Steam Injection

We consider two characteristic regimes of steam injection into a water pool (Figure 10). The first regime (Figure 10a) is characterized by considerable amount of a non-condensed steam (or non-condensable gases) that flows out of the blowdown pipe. The second (Figure 10b) is normally a result of relatively small flow rate of pure steam when all steam is condensed inside the blowdown pipe and only a hot condensate with low momentum flows out of the pipe.

In the first regime (Figure 10a) steam/gases flowing out of the pipe can create considerable momentum which may cause significant mixing and breakdown of stratification in the pool. This is addressed in detail in Chapter 3.

In the second regime (Figure 10b) steam injection provides negligible source of momentum which does not induce significant mixing in the pool while it provides considerable heat source for development of thermal stratification in the pool.

This regime is experimentally investigated in POOLEX test STB-20 [9] (Figure 4). Steam flow rate is controlled and the position of the water free surface is kept close to the outlet and inside the blowdown pipe [9]. As a result strong thermal stratification has developed during the heating phase of the experiment [9] (Figure 4).

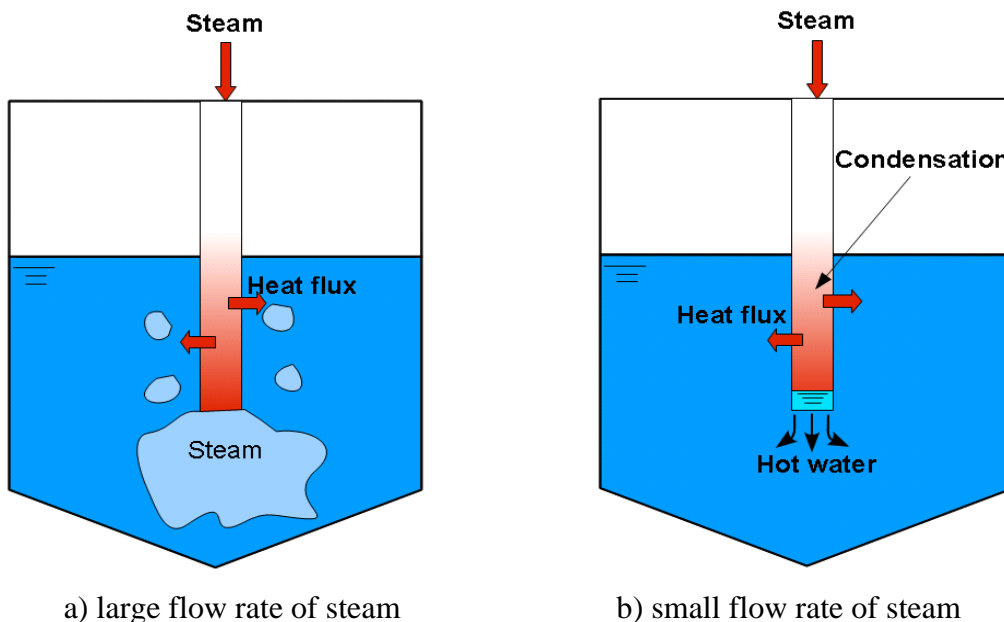


Figure 10: Two regimes of steam injection into a subcooled water pool

As it is shown in the previous section, modeling of direct steam injection with GOTHIC in this regime gives inadequate results, that is, mixing is predicted instead of stratification development.

It is important to mention also that small computational time step (and thus large computational costs) is required for simulation of steam injection with oscillations of condensation-evaporation inside the blowdown pipe.

In order to solve the problem of adequate and robust prediction of thermal stratification development we propose an “effective heat source” approach. In accordance with the experimental observations from POOLEX STB-20, we assume that momentum of the condensate flowing out of the blowdown pipe is negligibly small. Thus we assume that neither the steam nor the liquid flows out from the pipe in the GOTHIC model which introduces zero momentum in the pool. An effective heat source is assumed to be uniformly distributed along the surface of the pipe wall. The heat source is used to model thermal effect of steam injection (equivalent to the enthalpy of the steam flowing into the blowdown pipe). This heat source is considered to be the main cause of thermal stratification development.

The water pool geometry considered in further analysis is 2D axisymmetric. Only the liquid part of the tank volume is considered in the simulations in order to increase computational efficiency and to avoid possible numerical problems in resolving the top free surface of the liquid pool. Furthermore, the heat loss on the pool free surface is simulated with a time dependent heat flux.

Changes of water inventory in POOLEX STB-20 experiment are insignificant. Therefore we neglect such changes in further analysis and consider the volume of the liquid constant. Such assumption may not be valid in longer transients, when water inventory in the pool can vary significantly. In this case liquid free surface has to be explicitly modeled in the simulations, which can result in increase computational time.

## 2.4. Validation of Effective Heat Source Approach for Simulation of Stratification Development

### 2.4.1. Sensitivity to Boundary Conditions

Heat fluxes on the pool free surface and through the vessel walls were calculated with lumped parameter model presented in Section 2.1. In this model uniform pool temperature is assumed. In reality pool temperature is different at different elevations in the tank if thermal stratification has been developed.

Potential influence of boundary conditions on development of thermal stratification is studied in this section. In the simulations, cylindrical water tank was treated as 2D axisymmetric volume. Only liquid part is simulated. The liquid volume is divided into  $12 \times 30$  meshes in horizontal and in vertical directions respectively.

Three different kinds of thermal boundary conditions are used to simulate heat transfer through the tank walls, as shown in Figure 12. In all cases the heat loss from free surface is modeled by virtual thermal conductor made of steel wall with thickness of 0.01 cm. It is also assumed that all enthalpy of injected steam is transferred to the liquid part through submerged pipe surface and there is no mass influx into the pool. Heat fluxes used as boundary conditions on the pipe wall are presented in Figure 11a, and heat loss from free surface is shown in Figure 11b.

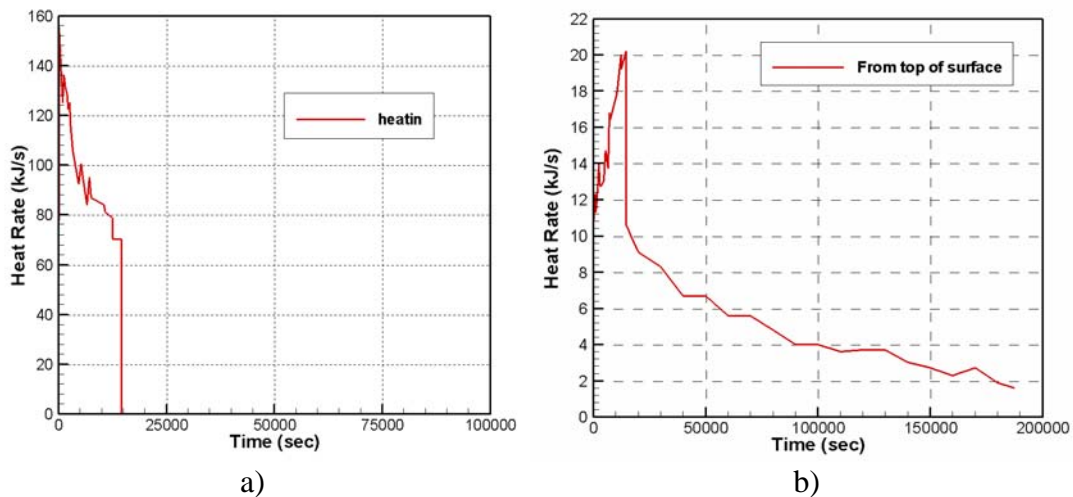


Figure 11: Heat rate: a) through the pipe wall; and b) on free surface

We denote as boundary conditions 1 (BC1) the case (Figure 12a) when transient heat losses are uniformly distributed along vertical and bottom vessel walls and are obtained from GOTHIC lumped parameter simulation (Section 2.1). In case of boundary conditions 2 (BC2), the thermal conductor which represents vessel side wall is connected with the lab (Figure 12b). In this case, the heat transfer between the side wall and the lab is simulated by a built-in heat transfer models in GOTHIC. Boundary conditions 3 (BC3) correspond to the case (Figure 12c) when heat loss through the bottom and side walls of the vessel to the lab are calculated by built-in model in

GOTHIC. In order to span the thermal conductor into the sub-volumes the conical bottom is been changed to a flat plate.

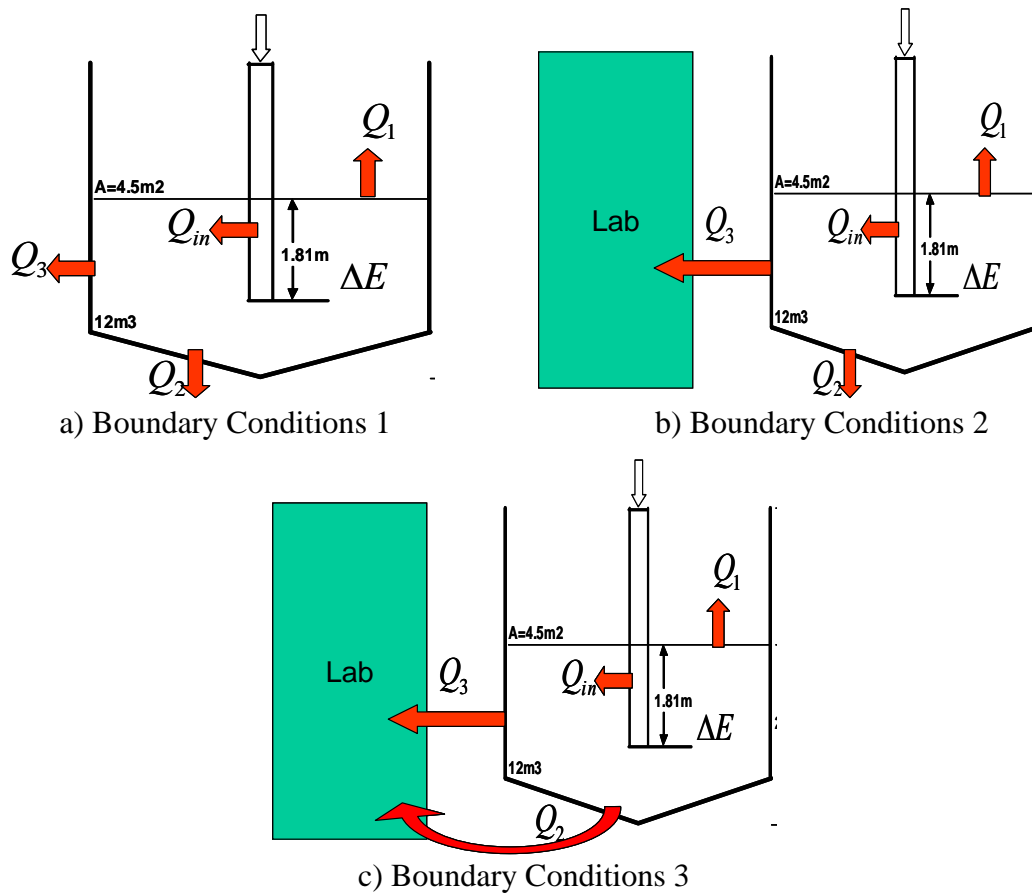


Figure 12: Schematics of boundary conditions BC1, BC2 and BC3

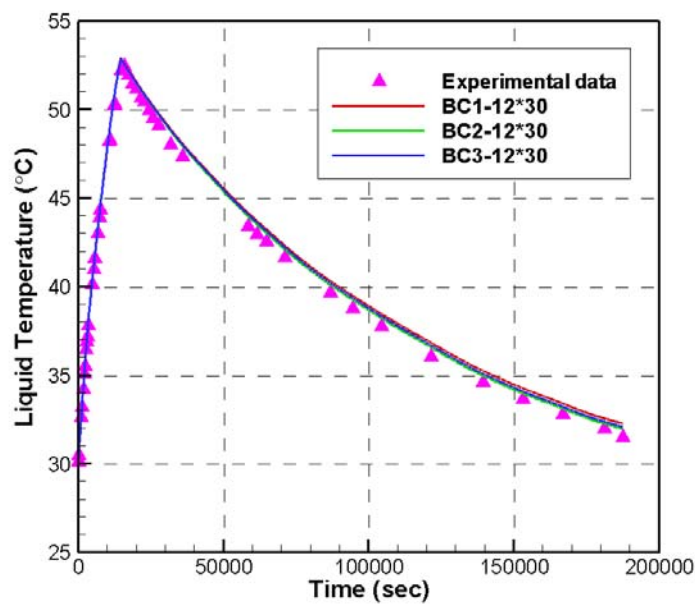


Figure 13: Averaged liquid temperature with different boundary condition

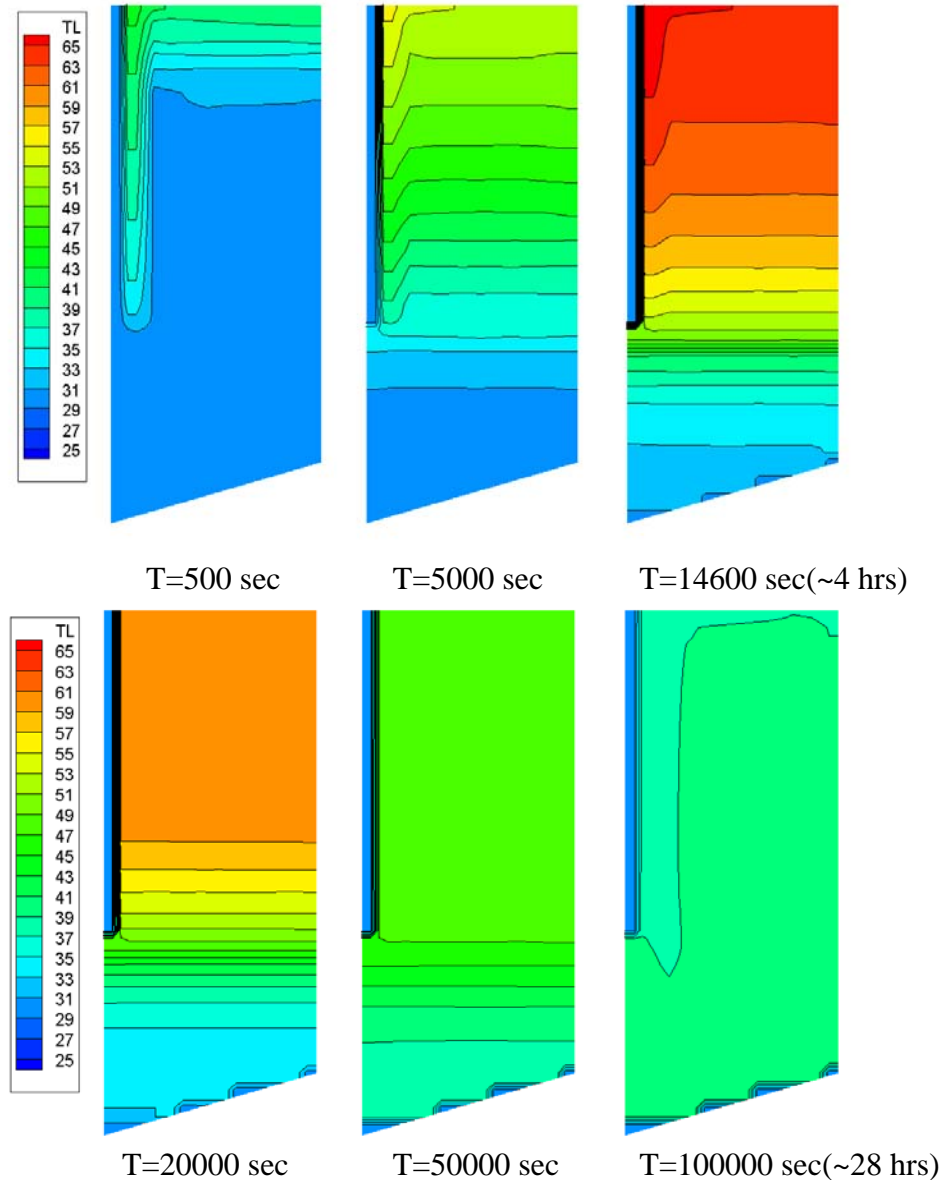
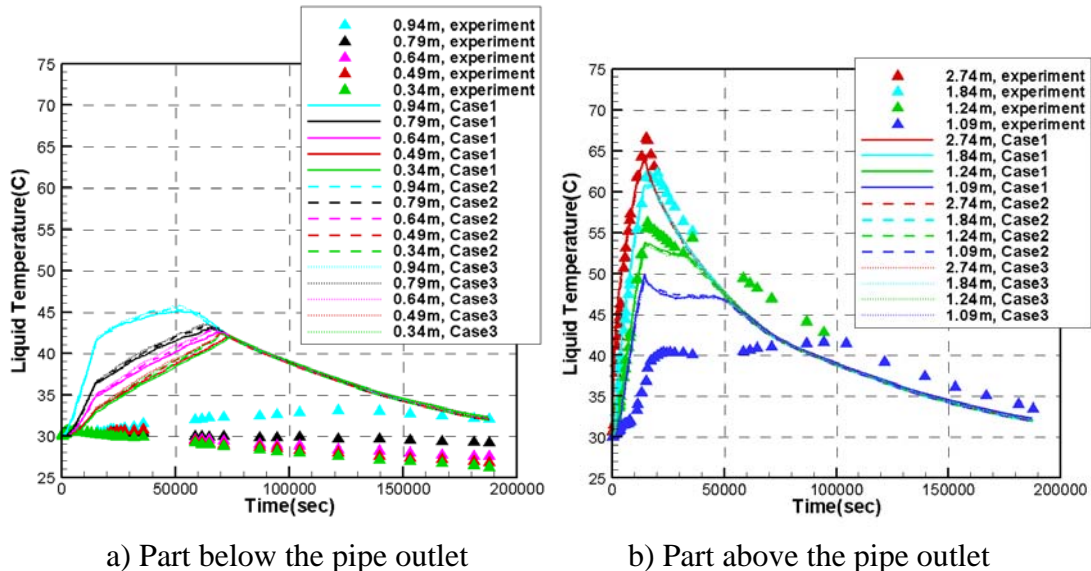


Figure 14: Temperature distribution in the pool calculated with BC1 and grid with 12x30 cells

The transient time for simulation is in total 187600 seconds (~52 hours). The computational time for simulations with different boundary condition is about 5 hours on a PC Pentium IV with 2.8 GHz processor. In Figure 13, we can see that the average liquid temperature is almost the same with different boundary conditions. It implies that the heat loss calculated with subdivided volume and with lumped parameter volume has almost identical effect in all considered cases.

The predicted temporal evolution of spatial temperature distribution in the pool is shown in Figure 14. Both heating and cooling phases of the experiment are presented. Development of hot layer on top during the heating phase and formation of isothermal layer in cooling phase are clearly visible even on the relatively coarse grid with 12x30 cells.

Figure 15 shows the temperature distribution predicted with different boundary conditions. There is a slight difference in the temperature distribution below the pipe outlet (Figure 15a). In that part, simulation with boundary condition 1 (BC1) has predicted slightly (less than 1 °C) lower temperature than that with the other boundary conditions for cooling phase. The reason is that the imposed heat flux using for BC1 has been obtained from lumped parameter simulation in which uniform temperature has been used. The real heat loss through the bottom wall should be smaller than that predicted with BC1 because liquid at the bottom layer is colder compared to the average liquid temperature used in BC1.



a) Part below the pipe outlet                      b) Part above the pipe outlet  
Figure 15: Temperature distribution in the simulation with different boundary conditions and comparison to experiment.

Simulations with built-in model in GOTHIC for thermal conductors are closer to reality. Since heat loss from side wall and bottom wall is quite small compared to the heat loss from the top free surface, the resulting difference due to the boundary conditions on the side and bottom walls is insignificant. The flat bottom can also be used to simplify the modeling for complex bottom geometry. Figure 15 also shows that using the flat bottom instead of the conic bottom in the boundary condition 3, has no significant effect on the simulation results.

Considerable over-prediction of temperature in the bottom layer is probably due to coarse grid resolution in the simulation. Effect of grid resolution is systematically addressed in the following section.

#### 2.4.2. Sensitivity to Grid Resolution Study

In the previous section of the report, 2D simulation in GOTHIC with grid 12×30 has been performed with different boundary condition and compared to experimental data. Although most of the simulation results show thermal stratification development and good agreement with measurement, still some deviations from experimental data has been observed in the bottom layer of tank. A probable reason is the excessive numerical diffusion in the simulations on coarse grids. In order to investigate

influence of numerical diffusion on simulation of thermal stratification, four grids with sequentially doubled space resolutions are used in GOTHIC for 2D simulations. The coarse grid resolution is  $12 \times 30$  with mesh size 0.1 m. Other tested grid resolutions are  $24 \times 59$  with mesh size 0.05 m and  $48 \times 118$  with mesh size 0.025 m. The finest grid resolution is  $48 \times 236$ , since a grid with  $96 \times 236$  is too computationally expensive to run.

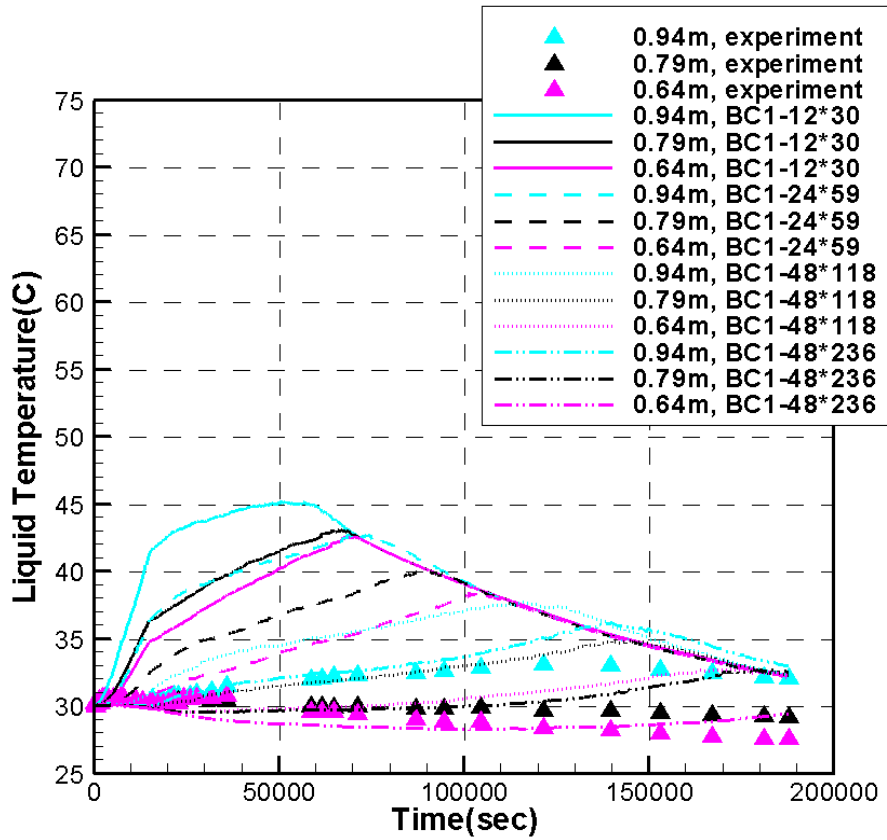
Since the simulation results is found to be insensitive to boundary conditions (see previous section), only the boundary condition 1 (BC1) with four fixed heat fluxes has been used for the grid sensitivity study.

From Figure 16, we can see the results with different grids scheme. Figure 15a shows the temperature distribution in the bottom part, i.e. below the pipe outlet. Results with grid  $48 \times 118$  and grid  $48 \times 236$  overlap each other in this part. This is an indication that grid resolution in horizontal direction has no big influence on the temperature distribution at the bottom of the tank. Results obtained with grid  $48 \times 118$  and  $48 \times 236$  are in much better agreement with the experimental data if compared to that obtained with other grids. The calculated temperature in the position of 0.64 m is close to the measured value. The temperature in the position of 0.94 m is over-predicted on the grid  $48 \times 236$  by  $\sim 3$  °C in comparison with the experiment. Such results confirm that the numerical error due to coarse grid in the bottom can be considerable in simulation of the thermal stratification development. Reasonably fine grid can help in reduction of numerical diffusion during simulation.

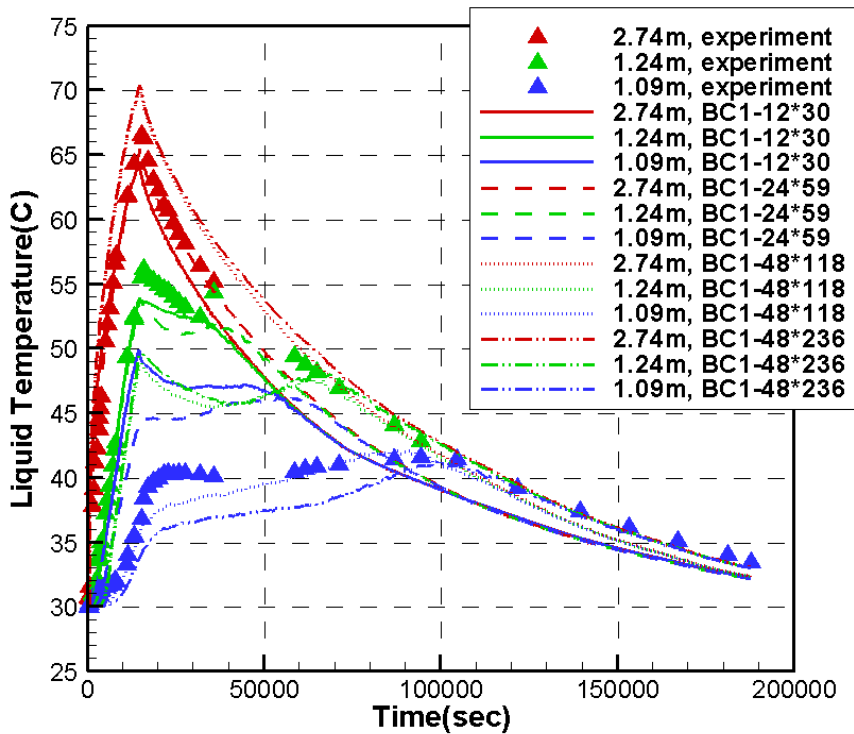
Figure 16b shows that some of the simulation results obtained on fine grid over-predict temperature gradient in the upper layer compared to the experimental data. The figure also shows temperature distribution above the pipe outlet. The temperature at 1.09 m, which is almost in the same plane with the pipe outlet, is higher with coarser grids than in the experimental data, and it is lower with grid  $48 \times 236$ . The calculated temperatures at 2.74 m with fine grids  $48 \times 118$  and  $48 \times 236$  are higher than in the experimental data, while coarser grid gives better agreement with the experimental data.

Another possible reason for the difference between simulation with finer grid and the experiment is that the momentum introduced by injected steam is ignored in the simulation. Although the steam has been totally condensed within pipe, the hot condensate coming from outlet of pipe can still introduce momentum in the liquid pool. This momentum is not taken into account to reduce possible computational expenses related to the resolution of free surface of liquid. On the other hand, there is a short period of venting and chugging in the blowdown pipe at the beginning of the experiment [9] and this could also introduce some initial momentum in the pool. Such momentum could result in partial mixing and decreases the top layer temperature while increases the middle layer temperature.

Same phenomenon can be observed in Figure 17, in which liquid temperature along height of pool is shown. Simulation results obtained with the finest grid  $48 \times 236$  for the bottom layer of the pool are in a good agreement with the experiment at all three time moments  $t = 14000$ ,  $30000$ , and  $100000$  seconds.



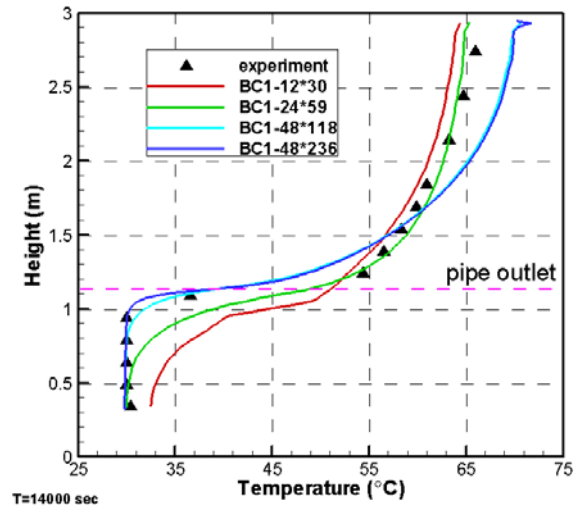
a) Pool layer below the pipe outlet



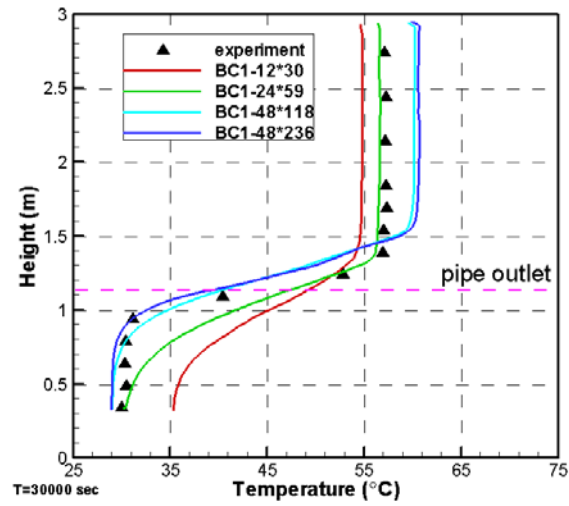
b) Pool layer above the pipe outlet

Figure 16: Temperature distribution obtained with different grid resolutions

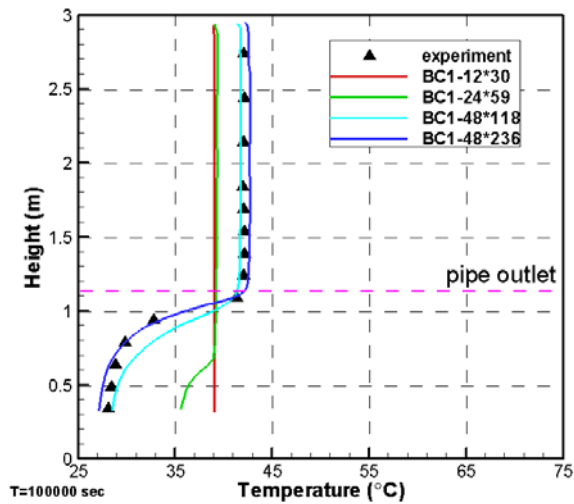




a) T=14000 second



b) T=30000 second



c) T=100000 second

Figure 17: Liquid temperature along elevation at different transient time.

At 14000 second (about 4 hours), the temperature distribution obtained with grid  $24 \times 59$  agree with the measured data in the part above the pipe outlet, while simulation with grid  $48 \times 118$  and  $48 \times 236$  over-predict temperature of this layer. Also in the figure, a thin unstably stratified layer at the free surface is visible. The layer is formed by the hot liquid that rises along the pipe wall and spreads over the pool free surface which is cooled from the top. Comparison of GOTHIC prediction with experimental data on temperature distribution suggests that GOTHIC seems to be capable in predicting convective overturning in the unstably stratified layer using  $k-\varepsilon$  turbulence model with sufficient grid resolution ( $48 \times 118$  in Figure 17a, b).

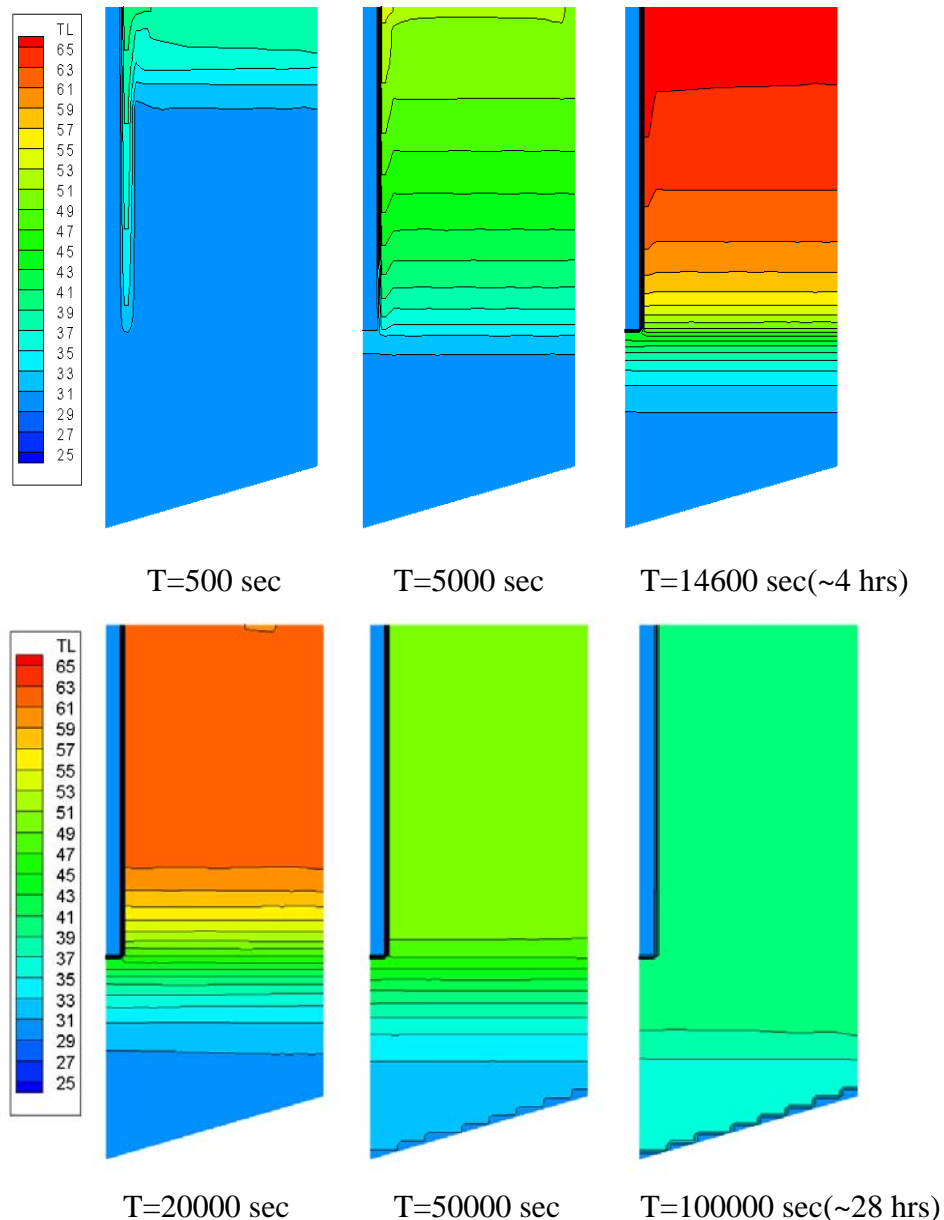


Figure 18: Temperature distribution in the pool grid of  $24 \times 59$

At time 30000 seconds (about 8 hours), a similar behavior can be found and the grid  $24 \times 59$  still shows good capability to predict temperature distribution in the upper layer. At time 100000 seconds (about 28 hours), the temperature distribution obtained with fine grids  $48 \times 118$  and  $48 \times 236$  agree with the measured data well both in the

upper part and the bottom part. The computational time for grid  $48 \times 236$  is about 17 days, while it takes about 5 hours with the coarsest grid.

Spatial distribution of the temperature obtained with different grids is shown in Figure 18 and Figure 19. Considerable improvement of the solution quality on refined grid can be observed at later stages of the transient cooling ( $> 20000$  seconds).

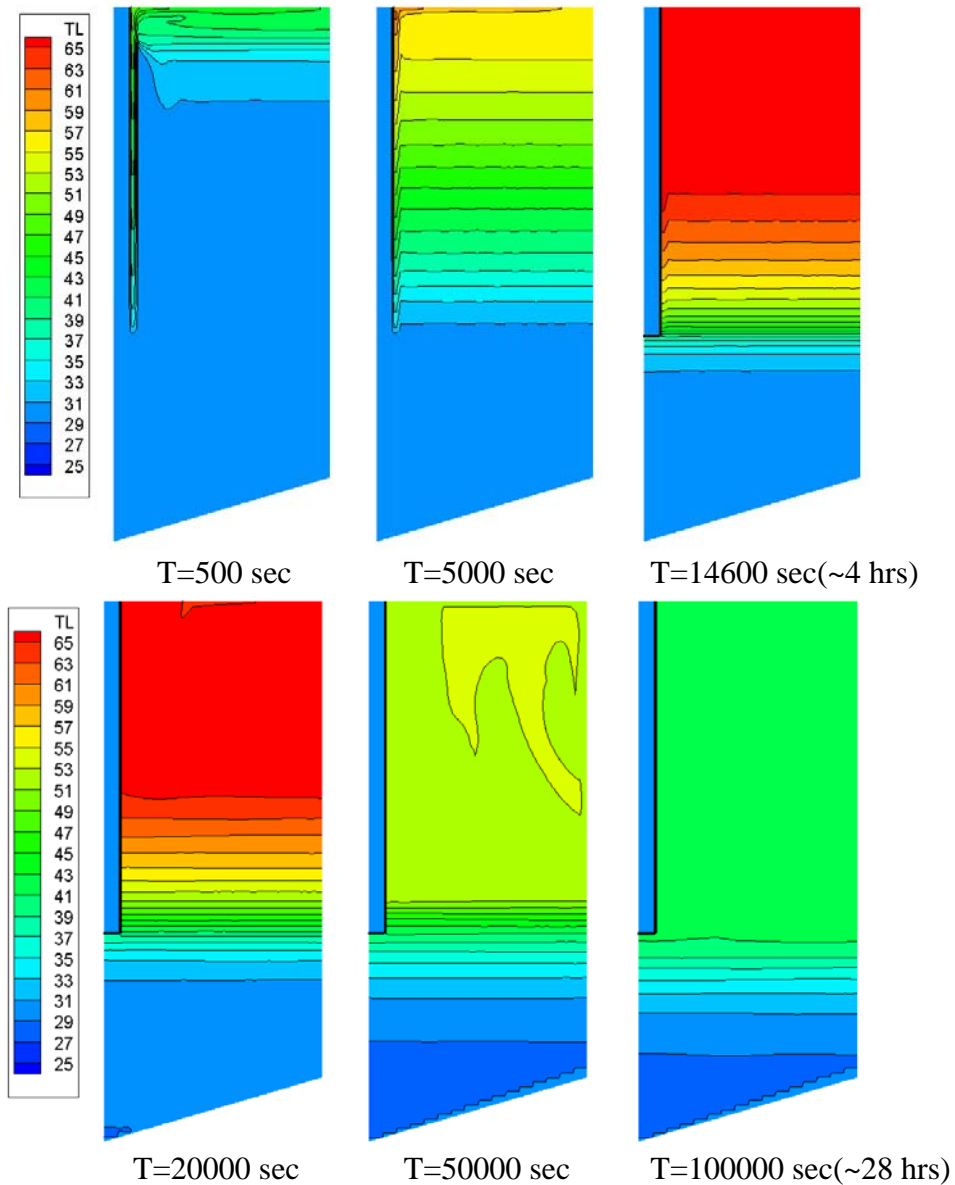


Figure 19: Temperature distribution in the pool grid of  $48 \times 118$

### 2.4.3. Sensitivity Study to Gas Space and Free Surface Modeling

The gas space of the tank has not been taken into account in previous simulation study. If water level increment is not negligible (e.g. as in the STB-21 test) then the gas space and free surface should be considered in modeling.

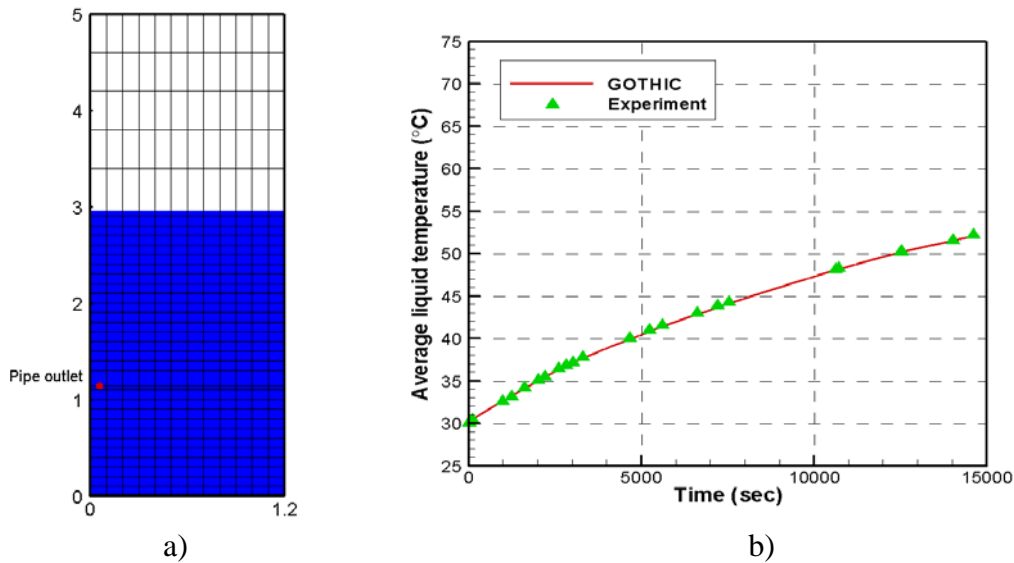


Figure 20: GOTHIC simulations: a) mesh with liquid and gas space; b) comparison of experimental and predicted averaged liquid temperature in STB-20

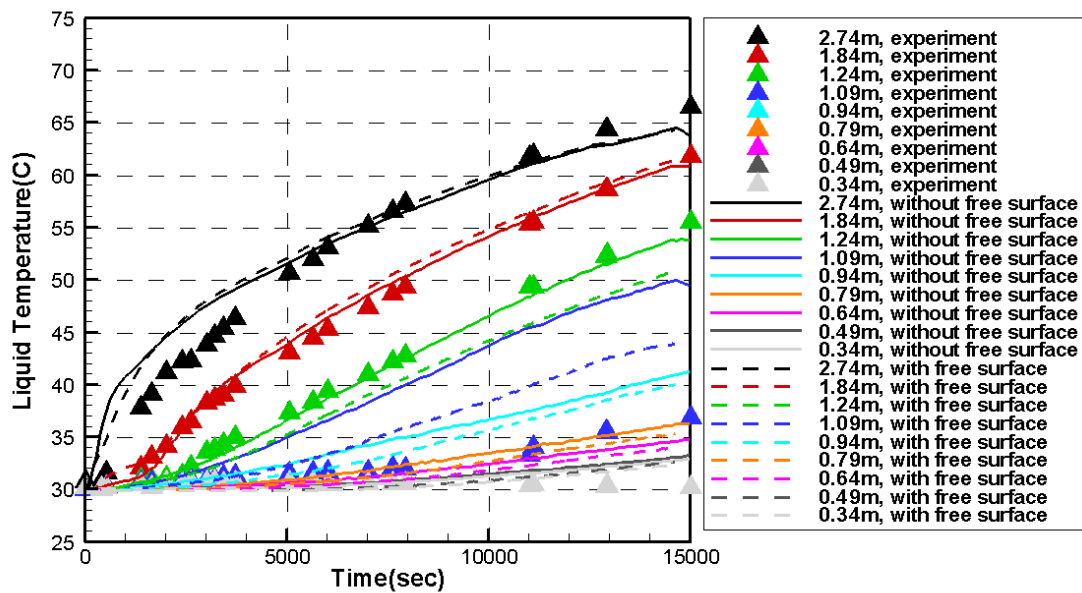


Figure 21: Temperature history in simulation with heat source and with/without pool free surface

Grid configuration with gas space is shown in Figure 20. The water pool geometry is modeled as 2D axisymmetric. The coarsest grid used in the analysis has 29 cells in the vertical direction for the liquid part, 1 cell for the liquid-gas interface, 4 cells for the gas space, and 12 cells in the horizontal direction. The mesh cell size in the liquid part is  $0.1\text{m} \times 0.1\text{m}$ ,  $0.5\text{m} \times 0.1\text{m}$  for the cell with interface, and  $0.4\text{m} \times 0.1\text{m}$  in the gas space of the tank (Figure 20a). Heat conduction through the blowdown pipe wall and through the tank walls is modeled with the GOTHIC models for thermal conductors. In addition, a large size lumped volume that is connected to a pressure boundary conditions simulates the lab atmosphere. Finally, a 3D connector is used to model flow and heat transfer between the lab and the pool in the open tank.

Results presented in Figure 20b suggest that GOTHIC can predict heat losses from the open tank and thus averaged liquid temperature in the POOLEX experiments. The average temperature predicted by GOTHIC models with and without gas space is practically identical.

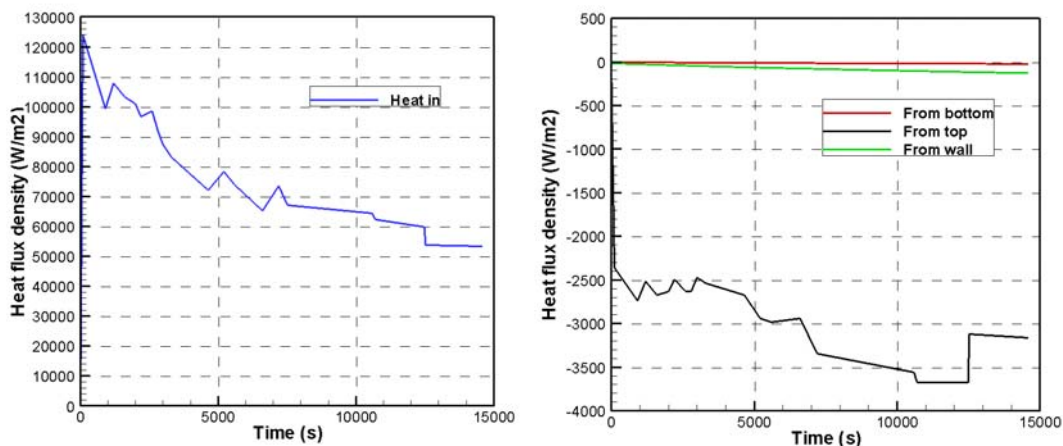
Figure 21 shows good agreement between experimental data for time dependent vertical temperature distribution in the STB-20 and results predicted by the GOTHIC with EHS model and with and without considering the gas space in the tank. Temperature of the very top layer of the pool is slightly overestimated (Figure 21), which can be attributed to the slight underestimation of the momentum in the effective heat source approach.

## 2.5. Application of Effective Heat Source Approach to Prediction of Stratification Development with CFD

A 2D simulation with CFD code, FLUENT, has also been carried out to get additional insight into the physics of thermal stratification development in heating phase and isothermal layer development during the cooling phase.

### 2.5.1. CFD Simulation of Heating Phase of the POOLEX STB-20 Experiment

Similar to the GOTHIC case, the model here is also 2D axisymmetric. However, only the liquid part is simulated and there is no mass influx. Four heat sources are imposed on the four sides of simulated domain and values of them obtained from lumped parameter simulation with GOTHIC are time-dependent, which is an attempt to have conditions similar with the experiment. The heat flux density imposed in this case is shown in Figure 22.



a) Heat influx through wall of tube      b) Heat loss from bottom, top and side wall  
Figure 22: Boundary conditions for heat fluxes

There are some small differences between modeling carried out with FLUENT and with GOTHIC, which generally have small effect on the result. For example FLUENT can use heat flux as thermal boundary condition. In GOTHIC thickness of thermal conductor has to be specified in order to provide a heat flux boundary condition. Heat capacity of thermal conductor in GOTHIC may affect result for short transient during heat transfer. For long quasi-steady transient, influence due to this difference between FLUENT and GOTHIC is negligible.

The transient time of simulation is 14600 and it takes about 25 days of computational time with time step 0.001 sec. The grid is shown in Figure 23. The size is 0.1 m for general square cells above conic bottom. The grid resolution is refined in the vicinity of the side wall, top surface and tube surface. Realizable  $k-\varepsilon$  model, pressure based solver and 1st order implicit time scheme are used in the simulation.

The average liquid temperature compared with the experimental data is shown in Figure 24. The difference is almost 3 degrees at the end of simulation. The reason for this is that geometry of the vessel bottom was approximated by simple conical shape and total water inventory was slightly different from experimental one.

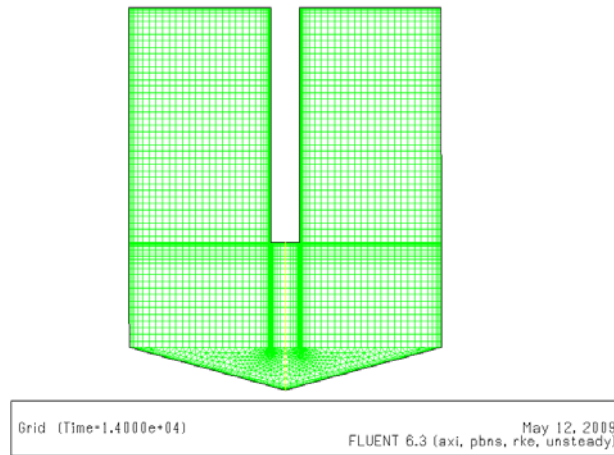


Figure 23: Grid in FLUENT simulation

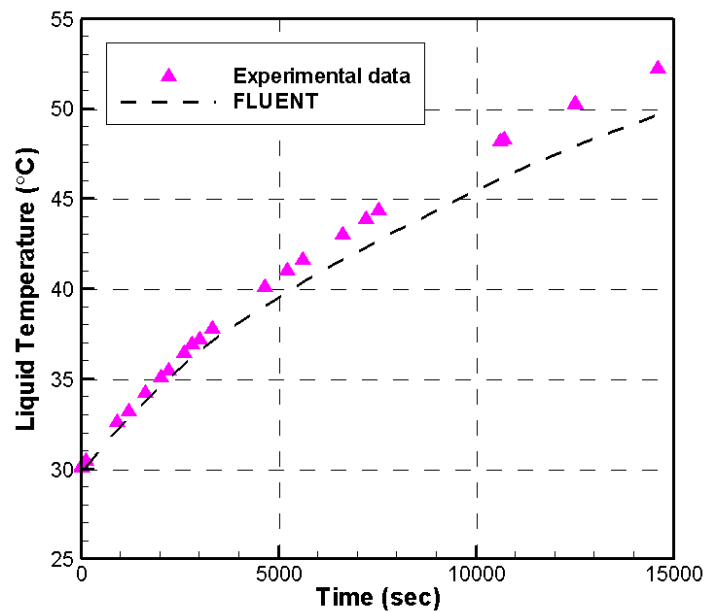
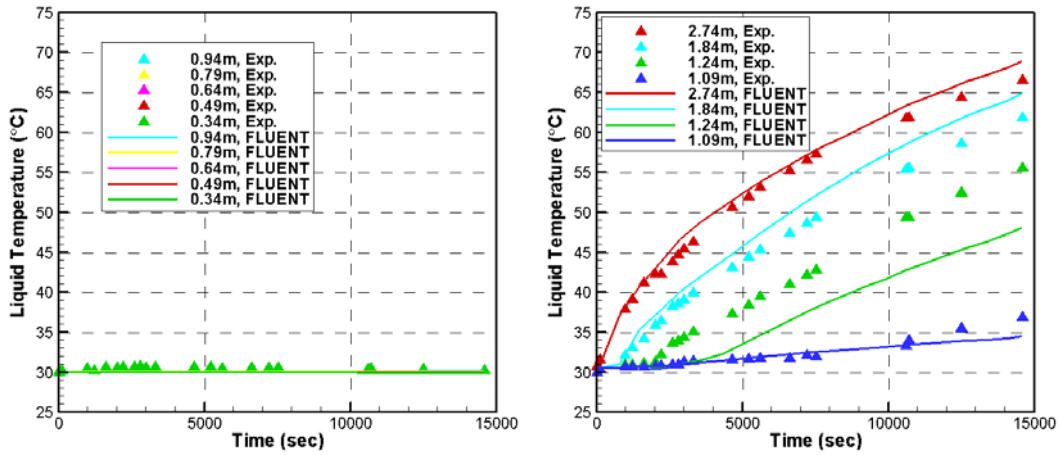


Figure 24: Average liquid temperature compared with experiment

Nevertheless, we can see from the figure of temperature distribution that the results are reasonably good. There is a clear thermal stratification above the outlet of pipe, while the part below the pipe outlet is kept at a constant temperature. Although some differences still exist, for example, the layers close to outlet of pipe. The temperature in this part has increased in the experiment but has not changed in simulation. The temperature distribution with the same position as in the experiment is shown in Figure 25.

Figure 26 shows the velocity magnitude field at 14000 seconds. In the part above outlet of pipe, liquid close to blowdown pipe wall flows upward with big velocity because of buoyancy force that is produced by the heat source. Such motion also

causes horizontal flow at the top surface. Since the heat loss on the side walls of the tank is so small, the downward flow is not strong. In the one isothermal layer, only the radial motion has formed to make the same temperature in the radial direction.

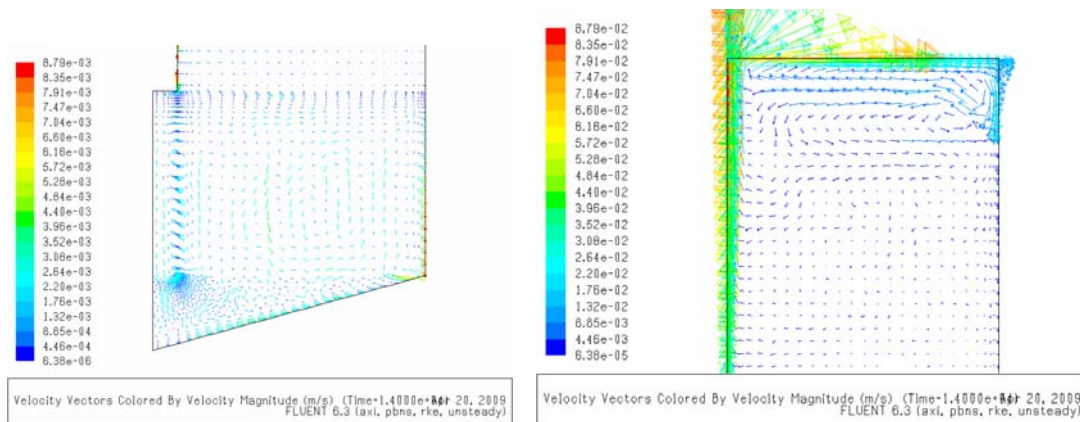


a) Below the pipe outlet

b) Above the pipe outlet

Figure 25: Temperature distribution compared with experiment

The plot in the bottom part shows a circulation. Fluid goes down along side wall and rises up on the other side. Even in the central part, a small circulation has formed. Such circulation ensures mixing in the part that has isothermal layers.



a) Below the pipe outlet

b) Above the pipe outlet

Figure 26: Velocity field at 14000 second

The Figure 27 shows temperature changes with height at 14000 second in transient time. The temperature predicted in CFD in the part below the outlet of blowdown pipe is almost completely isothermal until the layer closed to outlet of pipe. When the layer is higher than the outlet of pipe, the temperature has rapidly increased and stratified. The result of CFD simulation is generally consistent with the experimental data. Compared to the GOTHIC simulation, the CFD simulation shows good agreement in the parts below and above the outlet of the pipe.



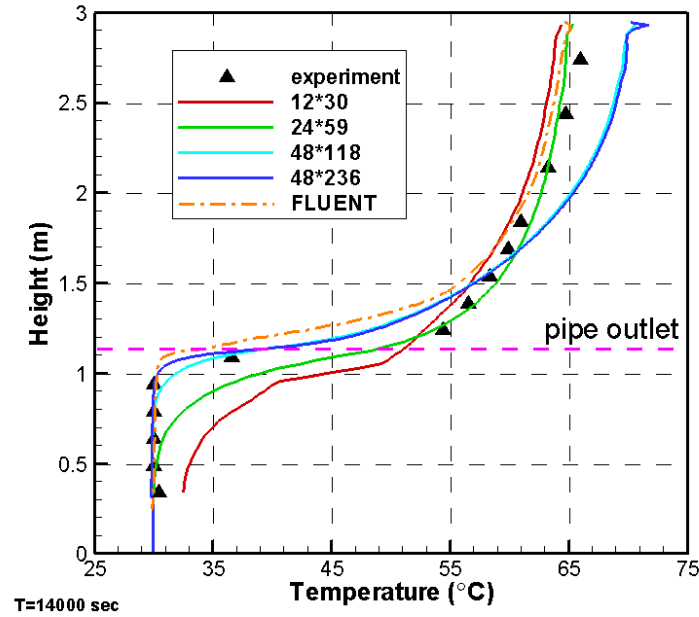


Figure 27: Vertical temperature distribution in the tank

Table 1: Computational efficiency

| Code                                 | FLUENT                          | GOTHIC                 |              |
|--------------------------------------|---------------------------------|------------------------|--------------|
| Computer                             | Intel(R) Xeon(R)<br>CPU 2.00GHz | Pentium IV,<br>2.8 GHz |              |
| Physical time                        | 14,600 s (~4 hrs)               | 187,600 s (~52 hrs)    |              |
| Number of grid cells                 | 3263                            | 48*118=5664            | 48*236=11328 |
| Computation time, days               | ~25 days                        | ~7 days                | ~15 days     |
| Maximum time step, s                 | 0.001                           | 1.0                    | 1.0          |
| Physical/Computational<br>time ratio | 0.06                            | 0.31                   | 0.144        |

### 2.5.2. CFD Simulation of Isothermal Layer Development during Cooling Phase

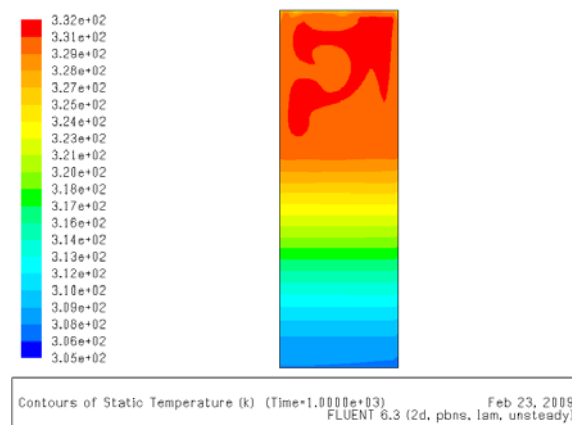
FLUENT is also used to simulate isothermal layer development with heat loss from top surface, side wall and bottom of wall. In this case, a small scale liquid domain with size 50cm×150cm has been used for theoretical analysis and also to reduce calculation time. Heat flux is imposed on the three walls to simulate isothermal layer propagation during the cooling phase in POOLEX experiment. Because steam injection has been terminated, the heat flux from the side of the blowdown pipe is set to zero during the cooling phase. In the calculation, a laminar Boussinesq model and

1<sup>st</sup>-order implicit solver have been used. The grid resolution is 50×150 with square mesh.

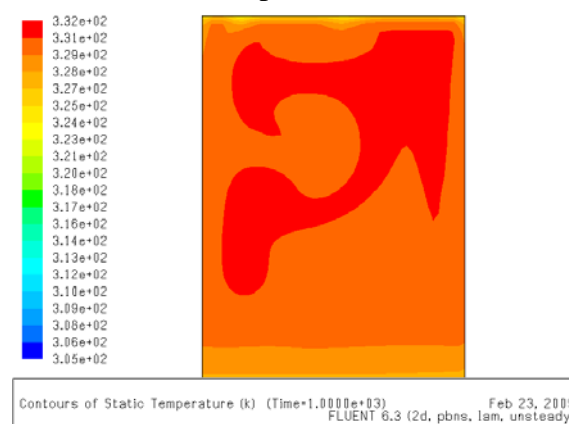
The values for the heat fluxes on the boundaries have also been taken from results of the lumped parameter GOTHIC simulation (Chapter 2.1). The CFD simulation has started from initial conditions with linear increased of the temperature from the bottom to the top. The temperature is 30 °C at the bottom and 75 °C at the top surface.

Figure 28 shows the temperature distribution at the end of simulation, i.e. 1000 seconds. There is an isothermal layer from top to middle, with temperature of about 57 °C. The temperature of the isothermal layer decreases from 75 °C initially, to about 57 °C while temperature at the bottom part has not changed during the transient. The figure shows that there is a small part with temperature lower than the isothermal layer. This is due to a big heat loss from the top to the outside.

Figure 29 shows the vorticity magnitude velocity at 1000 second. From Figure 26b, we can see some small circulation in the part of isothermal layer. This implies how the isothermal layer forms during the cooling process.



a) Whole computational domain



b) Top part of computational domain

Figure 28: Temperature distribution at 1000 second.

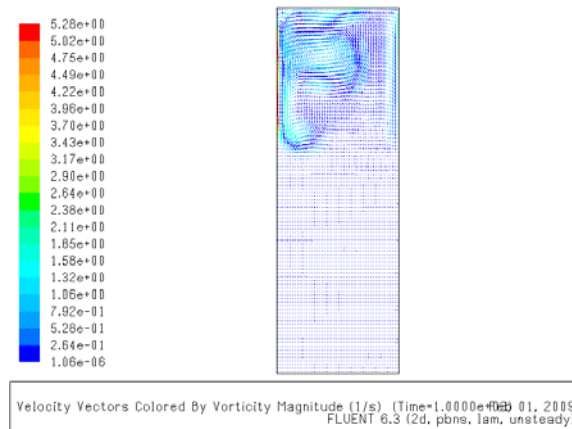
Figure 30 shows temperature change with elevation at different times. We can see the propagation of isothermal layer along with time. Corresponding to the elevation of isothermal layer, the propagation speed of isothermal layer could be estimated by the following equation:

$$v = \frac{dh}{dt} = \frac{\Delta h}{\Delta t} \approx \frac{0.0425}{900} = 4.72 \times 10^{-5} \text{ m/s} = 0.17 \text{ m/hr}$$

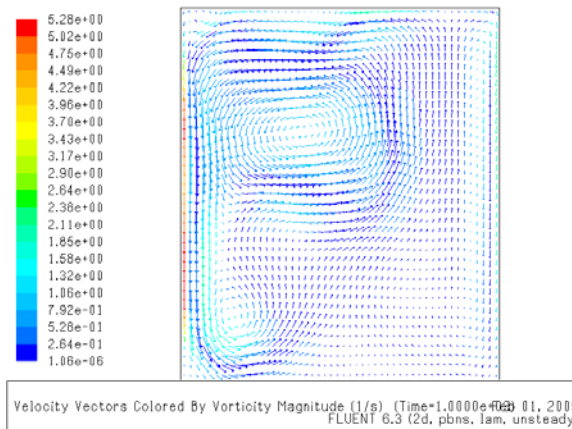
Data from the POOLEX experiment [9] can be used to estimate speed of isothermal layer propagation based on the measured time dependent temperature distribution in the cooling phase. From 20,000 seconds to 37,000 seconds, the isothermal layer goes down from elevation of thermocouple T111 to T107.

$$\begin{aligned} v &= \frac{dh}{dt} = \frac{\Delta h}{\Delta t} \approx \frac{600 \times 10^{-3}}{17000} \\ &= 3.53 \times 10^{-5} \text{ m/s} = 0.127 \text{ m/hr} \end{aligned}$$

Unfortunately experimental data is not detailed enough (e.g. heat flux on the top surface is not measured, vertical resolution of temperature distribution in experiment is 300 mm, etc.) to make accurate comparison with FLUENT simulations for the first 900 seconds. Nevertheless, the propagation speed predicted by FLUENT has the same order of magnitude as the estimated value from experimental data. We can conclude that FLUENT can be used to predict cooling process resolving microscale flow phenomena of the cooling phase.



a) Whole computational domain



b) Top part of computational domain

Figure 29: Vorticity Magnitude velocity distribution at 1000 second.

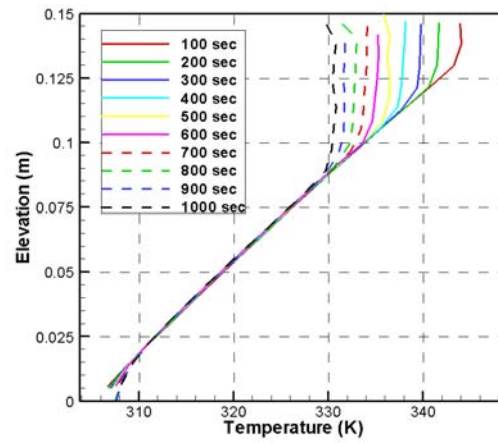


Figure 30: Temperature distribution along with elevation at different transient time.

## **2.6. Application of Effective Heat Source Approach to Simulation of Stratification Development in a Prototypic Size Pool**

In this section we study the issue of scale effect on development of stratification in a prototypical size BWR pressure suppression pool, which is considerably larger than any existing large scale integral experimental facility.

GOTHIC has been used for simulation of a water pool inside closed compartment with 20 m in diameter and 18.3 m in height. The wetwell volume is about 3000 m<sup>3</sup> including 1924 m<sup>3</sup> of water pool about 6 m deep. Injection of steam is provided through four pipes submerged into the pool for 4 m. In the simulation, the total steam flow rate is assumed at the level of 10 kg/s and the steam temperature is assumed to be 100 °C. With such steam injection condition, the ratio of injected energy rate to water volume is about 13.9 kJ/s·m<sup>3</sup>, compared to an average of 9 kJ/s·m<sup>3</sup> in test STB-20 of the POOLEX experiment.

The direct simulation with steam injection into tank has been carried out first. The results do not show any stratification as expected. Taking into account that heat rates per pool volume are close in the case of large scale pool and in the POOLEX STB-20, we use the same EHS approach to simulation of steam injection as it has been used in simulation of POOLEX. In the POOLEX simulations we use effective heat source on the submerged outside surface of the blowdown pipe to simulate steam injection. As shown in Figure 10b, all the steam is assumed to condense inside the pipe and the energy is transferred into the pool through the pipe walls. This approach has been validated against POOLEX STB-20 test and has shown reasonable agreement with the experimental data (see Chapter 2 for more details).

### **2.6.1. GOTHIC Model of a Prototypic Size Pool**

The volume of the water pool is closed therefore heat loss to atmosphere is not considered. The outside surface of the concrete wall of the pool is assumed to be thermally insulated, while the heat absorbed by the concrete wall is considered in the modelling. Three thermal conductors are used to model the heat transfer through the ceiling, sidewall and bottom wall separately.

For direct simulation with steam injection, four blowdown pipes are modeled as volume and the injected steam is supplied by four flow boundaries. The heat transfer through each pipe is simulated by one thermal conductor, as shown in Figure 31.

In the simulation with equivalent heat source, no pipe has been modeled and four spanned conductors are used to simulate the equivalent heat source to water pool.

The schematic of the GOTHIC model is shown in Figure 32. Grid with 9×9 meshes in the horizontal x, y plane and 14 mesh layers in vertical z direction has been used. There are 5 mesh layers for gas space and 9 mesh layers for liquid space. In order to get a detailed temperature distribution in z direction with such coarse grid

configuration, a finer grid with small vertical resolution has been used for the volume filled with water above the pipe outlet.

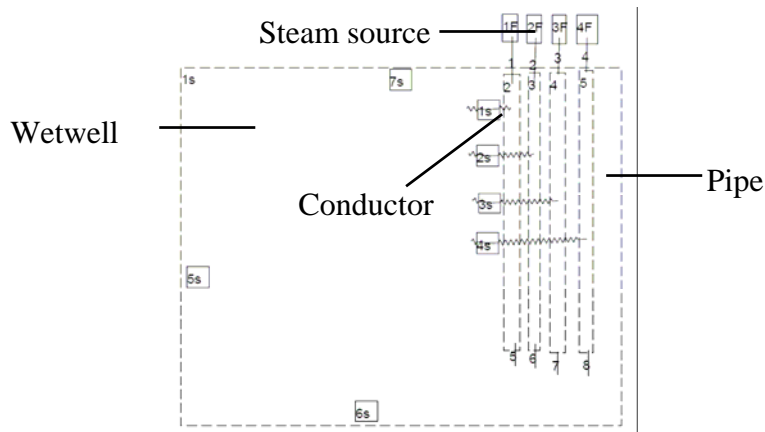


Figure 31: Input models with steam injection in GOTHIC

The initial condition for the water pool is atmospheric pressure and temperature about 20 °C. The injection of the steam starts at time  $t=0$ . The calculated transient time is 30 minutes which takes about 3 hours of computational time with GOTHIC.

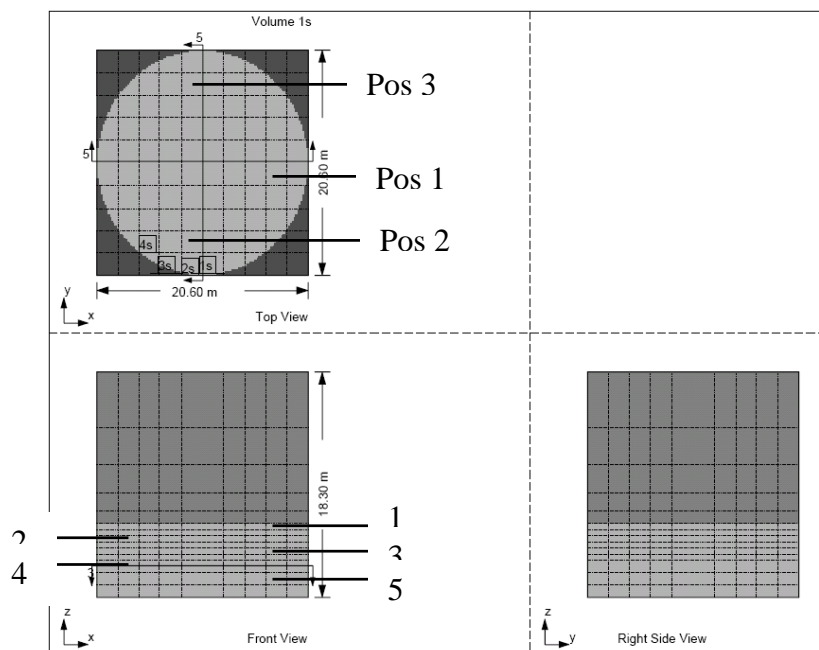


Figure 32: Grid configuration of large scale water pool in GOTHIC (1-5.75m, 2-4.75m, 3-3.75m, 4-2.5m, 5-1.5m)

### 2.6.2. Simulation of Direct Steam Injection into a Prototypic Size Subcooled Water Pool

Simulation of direct steam injection results in mixing of the pool (Figure 33). The temperature in the top layer is a little bit higher than in the lowest layer. It implies that the deficiency of GOTHIC models for simulation of direct steam injection also exists when GOTHIC is applied to large scale pools.

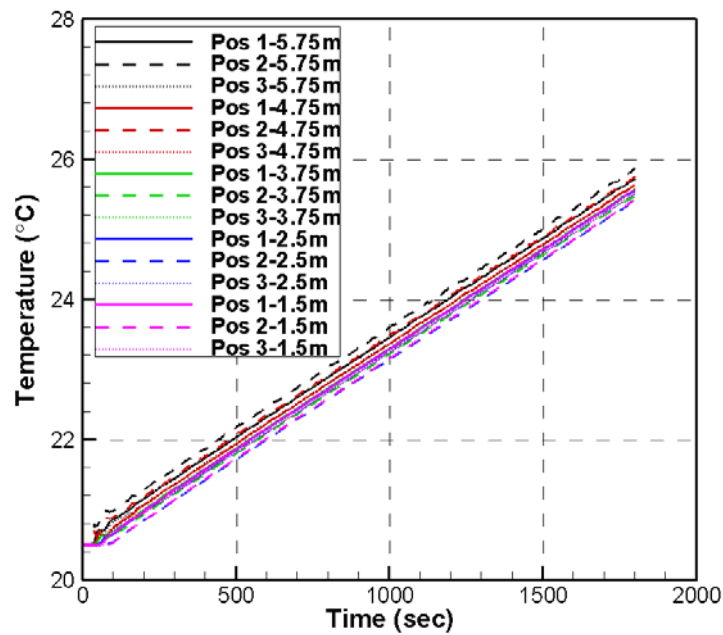


Figure 33: Temperature in the direct simulation with steam injection

### 2.6.3. Simulation of Stratification Development in a Prototypic Size Pool with Effective Heat Source Approach

Figure 34 shows development of thermal stratification during the transient simulation. The lines with same color represent the cell at the same elevation, but in different horizontal locations. Analysis of results suggests that at the same elevation water temperature has almost the same temperature. Thus obtained solution has practically pure 1D vertical thermal stratification as in the POOLEX tests. It means that it should be possible to apply 2D models for study of thermal stratification development in a large scale pool.

It is worth mentioning that the temperature difference between top and bottom layers obtained in GOTHIC simulation is only about 6 °C with 4 m submerged pipe which gives 1.5 °C/m temperature gradient. It is considerably smaller than temperature gradient obtained in the POOLEX STB-20 experiment at the same time after start of steam blowdown 3.9 °C/m (about 7°C with 1.8 m submerged pipe) [9]. Furthermore, temperature gradient in the part close to surface, 2 °C/m with large scale pool, is much smaller than 10 °C/m with experimental scale. This is probably due to coarse grid used in the simulation of large scale pool. Further investigation with fine grid resolution and detailed comparison with actual data is necessary to assess validity of the results and to understand the reasons for such differences between behavior of the integral facility and a prototypical size pressure suppression pool.

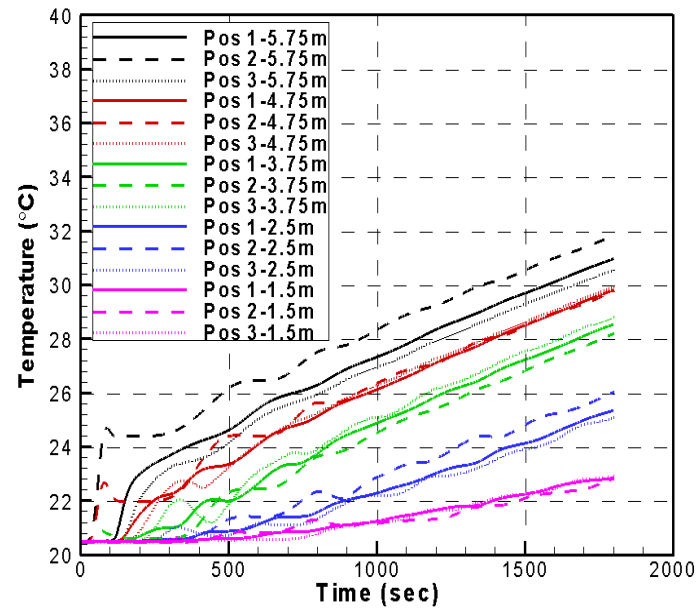


Figure 34: Temperature history in the simulation with equivalent heat source



### 3. EFFECTIVE MOMENTUM APPROACH TO PREDICTION OF MIXING IN A POOL

The important parameter for operation of the pressure suppression pool is time scale for mixing of stratified layers. This time scale defines how fast condensation capacity of the pressure suppression pool can be restored. In this chapter we discuss “effective momentum source” approach to simulation of mixing of initially stratified water pool. Importance of both direction and magnitude of effective momentum for mixing patterns in the pool is identified. It is demonstrated that it is possible to predict time scales for mixing in different layers of the pool if direction and magnitude of effective momentum are properly selected.

#### 3.1. Development and Implementation of Effective Momentum Approach in GOTHIC

In the present chapter we use the GOTHIC code for prediction of 2D mixing phenomena in a pool, and we use concept of effective momentum in order to take into account influence of gas injection into the pool. For validation of the simulation approach we use data on mixing of initially stratified pool in the POOLEX experiment STB-21 [9]. In the experiment with pure steam venting through a vertical pipe the thermal stratification formed in the pool during first stage of the experiment (4000 sec) at low steam flow rate. The established stratification is broken in around 600 seconds after rapid increase of the steam flow rate [9] (Figure 35).

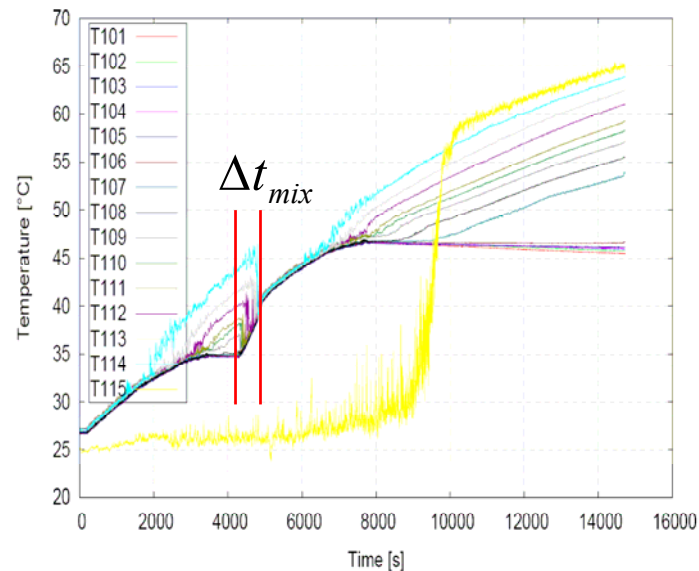


Figure 35: Temporal history of vertical temperature distribution in STB-21 [9]

Calculation of effective momentum for the case of steam venting through a vertical tube into a subcooled water pool is still an unsolved problem. Direction of effective momentum due to steam injection can change rapidly from downward to upward. Large scale motion of steam-water surface and buoyancy effects in small bubbles may counteract. Depending on steam mass flow rate and pool subcooling the steam

injection can be in different unsteady oscillatory regimes [45]. It is impossible at the moment to simulate directly such kind of oscillatory regimes in GOTHIC due to lack of appropriate models and closures. Also effect of small bubbles generation and collapse on effective momentum has to be investigated.

In the present work we use parametric simulations study with GOTHIC code and comparison with POOLEX STB-21 experimental data to investigate: how magnitude and direction of effective momentum can affect time scale for the pool mixing.

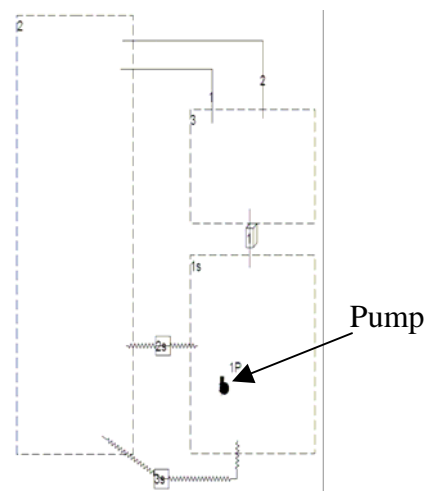


Figure 36: GOTHIC code model used for simulations with effective momentum simulated by pump

Figure 36 depicts open tank of the POOLEX facility and positions of thermocouples as well as the model used for GOTHIC simulation. The pool is modeled as distributed parameter volume 1s with 2D axisymmetric system. The vapor part (volume 3) and lab (volume 2) are represented with lumped parameter model. The approach to modeling of mixing phenomenon is the same as in the modeling of STB-20 of POOLEX. That is, heat source is used instead of modeling of direct steam injection. Heat rate calculated in STB-20 is used in the modeling in order to develop thermal stratification in the pool. To provide effective momentum induced by the steam injection, a pump (1P) has been added in the flow path 3, which connects two adjacent computational cells close to the outlet of the blowdown pipe. Thermal stratification has started to develop in the part above pipe outlet at the beginning. After 2000 sec, the pump is switched on to simulate the effect of the increased steam flow rate, whereas in STB-21 test, the steam flow rate has increased suddenly after 4000 sec.

### 3.2. Feasibility Study of Effective Momentum Approach in GOTHIC by Comparison with STB-21 Test Data from POOLEX

Figure 37 and Figure 38 show how mixing progress in different layers at upward and downward directed effective momentum provided by the pump. In Figure 37, the temperature in the lowest layer is still low, while above layer temperatures are totally mixed. In Figure 38, the order in which layers are mixed is reversed in comparison to simulation with upward momentum. The mixing began from low part and has propagated to the upper part. With upward momentum, circulation flow was formed firstly in the part above pump, while there is still no big heat and mass exchange between bottom and upper part. With downward momentum, the temperature in the layers below the outlet of blowdown pipe has uniform value because thermal stratification has only occurred above pipe outlet. As the pump is switched on, circulation flow has started from the bottom part. Liquid located on the pump side in the bottom part is pushed down and then rises up in the other side close to sidewall. The temperature of layers below the pipe outlet has immediately increased, to mix with the layer above pipe outlet. At the same time, the temperature in the lower layer above the pipe outlet has decreased to mix with bottom layers. And then the higher layer above pipe outlet has decreased in temperature and mixed with the lower part. The mixing time scale of one layer is defined to be the time of switching-on the pump to the time the temperature in such layer is same with the others. As seen from figure, it took about 36 seconds for bottom layer mixing with upper layer and 121 seconds for upper layer to mix with other layer.

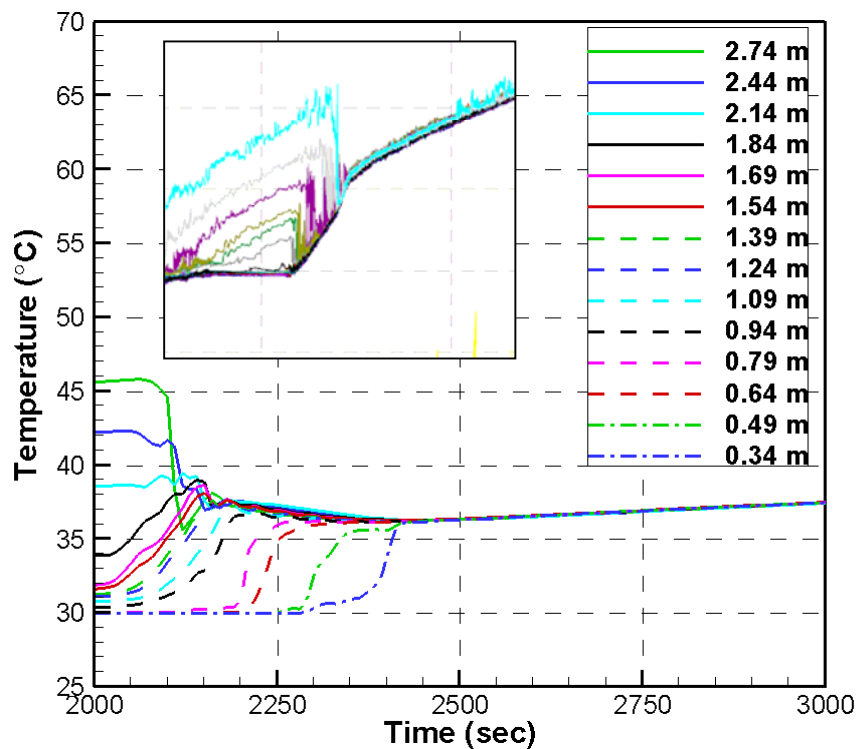


Figure 37: Mixing with upward direction of effective momentum provided by a pump with volumetric flow rate of  $0.0233 \text{ m}^3/\text{s}$  (STB-21 data [9] presented for qualitative comparison)

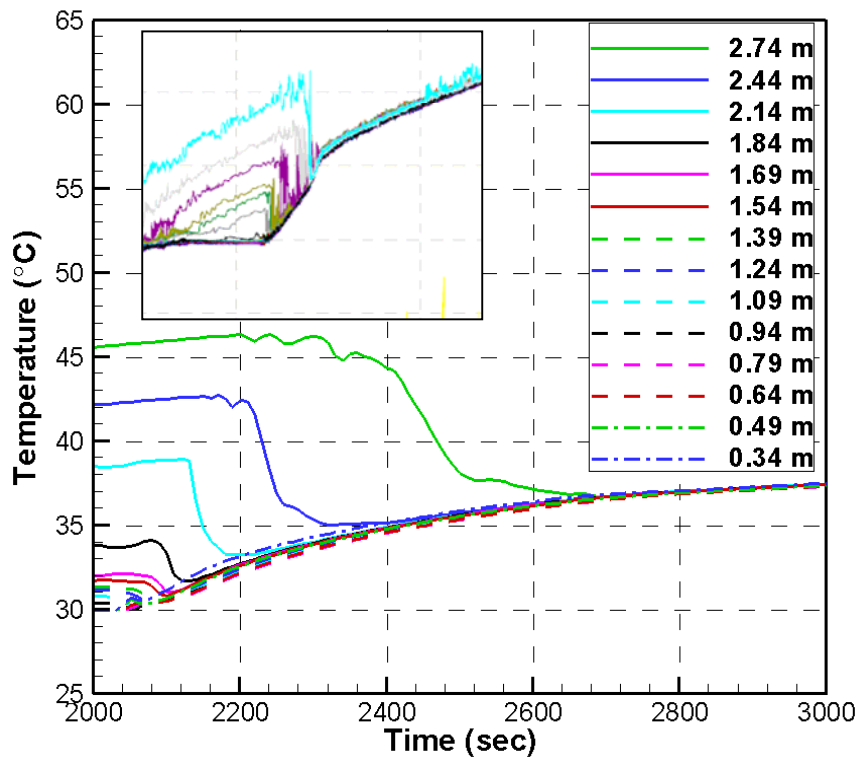


Figure 38: Mixing with downward direction of effective momentum provided by a pump with volumetric flow rate of  $0.0233 \text{ m}^3/\text{s}$  (STB-21 data [9] presented for qualitative comparison)

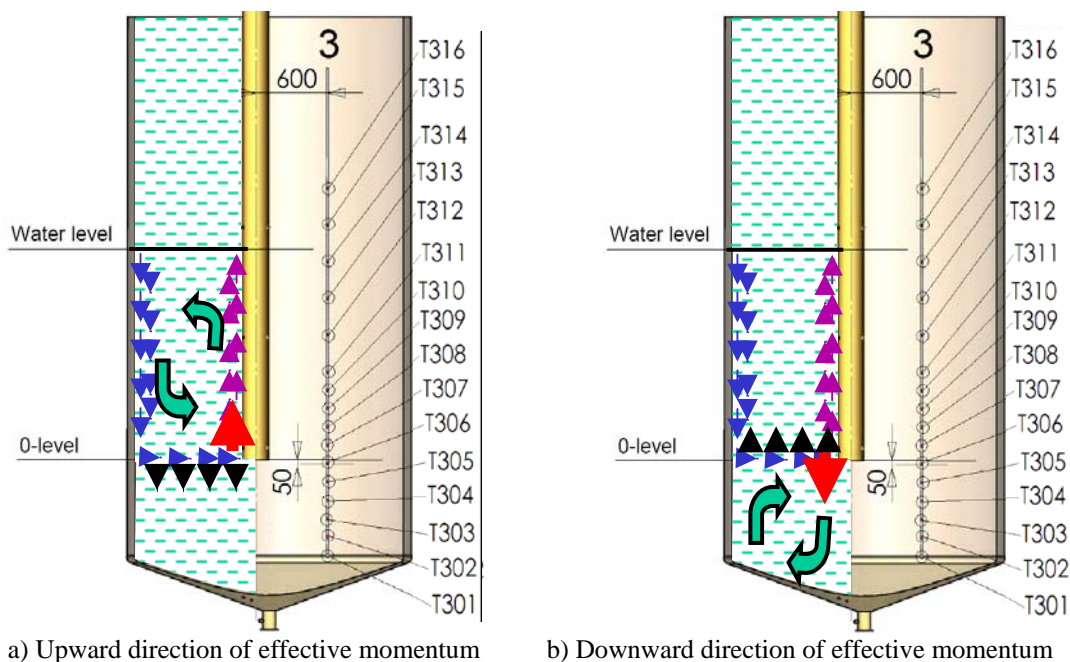
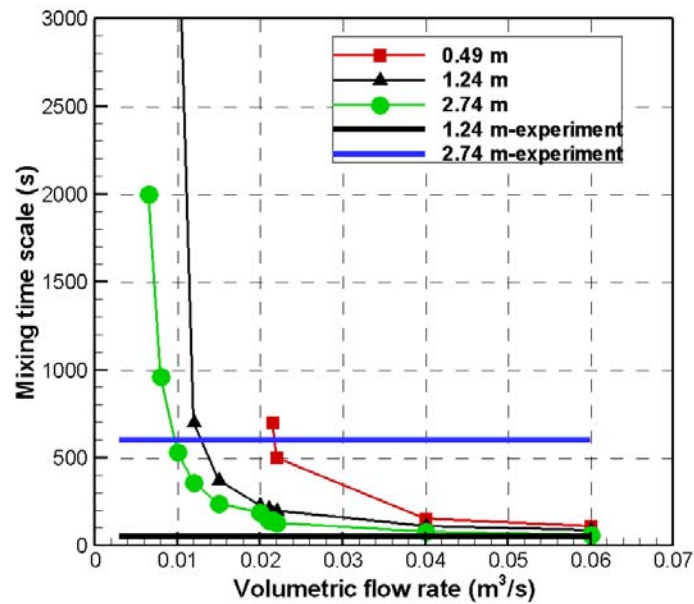


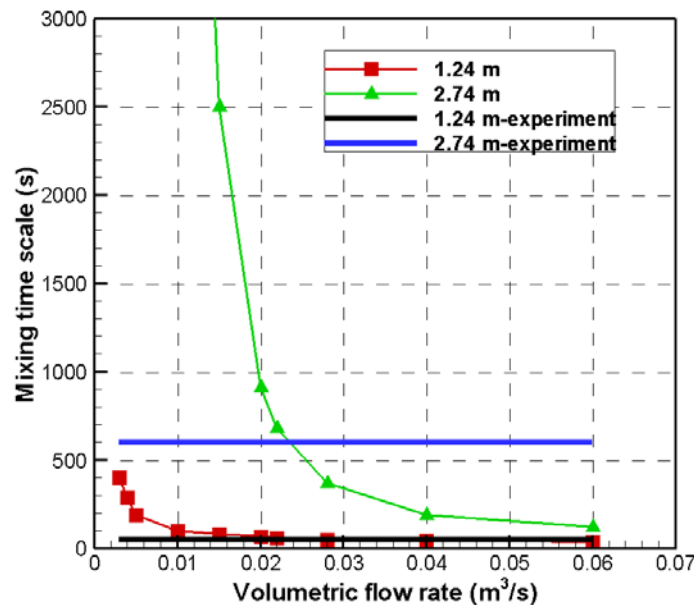
Figure 39: Mixing patterns depending on direction of effective momentum

Figure 40 shows the comparison observed in the STB-21 experiment (two horizontal lines) and calculated time scale for mixing in different horizontal layers of the pool as

a function of the water flow rate through the pump for different spatial orientations of the pump. Time scale for mixing is determined on the base of analysis of unsteady temperature field distribution. Mixing time scale for a layer is defined as time between start of pump (beginning of increased steam injection in experiment) to the point when temperature of the layer becomes the same with a neighboring (from top or from bottom) layer. E.g. “T114-experiment” on the Figure 37 shows the time necessary for mixing of the uppermost layer of the pool with the layer below it (identified by thermocouple T113 in experiment) starting from the injection of increased steam flow rate.



a)



b)

Figure 40: Calculated mixing time scale as a function of the pump volume flow rate: a) upward direction of momentum; b) downward direction of momentum.

Qualitatively and quantitatively different mixing behavior has been observed in the pool with different orientations of the pump and at different pump flow rates. If the pump flow rate is smaller than some threshold, then mixing time scale increases very fast. It is also found that in case of upward orientation of the effective momentum time scale for mixing of the layers above the pipe outlet was less than the time scale for mixing of the bottom part of the pool. And vice versa, if direction of the effective momentum is downward then the time scale for mixing of the bottom layers is smaller than for the upper layers.

Analysis of the Figure 40 suggests that the best agreement with the experimental data for the mixing time scales can be achieved for the downward direction of effective momentum and volumetric flow rate about  $0.0233 \text{ m}^3/\text{s}$ . In this case both time scales for mixing of bottom layer (identified as T107 in the figure) and upper layer (T114) can be reproduced in the GOTHIC simulation.

It is important to mention that steady volumetric flow rate of the pump is higher than volumetric flow rate of the steam in the experiment. From observations of the STB-21 experiment, a chugging regime has been obtained when steam flow rate increased to about  $210 \text{ g/s}$ . Chugging regime has relatively low frequency and high amplitude of pressure and flow rate oscillations. High amplitude flow oscillations in chugging regime can cause significant source of momentum which, in general, can be bigger than momentum estimated for a time averaged flow rate. Velocity of water inside the blowdown pipe can be, in principle, estimated based on temperature variations inside the pipe (Figure 41).

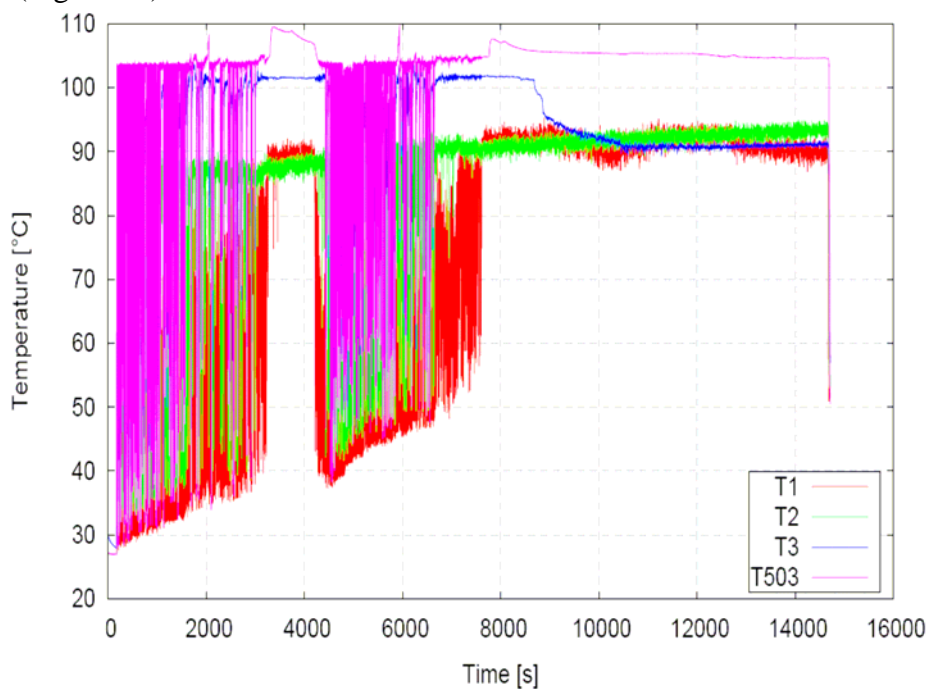


Figure 41: Temperature inside the blowdown pipe in STB-21 during heating phase

## **4. SIMULATION OF PPOOLEX TESTS WITH GOTHIC**

This chapter describes lumped parameter pre-test and post-test simulations for PPOOLEX experiment performed as a part of analytical support to the experimental activity at LUT.

Pre-test simulation results show that drywell and wetwell pressures can be kept within safety margins during quite long steam transients of injection at small flow rates, which is necessary for experiments on development of thermal stratification.

Post-test simulations show reasonable agreement with experimental data. Uncertainty in the experimental data measurements has to be taken into account. Correction of input data (within the ranges of experimental measurement error) for the steam inlet pressure to be at saturation conditions can significantly improve qualitative agreement between experimental and simulation data. More work is necessary for validation of GOTHIC against PPOOLEX data in order to clarify the influence of wall condensation in the drywell on the pressure level in the vessel.

### ***4.1. Pre-test Simulations with Lumped Parameter Model***

The important task in the GOTHIC validation is pre-calculation of the PPOOLEX experiment with GOTHIC. Such simulations can be considered as a “blind” testing for GOTHIC against future PPOOLEX experiment data. PPOOLEX is a closed pool. Pressure inside the pool is the limiting factor in the experiment. We use GOTHIC lumped parameter model to predict the pressure and temperature history during the experiment as a guideline of experiment. It is noticeable that thermal stratification predicted only by distributed parameter may affect actual pressure during the experiment.

#### **4.1.1. Simulation with pressure boundary**

The GOTHIC input for PPOOLEX experiment is shown in Figure 42. Drywell and wetwell are represented by volume 1s and volume 2s (Figure 42). Volume 3 and volume 4 are representing blowdown pipe and the lab correspondently. The large volume of  $10^7 \text{m}^3$  for lab is used. A blockage has also been used to model the real geometry of the drywell and wetwell (Figure 43 and Figure 44).

The table in Appendix 2 includes all parameters used in PPOOLEX calculations.

Six heat conductors are used in the input model of PPOOLEX. Conductor 1 and 2 were for heat transfer from drywell to the lab through the ceiling and side wall. Conductor 3 simulates the heat transfer between the drywell and wetwell and Conductor 4 models the heat transfer from blowdown pipe to wetwell. Conductor 5 and 6 are used for heat transfer from wetwell to lab through the side wall and bottom.

Two boundaries are used in the simulation for PPOOLEX experiment. Boundary 1 is connected to the drywell to supply the steam to inject into the drywell. Pressure boundary 2 is connected to the lab to keep the lab with atmospheric pressure.

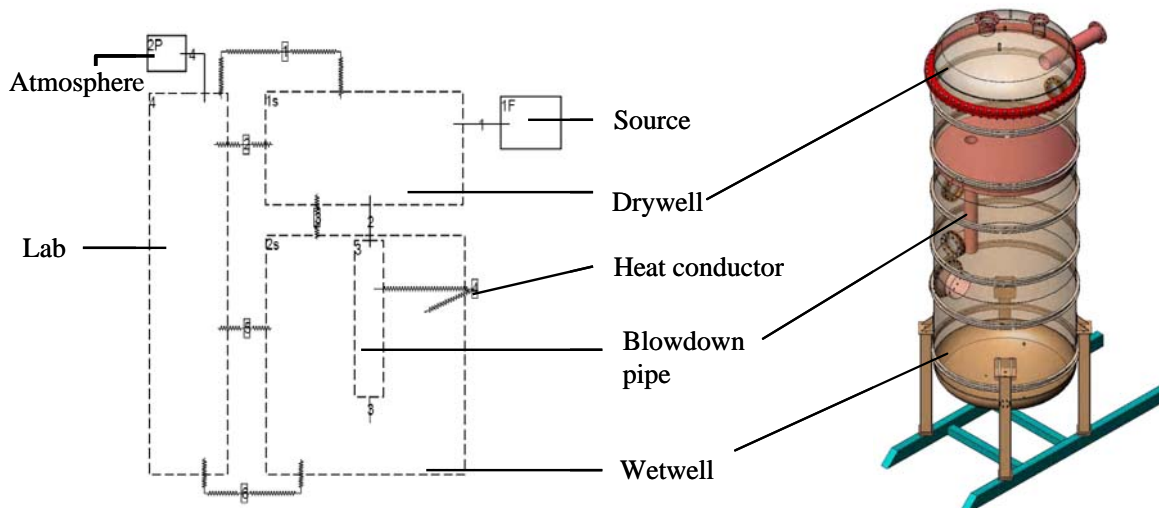


Figure 42: Schematic of PPOOLEX input with lumped parameter model in GOTHIC

In reality, the pressure of drywell increases during steam injection and then pressure of steam generator is controlled to make injection rate constantly. In that case, the steam is always superheated before injected into drywell. However, in the simulation it is difficult to control boundary conditions and change parameters according to the condition of drywell.

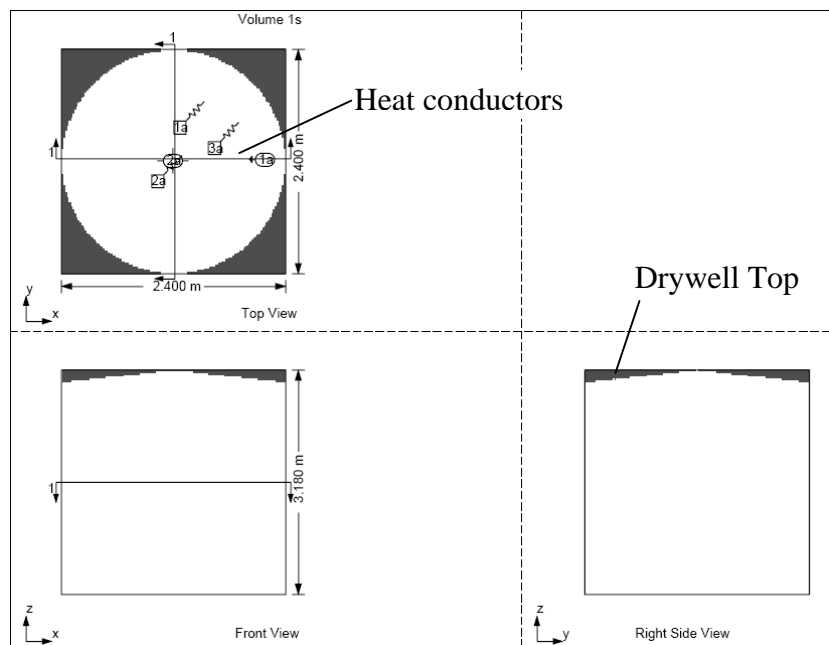


Figure 43: Representation of PPOOLEX drywell geometry in lumped model of GOTHIC

(Detailed information for heat conductors is in Appendix 2)



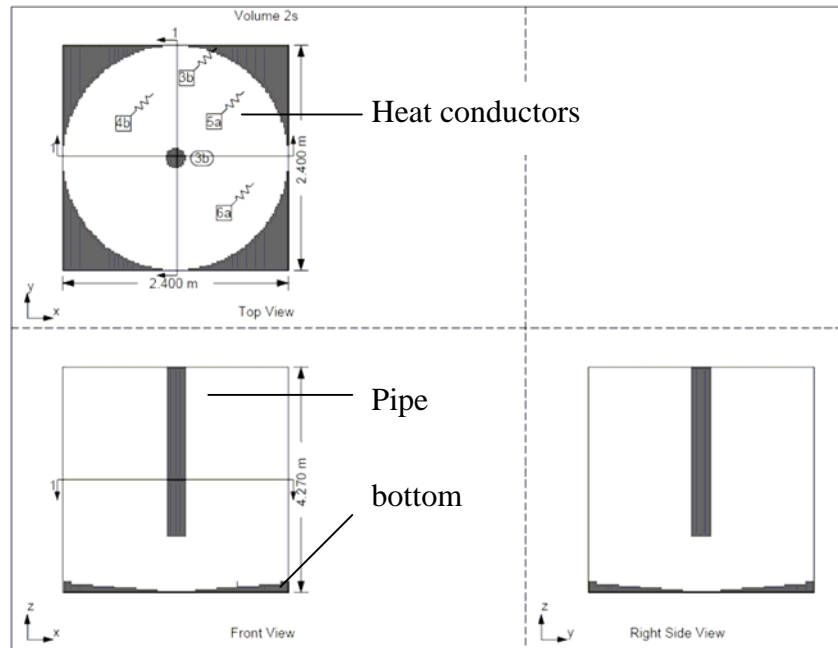


Figure 44: Grid for wetwell of PPOOLEX  
(Detailed information for heat conductors is in Appendix 2)

In order to supply the superheated steam into drywell the pressure boundary is used for boundary 1 and pressure at the steam line is increased from 110 kPa to 340 kPa linearly in time during heating phase. The temperature of injected steam changes from 114 °C to 147 °C linearly. The initial temperature inside the drywell and wetwell is assumed to be 30 °C. The initial temperature in the lab is set to 20 °C.

There is an isolate valve in the flow path which connects the pressure boundary and drywell. Steam injection lasts for 10000 seconds and is terminated by closing the isolate valve. The whole transient time is 160000 seconds.

Significant steam condensation in the drywell and blowdown pipe is observed in the preliminary calculation. Therefore two cases with different conditions are studied:

Case I: With heat transfer between drywell and lab.

Case II: With thermal insulation (zero heat flux at the outside wall of drywell) between the drywell wall and the lab.

#### **4.1.2. Analysis of Results**

The pressure in the drywell is close to the pressure of the boundary condition during the heating phase. Almost all the air in the drywell has impelled into the wetwell through blowdown tube during which hot steam has been injected. The air flows out of the tube and then moved up to the surface and has accumulated at the upper space of the wetwell. During the cooling phase, no steam supply was provided to the drywell. As a result the steam left in the drywell was cooled down and condensed quite quickly. Condensation in the drywell has caused fast pressure dropped in the drywell. The water in the wetwell is then pushed into drywell once the pressure in the

drywell became lower than in the wetwell, until balance of the pressures was established.

Figure 45 shows pressure history during heating and cooling phase. The pressure changes according to the physical picture described above. Since the blowdown tube has submerged, the pressure of wetwell is smaller than the pressure in the drywell. Blowdown tube has the same pressure to drywell, because small friction and loss coefficient is used for flow path connecting the drywell and the tube. In Case II the condensation rate in the drywell slows down because of the insulated outside wall, in comparison with Case I. Therefore the pressure in case II drops down later after injection.

In Figure 46, oscillation for vapor flow rate from boundary to drywell exists in the whole heating phase, even the jump is small for the pressure difference between pressure boundary and drywell and drywell and tube, which is shown in Figure 61 and Figure 62 in Appendix 3. It implies that vapor flow rate is very sensitive to the pressure difference.

Figure 47 shows the liquid to vapor phase change rate during the transient in Case I and Case II. One can see that the condensation rate in drywell in Case II is lower than in Case I. Most of steam is still condensed inside drywell in Case II, although the outside wall of drywell has been insulated. At the end of steam injection, oscillation is found for phase change, especially in the pipe. Such oscillation is consistent with the oscillation of pressure and flow rate. It is difficult to distinguish which one is the cause as they affect each other.

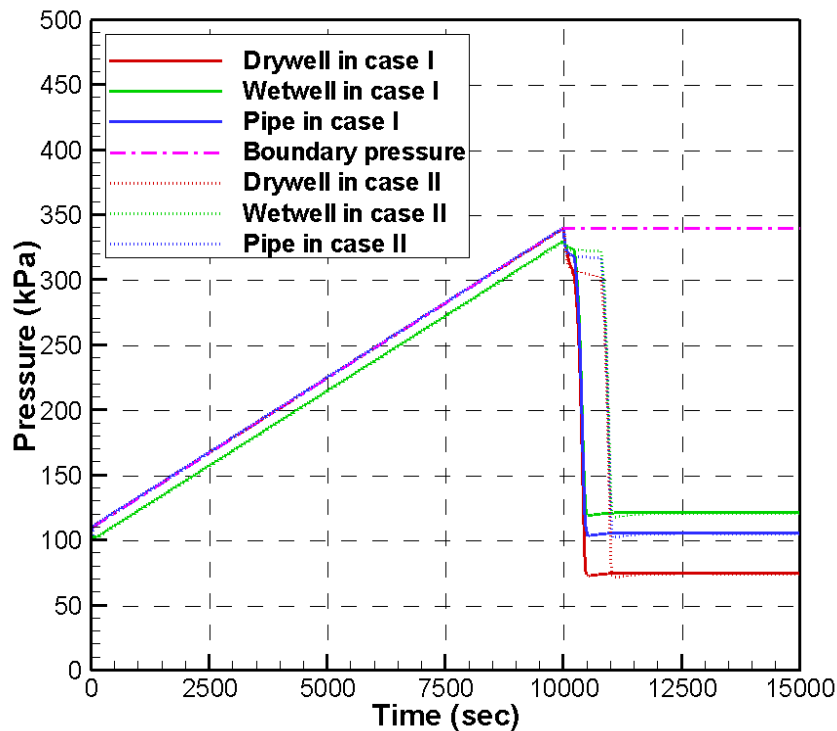


Figure 45: Pressure history in PPOOLEX simulation with pressure boundary condition

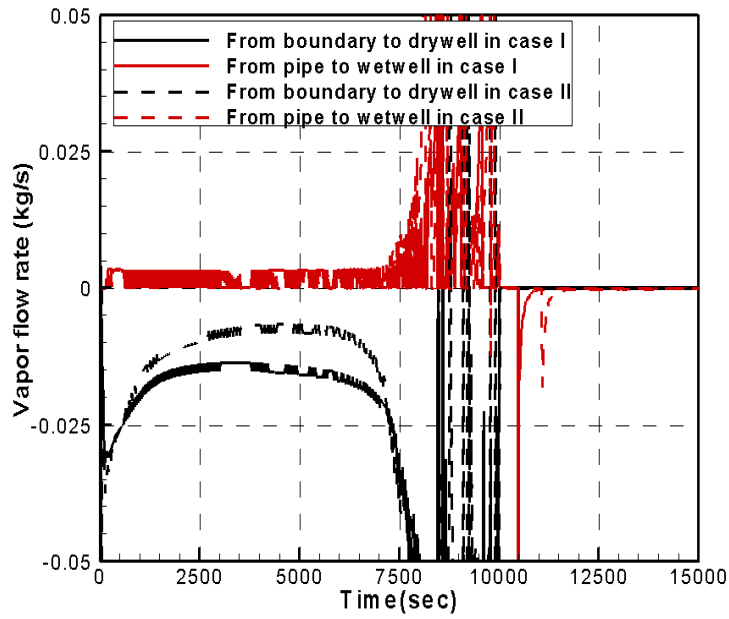


Figure 46: Vapor flow rate in PPOOLEX simulation with pressure boundary condition

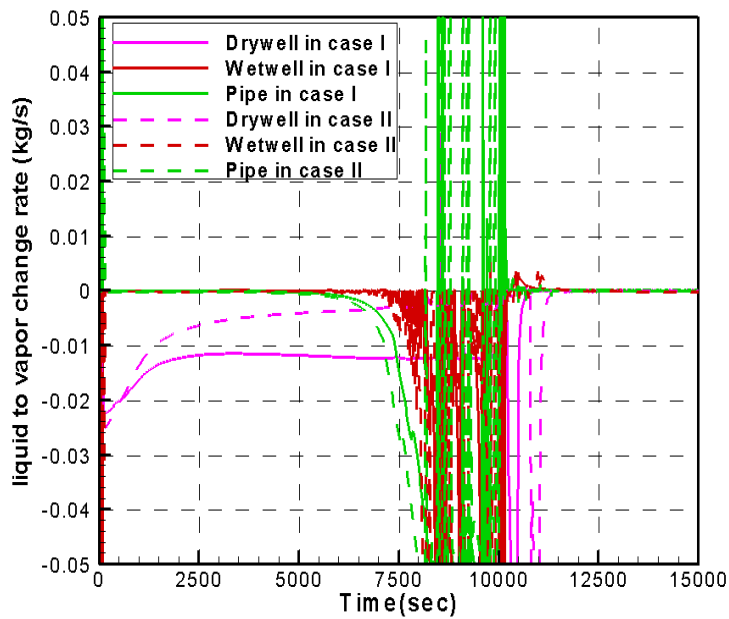


Figure 47: Liquid to vapor phase change rate in PPOOLEX simulation with pressure boundary

Figure 48 shows the history of average liquid temperature. It is instructive to note that the liquid temperature in the wetwell does not increase significantly in Case II in comparison with Case I. However, we know that steam injected in Case II is less than in Case I. That is a possible reason for small change on liquid temperature. If we can

supply large steam flow rate into drywell, it may produce big liquid temperature increasing.

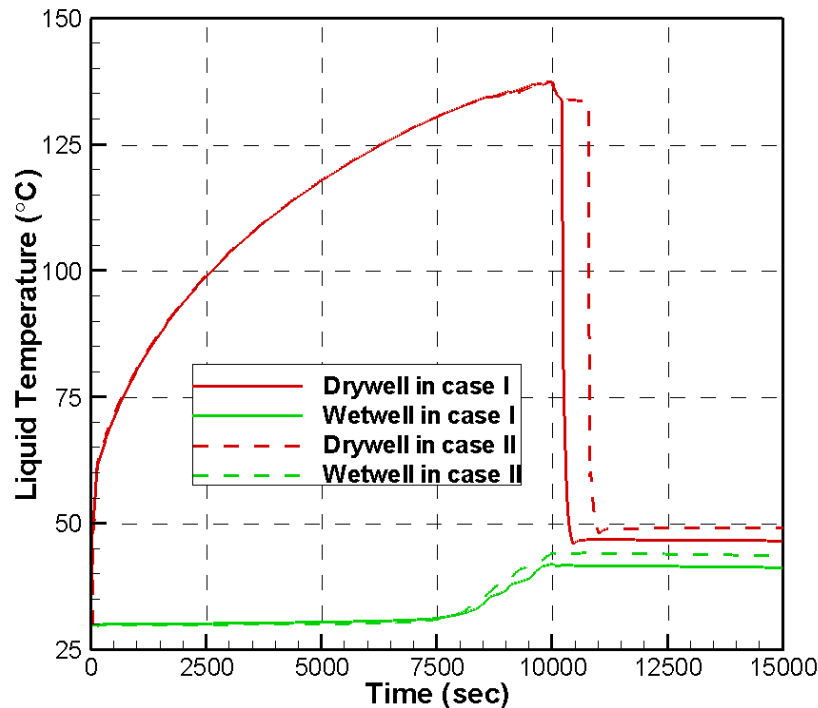


Figure 48: Liquid temperature in the tank in PPOOLEX simulation with pressure boundary

More plots of simulation with pressure boundary are shown in Appendix 3.

#### 4.1.3. Simulation with flow boundary

From the results of simulation with pressure boundary, we can see the flow rate is difficult to control during the steam injection. It is not consistent with the real experiment, in which steam flow rate could be controlled as constant value. Hence, flow boundary is used to supply steam during injection in the simulation.

Although the pressure of drywell has increased during steam injection, the steam flow rate still could be kept constant with flow boundary even the boundary pressure is lower than the pressure in the drywell. The pressure defined in the flow boundary is only used to determine the steam status. However, the big pressure with 187kPa and high temperature with 117 °C as shown in Appendix 2 are preferred to use for flow boundary to supply supersaturated steam at the beginning. The injection rate is 0.026kg/s according to the POOLEX experiment and it lasts 10,000 seconds. The check valve is not needed in the simulation. Other parameters are kept as simulation with pressure boundary.

#### 4.1.4. Analysis of Results

Figure 49 shows pressure in different compartments during the transient. Observed increase of the pressure during first 5000 seconds occurs because air is pushed from the drywell to the wetwell by the injected steam. Analysis of the phase change rates in Figure 50 shows that almost all injected steam has condensed in the drywell at the beginning of the transient. After about 5000 seconds condensation rate in the drywell is decreasing and only half of the steam is condensed in the drywell and the other half in the blowdown pipe.

In the simulation, the liquid temperature has risen up from 30 °C to about 35 °C. The temperature can be increased more if the big flow rate is defined for flow boundary.

There is a difficulty in defining numerical pressure boundary condition which would follow pressure change in the drywell. Therefore some differences between prediction and experimental data are expected.

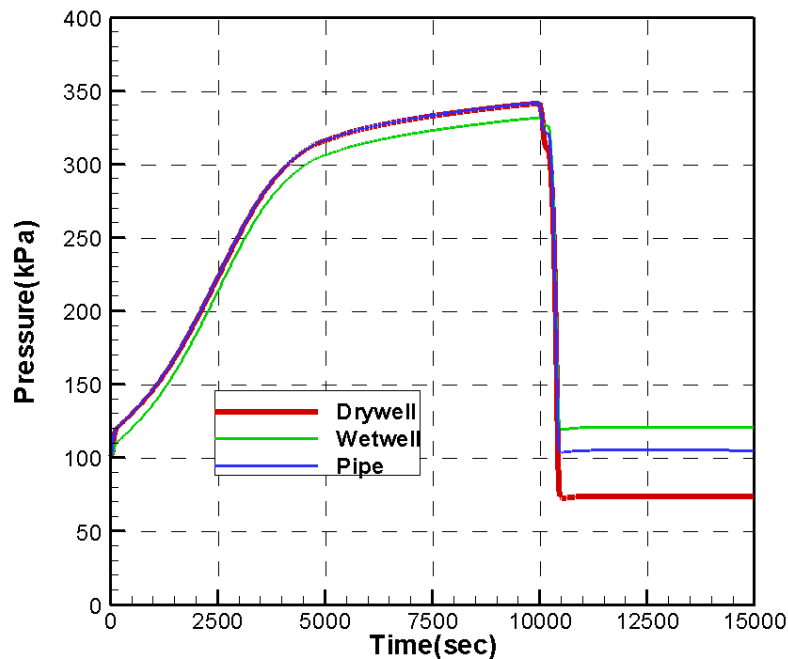


Figure 49: Pressure history in PPOOLEX simulation with flow boundary

More results of PPOOLEX simulations are shown in Appendix 3. From Figure 66 the pressure difference is almost flat during injection. However, there are still oscillations for vapor flow rate from pipe to wetwell, which can be seen from Figure 67. From plot of flow rate in Figure 68, the liquid part phase of the fluid is injected into the wetwell more than its steam part phase. Figure 69 shows the same character of water level with previous simulation.

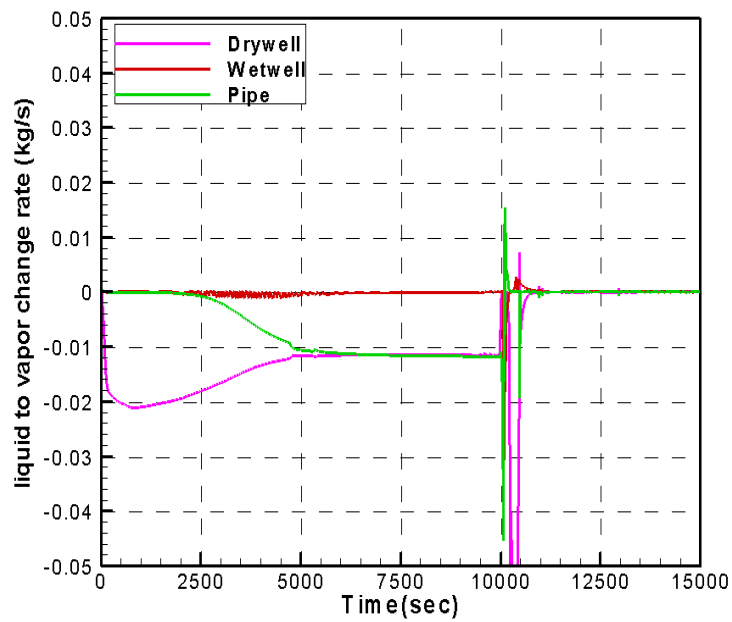


Figure 50: Liquid to vapor phase change rate in PPOOLEX simulation with flow boundary

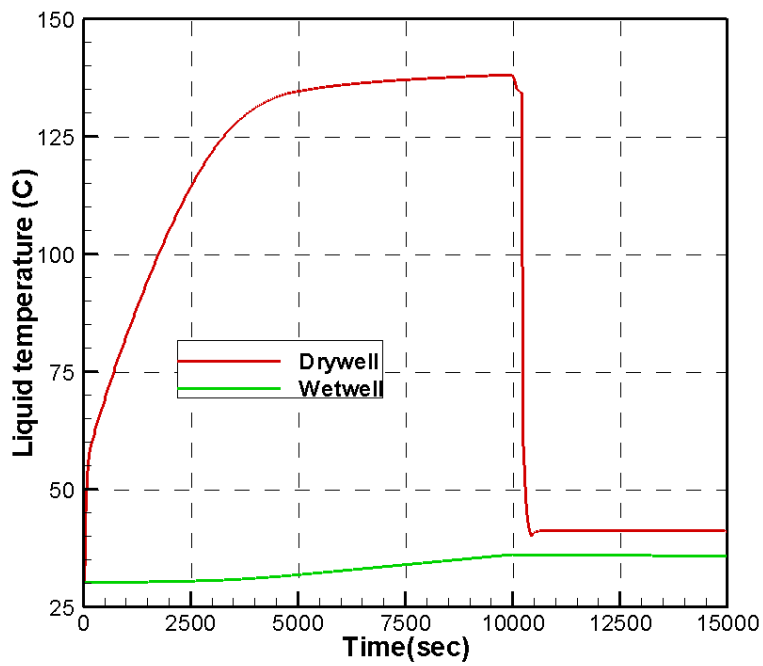


Figure 51: Liquid temperature in the tank in PPOOLEX simulation with flow boundary

## 4.2. Post-test lumped parameter simulation

The results and initial conditions of the thermal stratification experiment with the PPOOLEX test facility has been presented in the NKS report [10]. Six experiments have been carried out and heat-up periods of several thousand seconds by steam injection into the drywell compartment and into the wetwell water pool are measured. Some tests have shown thermal stratification in the wetwell. In the present part, the initial conditions in test STR-04 are used as initial boundary conditions in lumped parameter modeling with GOTHIC, to validate the GOTHIC code capability for prediction of pressure during steam injection. The inventory of injected steam, in terms of total energy injected, is critical to final results of pressure and averaged temperature. Hence flow boundary is used for modeling. The steam flow rate is function of time, which is shown in Figure 52. The boundary pressure and injected steam temperature are shown together with following results.

Figure 53 shows the predicted pressure in the three compartments. After about 2000 seconds, the pressure in the simulation is apparently overestimated compared to the measured data, which is equal to boundary pressure in the experiment. From the gas volume fraction in the drywell, as shown in Figure 54, over 90 percent of the gas in the drywell after that moment is steam. Figure 55 shows that the vapor temperature in the simulation is also higher than the measured data.

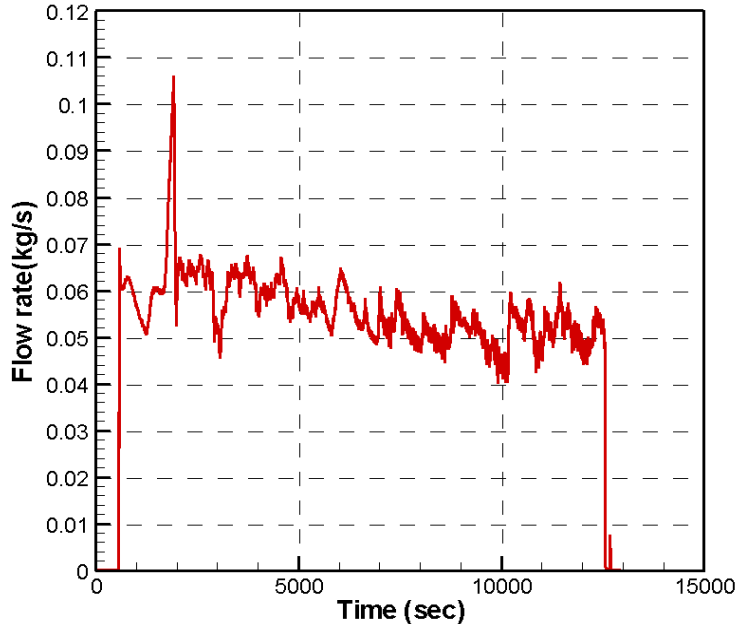


Figure 52: Steam flow rate supplied by flow boundary

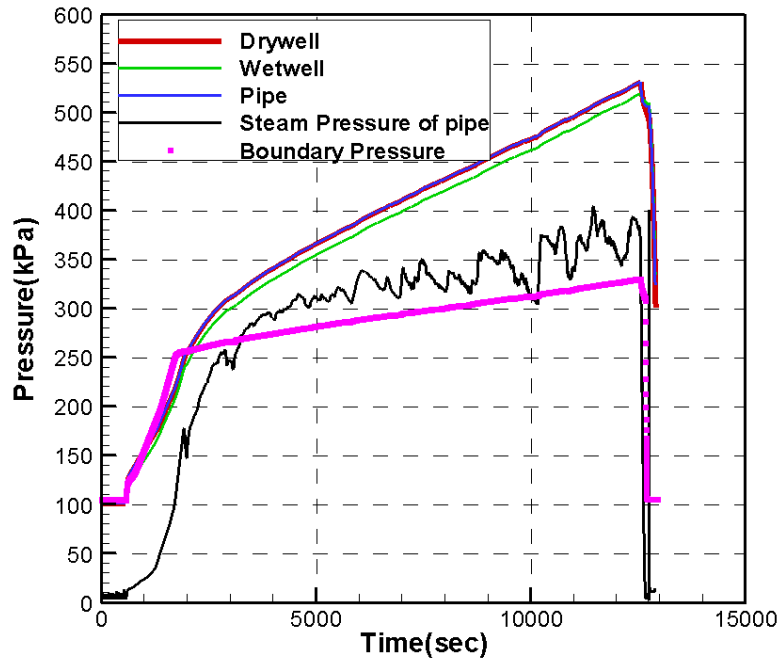


Figure 53: Total pressure in the drywell, wetwell, blowdown pipe and steam partial pressure in pipe, compared with steam inflow boundary pressure

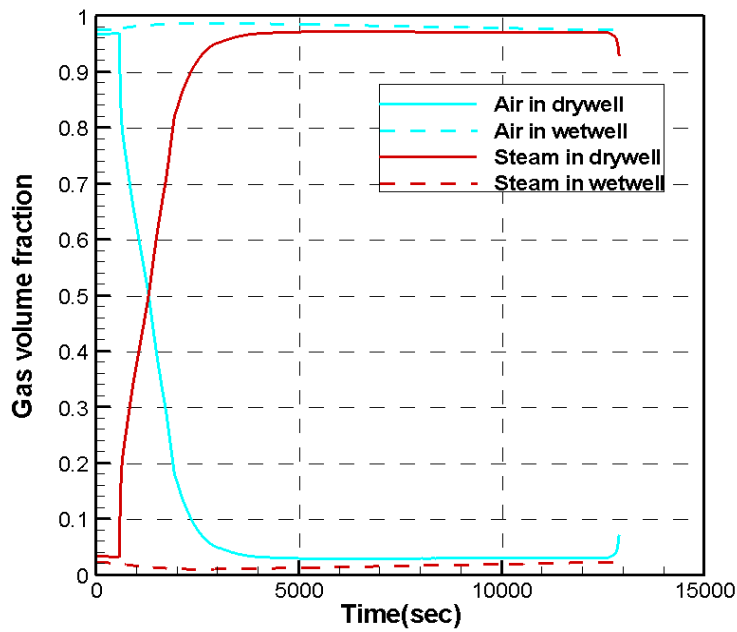


Figure 54: Air and steam volume fraction in the drywell and wetwell



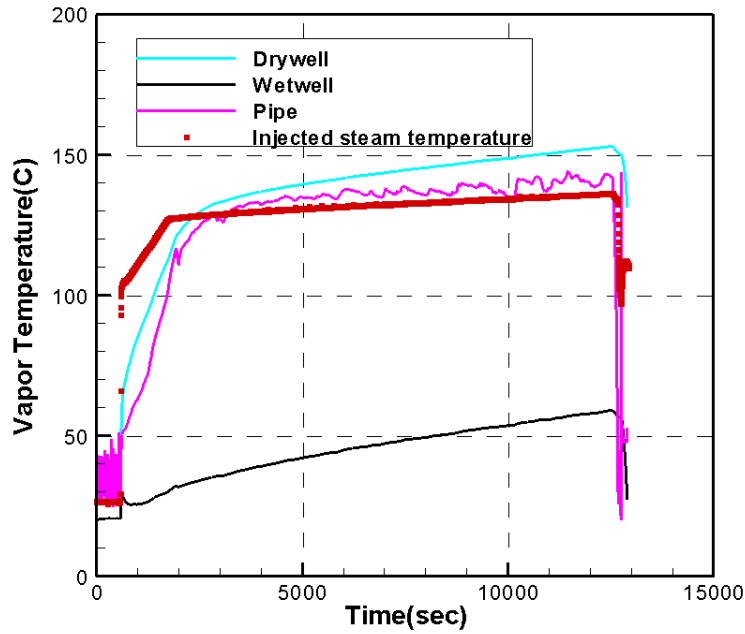


Figure 55: Vapor temperature in the drywell, wetwell, pipe and injected steam temperature

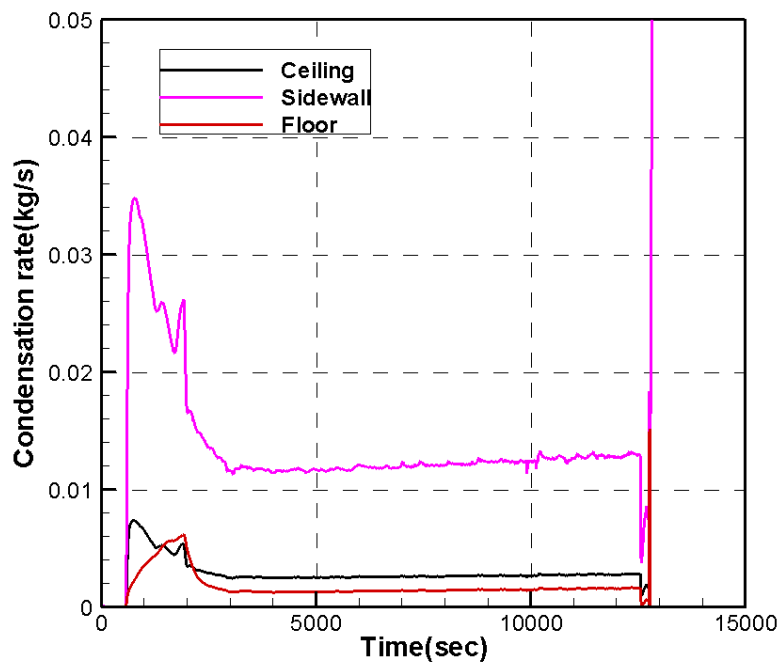


Figure 56: Condensation rate in the drywell for different part

Comparison of results of pre-test simulation and post-test simulation shows that the results of modeling with flow boundary conditions are much more reasonable and closer to the experimental data. With big flow rate steam injection, big liquid temperature increment can be obtained and thermal stratification can be observed easily. From Figure 57, wetwell liquid temperature in the simulation with experimental steam flow rate is close to the experimental averaged liquid temperature of the wetwell. However, pressure in simulation with experimental steam flow rate is over-estimated compared to experimental data.

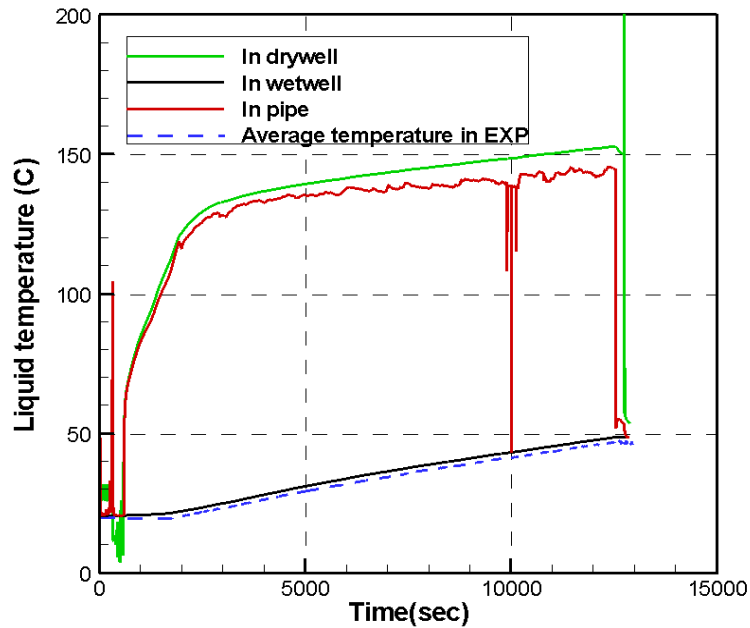


Figure 57: Liquid temperature in simulation and experimental average liquid temperature in the wetwell

Analysis of simulation results suggests that it is probable that air is injected also from flow boundary and accumulated in the wetwell resulting in increased pressure. It is found in the simulation that total non-condensable gas in the tank has increased from about 26 kg at the beginning to 49 kg at the end of transient, as shown in Figure 58. In the simulation, measured steam temperature of T1106 at inlet plenum is used as boundary temperature in the simulation, while steam pressure of P1102 at inlet plenum is used as boundary pressure. Measured temperature of T1106 is always lower than saturated temperature in measured pressure of P1102, which means air is taken into account by GOTHIC in given pressure and temperature, and injected through the boundary.

Boundary pressure is considered instead of saturated pressure corresponding to measured temperature in the simulation. Figure 59 shows that the pressure in the drywell and wetwell is close to the measured pressure. Calculated liquid temperature of wetwell is a little higher than wetwell averaged liquid temperature of experiment as shown in Figure 60, probably because of lumped parameter simulation which makes the vapor temperature and the liquid temperature close in value. Investigation of simulation and comparison to experimental data about wall condensation will be done in the future. More details are presented in Appendix 3.

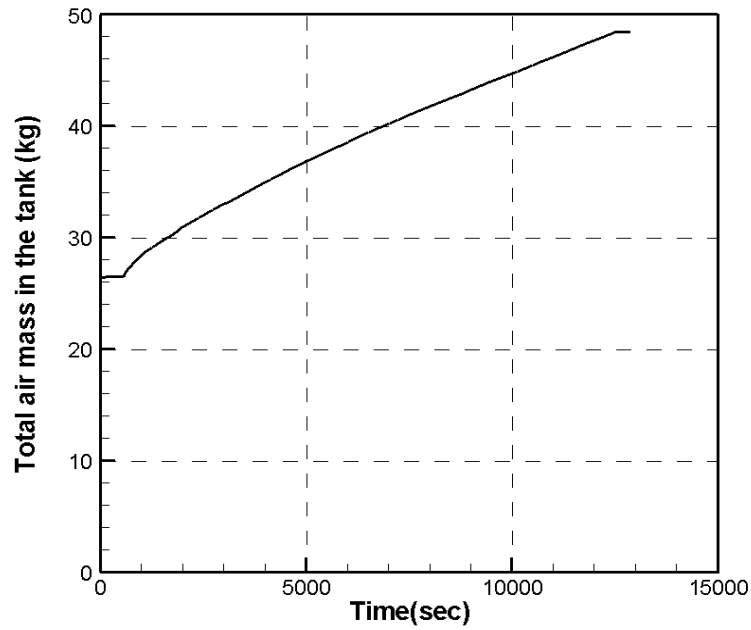


Figure 58: Total predicted air mass in the tank

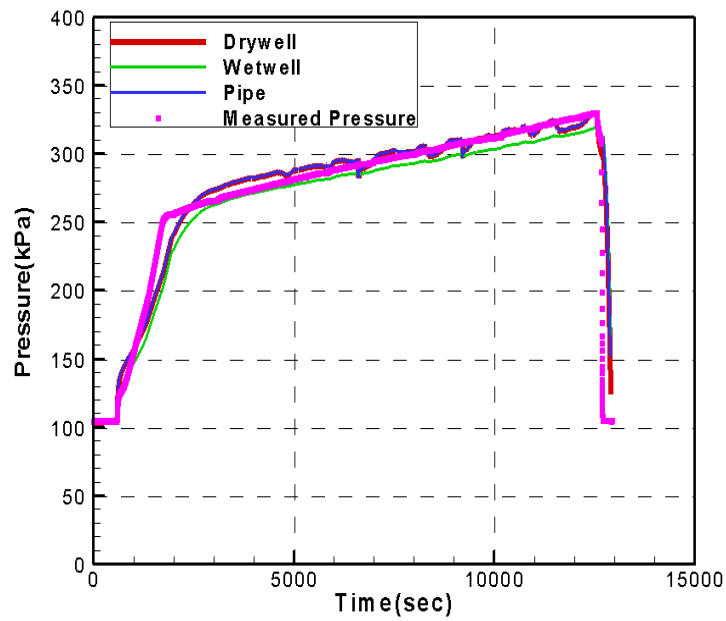


Figure 59: Pressure in the drywell, wetwell, blowdown pipe and steam partial pressure in pipe in simulation with improved boundary pressure, compared with measured pressure

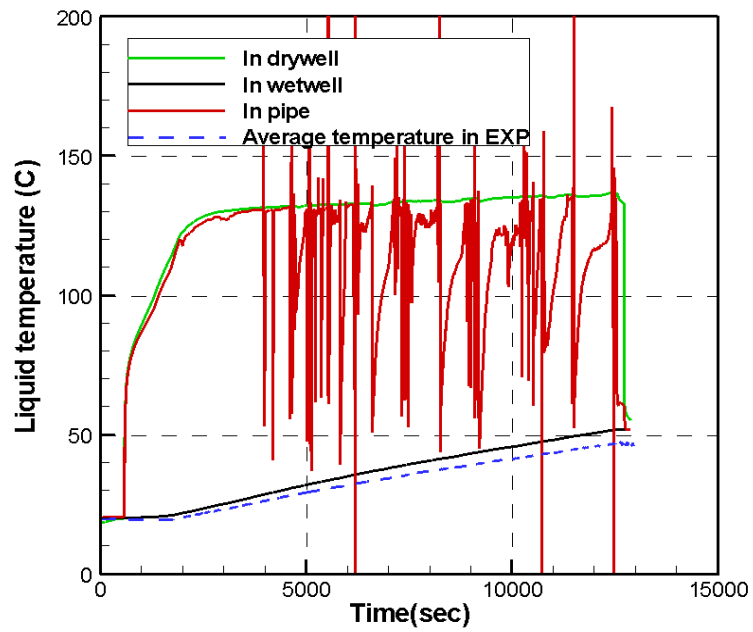


Figure 60: Liquid temperature in the drywell, wetwell, blowdown pipe in simulation with improved boundary pressure, compared with wetwell averaged liquid temperature in experiment

## **5. SUMMARY AND OUTLOOK**

Presented work contributes to development and sustaining of expertise at KTH in the field of containment thermal-hydraulics under support of the NORTHNET Roadmap 3 (Containment Thermal Hydraulics). Analytical support and leverage on data of POOLEX/PPOOLEX experiments at Lappeenranta University of Technology (LUT) is additional important element of the present work.

Focus of the present work is on assessment of present capabilities of containment thermal hydraulic codes (specifically GOTHIC) to predict condensation, stratification and mixing phenomena in a BWR pressure suppression pool. Two major questions of safety importance are to be addressed with the codes:

- (a) Conditions for onset of thermal stratification development and its speed.
- (b) Time scale for breakdown of stratified layers in the pool.

Main conclusions and results of the present work can be summarized as follows:

- (i) Reliable and computationally affordable prediction of thermal stratification development and mixing time scales in case of steam injection into a large subcooled pool is yet unsolved for contemporary simulation methods. Major problems are due to long time transients, complex geometry, complex physics of mixed (forced/natural) turbulent convection at high Rayleigh numbers, and potential instabilities in direct contact condensation of steam in different flow regimes (Chapter 1).
- (ii) The GOTHIC code predicts artificial mixing in the pool in case of direct simulation of steam injection into a subcooled water pool even if experimental data (e.g. POOLEX tests) shows development of stratification. Besides that, attempts to simulate direct contact condensation are computationally expensive due to severe limitations on the computational time step (Chapter 2).
- (iii) In the present work we propose to develop appropriate models which can take into account heat and momentum fluxes due to steam injection. Namely we propose two approaches (Chapter 2):
  - (a) Effective heat source approach
  - (b) Effective momentum approach

Effective heat source approach can be applied for simulation of thermal stratification development in the case of relatively small steam flow rate when effective momentum due to steam injection is small.

Effective momentum approach can be used at larger steam flow rates when motion of steam-water interface creates significant momentum sufficient for breakdown and mixing of stratified layers.

In both approaches no direct simulation of steam injection has been used. Instead effective values (and direction for momentum) of heat and momentum are calculated with appropriate subgrid models.

- (iv) Validation against POOLEX data and grid sensitivity study for effective heat source approach has been performed with the GOTHIC code and with CFD code Fluent. It is demonstrated that development of thermal stratification can be predicted with the GOTHIC code reasonably well with reasonable computational expenses both for relatively large scale experiments (POOLEX) and for prototypic scale pools (Chapter 2). CFD

also shows decent quality results but it is rather expensive in terms of computational time in comparison with GOTHIC. Attractive feature of CFD approach is that it allows considering separate effect phenomena with minimum modeling assumptions which gives very useful insights into basic physics of the problem.

- (v) Feasibility of effective momentum approach has been demonstrated in Chapter 3. We have shown in the parametric study that with appropriate momentum direction and magnitude it is possible to reproduce from the numerical simulation the characteristic time scales for mixing in different layers. A physically sound model still has to be developed for calculation of effective momentum which depends on conditions of steam injection (steam flow rate, water subcooling, concentration of non-condensable gases, flow regime, etc.)
- (vi) Lumped parameter pre-test and post-test simulations for PPOOLEX experiment have been performed as part of analytical support to the experimental activity at LUT (Chapter 4). Results have shown that the drywell and wetwell pressures can be kept within safety margins during quite long steam transients of injection at small flow rates, which is necessary for development of thermal stratification. Post-test simulations have also shown reasonable agreement with experimental data. Although we have to take into account some uncertainty in the experimental data measurements. Namely exact experimental data suggest subcooled conditions for steam injection, which leads to problems in GOTHIC simulations. Correction of input data for the steam inlet pressure within the ranges of experimental measurement error can significantly improve qualitative agreement between experimental and simulation data. More work is necessary for validation of GOTHIC against PPOOLEX data in order to clarify the influence of wall condensation in the drywell on the pressure level in the vessel.

### **Next steps:**

Based on the achievements of the current project we propose:

- (i) develop effective heat source and effective momentum models and approaches to prediction of thermal stratification and mixing in a BWR pressure suppression pool;
- (ii) validate capability of modified tools (codes, models) in predicting key behaviors and parameters of suppression pools;
- (iii) to continue leverage on and collaborate with the closely related experimental program conducted at Lappeenranta University of Technology (LUT) on condensation pools, namely POOLEX and PPOOLEX experiments.

We have made considerable step forward in qualification of the tools for prediction of condensation, stratification and mixing in a BWR suppression pool. Yet we believe that mission on development and sustaining of expertise in the field of containment thermal-hydraulics is neither accomplished nor impossible.

The mission is not accomplished because identified in the present work limitations in the prediction of thermal stratification and especially mixing are still there. Direct application of the GOTHIC code models to prediction of dynamics of the pressure suppression pool is impractical for industrial purposes. Main reasons for that are (i) low fidelity and (ii) low computational efficiency of the computational tool when direct simulation of steam injection into a subcooled pool is employed. Ironically GOTHIC almost never use such “direct simulation” approaches. The code is built on a set of well validated subgrid scale models for resolution of separate effect multiphase heat and mass transfer phenomena. Such multiscale approach and the set of effective models are the real reasons for robustness, reliability and efficiency of GOTHIC prediction in other cases.

We believe that mission on development of better approaches to modeling of stratification and mixing is not impossible because identified limitations in the code prediction are amenable for improvement, as it is demonstrated in the current work. New capabilities which can become available for industrial applications with “effective heat source” and “effective momentum” approaches are worth the effort on model development, validation and implementation. There are scientific, technical, and organizational challenges on the way toward eventual implementation of new models in the GOTHIC code. Therefore there is no guarantee that implementation of the developed models in the standard GOTHIC code will happen within the project time frame, on the other hand we do not exclude such a possibility and will work toward this goal. In fact we have reached an unwritten agreement with the GOTHIC developers that necessary part of the source code can be given to us for model development and implementation.

Another key ingredient for success of the future project will be continuation of mutually interesting collaboration with Lappeenranta University of Technology (LUT). POOLEX and PPOOLEX experiments funded within the long term SAFIR program are unique sources of detailed data which will be necessary for model development and code validation purposes. On the other hand, analytical support from KTH for design, modifications of the facility, development of experimental procedures can be beneficial as guidance toward most interesting for code validation experimental regimes.

## **6. ACKNOWLEDGEMENT**

Financial support from the NORTHNET RM3 and Nordic Nuclear Safety Program (NKS) is greatly acknowledged.



## **7. REFERENCES**

1. Varzaly, A.M., Grafton, W.A., Chang, H., Mitchell, M.K., "Mark III, 1977. Confirmatory test program, 1: 3 scale condensation and stratification phenomena-test series 5807," General Electric Report, NEDE-21596-P, March 1977.
2. Varzaly, A.M., Grafton, W.A., Seely, D.S., "Mark III, 1978. Confirmatory test program, full scale condensation and stratification phenomena-test series 5707," General Electric Report, NEDE-21853-P, August 1978.
3. Varzaly, A.M., Yu, K.P., Kerinenen, J.A., "Mark III, 1980. Confirmatory test program, 1:9 area scale multicell condensation and stratification phenomena-test series 6003," General Electric Report, NEDE-24720-P, January 1980.
4. Peterson, P.F., Rao, I.J., Schrock, V.E., "Transient thermal stratification in pools with shallow buoyant jets," In: Hassan, Y.A., Hochreiter, L.E. (Eds.), Nuclear Reactor Thermal Hydraulics, HTD-Vol. 190. ASME, New York, pp. 55–62, 1991.
5. Kataoka, Y., Fukui, T., Hatamiya, S., "Experimental study on convection heat transfer along a vertical flat plate between different temperature pools," ANS National Heat Transfer Conference, Minneapolis, 28-31 July, 1991.
6. Fox, R.J., "Temperature distribution in pools with shallow buoyant jets," Fifth International Topical Meeting on Nuclear Reactor Thermal Hydraulics (NURETH-5), September 21-24, Salt Lake City, Utah. pp. 1227-1234, 1992.
7. Smith, B.L., Dury, T.V., Huggenberger, M., Nöthiger, N., "Analysis of single-phase mixing experiments in open pools," In: Cheung, F.B., Peterson, P.F. (Eds.), Thermal Hydraulics of Advanced and Special Purpose Reactors, ASME HTD, vol. 209. ASME, New York, pp. 91-100, 1992.
8. Ling, C., Kyoung, S.W., Ishii, M., Lim, J., Han, J., "Suppression pool mixing and condensation tests in PUMA facility," International Conference on Nuclear Engineering, ICONE, 2006.
9. Laine, J., Puustinen, M., "Thermal stratification experiments with the condensation pool test rig," NKS-117, 2006.
10. Puustinen, M., Laine, J., Räsänen, A., "PPOOLEX experiments on thermal stratification and mixing". Research report CONDEX 1/2008, NKS-198, 2009.
11. Norman, T.L., Park, H.S., Revankar, S.T., Ishii, M., Kelly, J.M., "Thermal stratification and mixing in an open water pool by submerged mixtures of steam and air," ASME International Mechanical Engineering Congress and Exposition, IMECE2006 - Nuclear Engineering, 2006.
12. Peterson, P.F., "Scaling and analysis of mixing in large stratified volumes," International Journal of Heat and Mass Transfer, 37, pp.97-106, 1994.
13. Peterson, P.F., Gamble, R., "Scaling for forced-convection augmentation of heat and mass transfer in large enclosures by injected jets," Trans. Am. Nucl. Soc., 78, pp.265-266, 1998.
14. Gamble, R. E., Nguyen, T. T., Peterson, P. F., "Pressure suppression pool mixing in passive advanced BWR plants," Nuclear Engineering and Design, 204, pp.321-336, 2000.
15. Kuhn, S.Z., Kang, H.K., Peterson, P.F., "Study of Mixing and Augmentation of Natural Convection Heat Transfer by a Forced Jet in a Large Enclosure," Journal of Heat Transfer, Volume 124, Issue 4, pp. 660-666, 2002.
16. Zhao, H., "Computation of mixing in large stably stratified enclosures," Ph.D. Dissertation. University of California, Berkeley, 2003.

17. Niu, F., Zhao, H., Per F. Peterson, P.F., Joel Woodcock and Robert E. Henry, "Investigation of mixed convection in a large rectangular enclosure," Nuclear Engineering and Design, Volume 237, Issue 10, May 2007, Pages 1025-1032.
18. Zhao, H., Peterson, P.F., "One-dimensional analysis of thermal stratification in AHTR and SFR coolant pools. Proceedings - 12th International Topical Meeting on Nuclear Reactor Thermal Hydraulics, NURETH-12, 2007.
19. Li, H., Kudinov, P., "An approach toward simulation and analysis of thermal stratification and mixing in a pressure suppression pool," NUTHOS-7, Seoul, Korea, October 5-9, 2008, Paper 243.
20. Li, H. and Kudinov, P., "An Approach for Simulation of Mixing in a Stratified Pool with the GOTHIC code," ANS Transactions, 2009.
21. Li, H. and Kudinov, P., "Effective Approaches to Simulation of Thermal Stratification and Mixing in a Pressure Suppression Pool," CFD4NRS-3 Workshop, Bethesda, MD, USA, September 14-16, 2010.
22. Nourgaliev, R.R., Dinh, T.N., "The investigation of turbulence characteristics in an internally-heated unstably-stratified fluid layer," Nuclear engineering and design, 178, pp.235-258, 1997.
23. "GOTHIC containment analysis package qualification report," Version 7.2a (QA), EPRI, Palo Alto, CA, 2006.
24. "GOTHIC containment analysis package user manual," Version 7.2a (QA), EPRI, Palo Alto, CA, 2006.
25. "GOTHIC containment analysis package technical manual," Version 7.2a, EPRI, Palo Alto, CA, 2006.
26. "The Marviken Full Scale Containment Experiment, Second Series, Description of the Test Facility", AB Atomenergi Sweden, MXB-101, March, 1977.
27. Andreani, M., "Pretest calculations of phase A of ISP-42 (PANDA) using the GOTHIC containment code and comparison with the experimental results," Nuclear Technology, 148, pp.35-47, 2006.
28. Andreani, M., Putz, F., Dury, T.V., Gjerloev, C., Smith, B.L., "On the application of field codes to the analysis of gas mixing in large volumes: case studies using CFX and GOTHIC," Annals of Nuclear Energy, Volume 30, Issue 6, April 2003, Pages 685-714.
29. Wiles, L.E., George, T.L., "Thermal-Hydraulic Analysis of the Nuclear Power Engineering Corporation Containment Experiments with GOTHIC," Nuclear Technology, Volume 142, Number 1, April 2003, Pages 77-91.
30. Gavrilas, M., Todreas, N.E., Driscoll, M.J., "The design and evaluation of a passively cooled containment for a high-rating pressurized water reactor," Nuclear Engineering and Design, Volume 200, Issues 1-2, August 2000, Pages 233-249.
31. Weimer, J.C., Faeth, G.M., Olson, D.R., "Penetration of vapor jets submerged in subcooled liquids," American Institute of Chemical Engineering Journal 19 (3), 552-558, 1973.
32. Chun, M. H., Kim, Y. S., Park, J. W., "An investigation of direct condensation of steam jet in subcooled water," International Communications in Heat and Mass Transfer, 23, pp.947-958, 1996.
33. Kim, Y. S., Park, J. W., Song, C. H., "Investigation of the steam-water direct contact condensation heat transfer coefficients using interfacial transport models," International Communications in Heat and Mass Transfer, 31 n3, 397- 408, 2004.
34. Song, C. H., Cho, S., Kim, H. Y., Bae, Y. Y., Chung, M. K., "Characterization of direct contact condensation of steam jets discharge into a subcooled water," IAEA TCM, PSI, Viligen, pp.1-12, 1998.

35. Kerney, P.J., Fathe, G.M., Olson, D.R., "Penetration characteristics of submerged jet," *American Institute of Chemical Engineering Journal* 18 (3), 548-553, 1972.
36. Chun, M.H., Kim, Y.S., Park, J.W., "An investigation of direct condensation of steam jet in subcooled water," *International Communications in Heat and Mass Transfer* 23, 947-958, 1996.
37. Kim, H.W., Bae, Y.Y., Song, C.H., Park, J.K., Choi, S.M., "Characterization of direct contact condensation of steam jets discharging into a subcooled water," *International Journal of Energy Research* 25, 239-252, 2001.
38. Wu, X.Z., Yan, J.J., Shao, S.F., Cao, Y., Liu, J.P., "Experimental study on the condensation of supersonic steam jet submerged in quiescent subcooled water: steam plume shape and heat transfer," *International Journal of Multiphase Flow* 33, 1296-1307, 2007.
39. Gebhart, B., Jaluria, Y., Mahajan, R.L., Sammakia, B., "Buoyancy Induced Flows and Transport." Hemisphere, New York, 1988.
40. Kudo, A., Egusa, T., Toda, S., "Basic study on vapor suppression," *Proc. Fifth Int. Heat Transfer Conf.* 3, pp.221-225, 1974.
41. Cumo, W., Farello, G.E., Ferrari, G., "Direct heat transfer in pressure-suppression systems," *Proc. Sixth Int. Heat Transfer Conf.* 5, pp.101-106, 1978.
42. Simpson, M.E., Chan, C.K., "Hydrodynamics of a subsonic vapor jet in subcooled liquid," *J. Heat Transfer* 104, 271-278, 1982.
43. Tin, G.D., Lavagno, E., Malandrone, M., "Pressure and temperature measurements in a vapour condensing jet," *Proc. Seventh Int. heat Transfer Conf.* 6, 159-164, 1982.
44. Nariai, H., Aya, I., "Fluid and pressure oscillations occurring at direct contact condensation of steam flow with cold water," *Nucl. Eng. Des.* 95, 35-45, 1986.
45. Lahey, R.T., Moody, F.J., "The Thermal Hydraulics of a Boiling Water Reactor, second ed.," American Nuclear Society, Illinois, 582 p., 1993.
46. Fitzsimmons, G.W., Galyard, D.L, Nixon, R.B., Mann, M.J. and Yu, K.P., "Mark I Containment Program, Full Scale Test Program Final Report," General Electric Report, NEDE-24539, August 1979.
47. Tanskanen V., Lakehal, D., Puustinen, M., "Validation of direct contact condensation CFD models against condensation pool experiment," *XCFD4NRS OECD Conf.*, Grenoble, Sep. 12-15, 2008.
48. Moon, Y.-T., Lee, H.-D., Park, G.-C., "CFD simulation of steam jet-induced thermal mixing in subcooled water pool," *Nuclear Engineering and Design*, 239, pp.2849-2863, 2009.
49. Chan, C.K., Lee, C.K.B., "A regime map for direct contact condensation," *International Journal of Multiphase Flow*, 8 (1), 11-20, 1982.
50. Liang, K.S., Griffith, P., "Experimental and analytical study of direct contact condensation of steam in water," *Nuclear Engineering and Design* 147, 425-435, 1994.
51. Cho, S., Song, C.H., Park, C.K., Yang, S.K., Chung, M.K., "Experimental study on dynamic pressure pulse in direct contact condensation of steam Jets Discharging into Subcooled Water, NTHAS98, 291, 1997.
52. Youn, D.H., Ko, K.B., Lee, Y.Y., Kim, M.H., Bae, Y.Y., and Park, J.K., "The direct contact condensation of steam in a pool at low mass flux," *Journal of Nuclear Science and Technology*, 40 (10), 881-885, 2003.
53. Petrovic-de With, A., Calay, R.K., and With, G., "Three dimensional regime map for direct contact condensation of steam injected into water," *International Journal of Heat and Mass Transfer*, 50, 1762-1770, 2007.

54. Song, C.H., Baek, W.P., Chung, M.K., and Park, J.K., “Multi-dimensional thermal-hydraulic phenomena in advanced nuclear reactor systems: current status and perspectives of the R&D program at KAERI,” Proceedings International Conference on Nuclear Reactor Thermal Hydraulics (NURETH-10), Seoul, Korea, October 5-9, Paper I00121, 2003.
55. Kang, H.S., Song, C.H., “CFD Analysis for Thermal Mixing in a Subcooled Water Tank under a High Steam Mass Flux Discharge Condition,” Nuclear Engineering and Design, 238 (3), 492-501, 2008.
56. Austin, S., and Baisley, D., “System 80+Summary of Program to Evaluate DCRT Issues Related to the Safety Depressurization System and IRWST – Task 12,” ABB-CE Documentation, 1992.
57. Zurigat, Y.H., Ghajar, A.J., “Heat transfer and stratification in sensible heat storage systems,” In Thermal Energy Storage Systems and Applications. Eds. Dincer & Rosen. Wiley, New York. 2002.

## Appendix 1

Table A1-1: Parameters for lumped parameter modeling of STB-20

|  |                                      |
|--|--------------------------------------|
| <b>INITIAL CONDITION</b>                 |                                      |
| Pool liquid and vapor temperature (°C)   | 30                                   |
| Pool pressure (kPa)                      | 105.353                              |
| Liquid fraction in the pool              | 0.533                                |
| Pipe liquid and vapor temperature (°C)   | 30                                   |
| Pipe pressure (kPa)                      | 101.353                              |
| Liquid fraction in the pipe              | 0.469                                |
| liquid and vapor temperature in lab (°C) | 24                                   |
| Lab pressure (kPa)                       | 101.353                              |
| Liquid fraction in lab                   | 0                                    |
| <b>BOUNDARY 1 (Flow)</b>                 |                                      |
| Steam Source Pressure (kPa)              | Time dependent experimental data [9] |
| Steam Flow (kg/s)                        | Time dependent experimental data [9] |
| Temperature (°C)                         | Time dependent experimental data [9] |
| Steam Fraction                           | 1                                    |
| Elevation (m)                            | 6.9                                  |
| <b>BOUNDARY 2 (Pressure)</b>             |                                      |
| Pressure (kPa)                           | 101.353                              |
| Temperature (°C)                         | 20                                   |
| Air Fraction                             | 1                                    |
| Elevation (m)                            | 9                                    |
| <b>VOLUME 1</b>                          |                                      |
|  | (Blowdown pipe model)                |
| Volume (m <sup>3</sup> )                 | 0.149                                |
| Hydraulics diameter (m)                  | 0.2141                               |
| Bottom Elevation (m)                     | 0.857                                |
| Height (m)                               | 4.143                                |
| <b>VOLUME 2s</b>                         |                                      |
|  | (Pool model)                         |
| Volume (m <sup>3</sup> )                 | 22.5                                 |
| Hydraulic diameter (m)                   | 2.4                                  |
| Bottom Elevation (m)                     | 0                                    |
| Height (m)                               | 5                                    |
| <b>VOLUME 3</b>                          |                                      |
|  | (Lab model)                          |
| Volume (m <sup>3</sup> )                 | 10 <sup>7</sup>                      |
| Hydraulics diameter (m)                  | 15                                   |
| Bottom Elevation (m)                     | -1                                   |

|                                |                                      |
|--------------------------------|--------------------------------------|
| Height (m)                     | 10                                   |
| <b>JUNCTION 1</b>              | (Connects flow boundary to pipe)     |
| End elevation (m)              | 4.5                                  |
| Start elevation (m)            | 6.9                                  |
| Hydraulic diameter (m)         | 0.2141                               |
| Flow area (m <sup>2</sup> )    | 0.036                                |
| Inertia length (m)             | 0.01                                 |
| Friction length (m)            | 0.01                                 |
| <b>JUNCTION 2</b>              | (Connects blowdown pipe to pool)     |
| End elevation (m)              | 0.857                                |
| Start elevation (m)            | 0.757                                |
| Hydraulic diameter (m)         | 0.2141                               |
| Flow area (m <sup>2</sup> )    | 0.036                                |
| Inertia length (m)             | 4.143                                |
| Friction length (m)            | 4.143                                |
| <b>JUNCTION 3</b>              | (Connects lab to pool)               |
| End elevation (m)              | 4.5                                  |
| Start elevation (m)            | 5.05                                 |
| Hydraulic diameter (m)         | 2.4                                  |
| Flow area (m <sup>2</sup> )    | 2.25                                 |
| Inertia length (m)             | 5                                    |
| Friction length (m)            | 5                                    |
| <b>JUNCTION 4</b>              | (Connects pressure boundary to lab)  |
| End elevation (m)              | 8.9                                  |
| Start elevation (m)            | 9                                    |
| Hydraulic diameter (m)         | 1                                    |
| Flow area (m <sup>2</sup> )    | 3                                    |
| Inertia length (m)             | 0.01                                 |
| Friction length (m)            | 0.01                                 |
| <b>JUNCTION 5</b>              | (Connects lab to pool)               |
| End elevation (m)              | 4.508                                |
| Start elevation (m)            | 5.05                                 |
| Hydraulic diameter (m)         | 2.4                                  |
| Flow area (m <sup>2</sup> )    | 2.25                                 |
| Inertia length (m)             | 5                                    |
| Friction length (m)            | 5                                    |
| <b>CONDUCTOR 1</b>             | (Pipe wall in gas space of pool)     |
| Thickness (cm)                 | 0.25                                 |
| Surface area (m <sup>2</sup> ) | 1.379                                |
| Initial temperature (°C)       | 30                                   |
| <b>CONDUCTOR 2</b>             | (Pipe wall in liquid space of pool ) |

|                                |                                 |
|--------------------------------|---------------------------------|
| Thickness (cm)                 | 0.25                            |
| Surface area (m <sup>2</sup> ) | 1.2174                          |
| Initial temperature (°C)       | 30                              |
|                                |                                 |
| <b>CONDUCTOR 3</b>             | (Tank sidewall in gas space)    |
| Thickness (cm)                 | 4                               |
| Surface area (m <sup>2</sup> ) | 15.46                           |
| Initial temperature (°C)       | 30                              |
|                                |                                 |
| <b>CONDUCTOR 4</b>             | (Tank sidewall in liquid space) |
| Thickness (cm)                 | 4                               |
| Surface area (m <sup>2</sup> ) | 20.11                           |
| Initial temperature (°C)       | 30                              |
|                                |                                 |
| <b>CONDUCTOR 5</b>             | (Bottom wall of the tank)       |
| Thickness (cm)                 | 5                               |
| Surface area (m <sup>2</sup> ) | 4.5                             |
| Initial temperature (°C)       | 30                              |

Table A1-2: Parameters for 2D modeling of STB-20

| In 2D modeling of pool without gas space |   |
|--|---|
| INITIAL CONDITION                        |   |
| Pool liquid and vapor temperature (°C)   | 30  |
| Pool pressure (kPa)                      | 105.353                                     |
| liquid and vapor temperature in lab (°C) | 24  |
| Lab pressure (kPa)                       | 101.353                                     |
| Liquid fraction in lab                   | 0   |
|  |   |
| VOLUME 1s                                | (Liquid part of the pool)                   |
| Volume (m <sup>3</sup> )                 | 12  |
| Hydraulic diameter (m)                   | 2.4   |
| Bottom Elevation (m)                     | 1   |
| Height (m)                               | 2.95  |
|  |   |
| VOLUME 2                                 | (Lab model)                                 |
| Volume (m <sup>3</sup> )                 | 10 <sup>7</sup>                             |
| Hydraulics diameter (m)                  | 15  |
| Bottom Elevation (m)                     | -1  |
| Height (m)                               | 10  |
|  |   |
| CONDUCTOR 1s                             | (Pipe wall in liquid space of pool )        |
| Thickness (cm)                           | 0.25  |
| Surface area (m <sup>2</sup> )           | 1.2174                                      |
| Initial temperature (°C)                 | 30  |
|  |   |
| CONDUCTOR 2s                             | (Virtual wall of free surface in the pool ) |
| Thickness (cm)                           | 0.01  |
| Surface area (m <sup>2</sup> )           | 4.5   |
| Initial temperature (°C)                 | 30  |
|  |   |
| CONDUCTOR 3s                             | (Tank sidewall in liquid space)             |
| Thickness (cm)                           | 4   |
| Surface area (m <sup>2</sup> )           | 20.11                                       |
| Initial temperature (°C)                 | 30  |
|  |   |
| CONDUCTOR 4s                             | (Bottom wall of the tank)                   |
| Thickness (cm)                           | 5   |
| Surface area (m <sup>2</sup> )           | 4.5   |
| Initial temperature (°C)                 | 30  |
|  |   |
| In 2D modeling of pool without gas space |   |
| INITIAL CONDITION                        |   |
| Pool liquid and vapor temperature (°C)   | 30  |
| Pool pressure (kPa)                      | 105.353                                     |



|   |                 |
|---|-----------------|
| liquid and vapor temperature in lab (°C)                | 24              |
| Lab pressure (kPa)                                      | 101.353         |
| Liquid fraction in lab                                  | 0               |
| <b>BOUNDARY 1 (Pressure)</b>                            |                 |
| Pressure (kPa)  | 101.353         |
| Temperature (°C)  | 20              |
| Air Fraction  | 1               |
| Elevation (m)   | 9               |
| <b>VOLUME 1s (Pool model)</b>                           |                 |
| Volume (m <sup>3</sup> )                                | 21.225          |
| Hydraulic diameter (m)                                  | 2.4             |
| Bottom Elevation (m)                                    | 0               |
| Height (m)  | 5               |
| <b>VOLUME 2 (Lab model)</b>                             |                 |
| Volume (m <sup>3</sup> )                                | 10 <sup>7</sup> |
| Hydraulics diameter (m)                                 | 15              |
| Bottom Elevation (m)                                    | 5               |
| Height (m)  | 16              |
| <b>CONDUCTOR 1s (Pipe wall in liquid space of pool)</b> |                 |
| Thickness (cm)  | 0.25            |
| Surface area (m <sup>2</sup> )                          | 1.2174          |
| Initial temperature (°C)                                | 30              |
| <b>CONDUCTOR 2s (Tank sidewall in liquid space)</b>     |                 |
| Thickness (cm)  | 4               |
| Surface area (m <sup>2</sup> )                          | 35.57           |
| Initial temperature (°C)                                | 30              |
| <b>CONDUCTOR 3s (Bottom wall of the tank)</b>           |                 |
| Thickness (cm)  | 5               |
| Surface area (m <sup>2</sup> )                          | 4.5             |
| Initial temperature (°C)                                | 30              |
| <b>JUNCTION 1 (Connects pressure boundary to lab)</b>   |                 |
| End elevation (m)                                       | 8.9             |
| Start elevation (m)                                     | 9               |
| Hydraulic diameter (m)                                  | 1               |
| Flow area (m <sup>2</sup> )                             | 3               |
| Inertia length (m)                                      | 0.01            |
| Friction length (m)                                     | 0.01            |
| <b>3D CONNECTOR (Connects lab and pool)</b>             |                 |
| Forward loss coefficient                                | 1               |

|                          |          |
|--------------------------|----------|
| Reverse loss coefficient | 1        |
| Lumped volume momentum   | Conserve |

## Appendix 2

The following table includes all of parameters used in PPOOLEX calculation with GOTHIC. The pure steam with flow rate of 0.026 kg/s is injected into drywell through a horizontal pipe. The pressure and temperature of steam are shown in table. There are air and steam mixture in the drywell and wetwell before injection. The initial pressure and temperature are also shown in the table.

|                              |                       |
|------------------------------|-----------------------|
| <b>INITIAL CONDITION</b>     |                       |
| Pressure (kPa)               | 101.353               |
| Vapor Temperature (°C)       | 30                    |
| Liquid Temperature (°C)      | 30                    |
| Liquid fraction in wetwell   | 0.637                 |
| Liquid fraction in pipe      | 0.513                 |
|                              |                       |
| <b>BOUNDARY 1 (Flow)</b>     |                       |
| Steam Source Pressure (kPa)  | 187                   |
| Steam Flow (kg/s)            | 0.026                 |
| Temperature (°C)             | 117                   |
| Steam Fraction               | 1                     |
| Elevation (m)                | 6.342                 |
|                              |                       |
| <b>BOUNDARY 2 (Pressure)</b> |                       |
| Pressure (kPa)               | 101.1                 |
| Temperature (°C)             | 20                    |
| Air Fraction                 | 1                     |
| Elevation (m)                | 9                     |
|                              |                       |
| <b>VOLUME 1s</b>             | (Dry well model)      |
| Volume (m <sup>3</sup> )     | 13.3                  |
| Hydraulics diameter (m)      | 2.4                   |
| Bottom Elevation (m)         | 4.27                  |
| Height (m)                   | 3.18                  |
|                              |                       |
| <b>VOLUME 2s</b>             | (Wetwell model)       |
| Volume (m <sup>3</sup> )     | 17.8                  |
| Hydraulic diameter (m)       | 2.4                   |
| Bottom Elevation (m)         | 0                     |
| Height (m)                   | 4.27                  |
|                              |                       |
| <b>VOLUME 3</b>              | (Blowdown pipe model) |
| Volume (m <sup>3</sup> )     | 0.1                   |
| Hydraulics diameter (m)      | 0.2                   |
| Bottom Elevation (m)         | 1.087                 |
| Height (m)                   | 3.183                 |
|                              |                       |

|                                |   |
|--------------------------------|---|
| <b>VOLUME 4</b>                | (Lab model)                             |
| Volume (m <sup>3</sup> )       | 10 <sup>7</sup>                         |
| Hydraulics diameter (m)        | 15                                      |
| Bottom Elevation (m)           | -1                                      |
| Height (m)                     | 10                                      |
|                                |   |
| <b>JUNCTION 1</b>              | (Connects flow boundary to drywell)     |
| End elevation (m)              | 6.342                                   |
| Start elevation (m)            | 6.342                                   |
| Hydraulic diameter (m)         | 0.2141                                  |
| Flow area (m <sup>2</sup> )    | 0.036                                   |
| Inertia length (m)             | 0.01                                    |
| Friction length (m)            | 0.01                                    |
|                                |   |
| <b>JUNCTION 2</b>              | (Connects drywell to blowdown pipe)     |
| End elevation (m)              | 4.27                                    |
| Start elevation (m)            | 4.255                                   |
| Hydraulic diameter (m)         | 0.2                                     |
| Flow area (m <sup>2</sup> )    | 0.0314                                  |
| Inertia length (m)             | 1.59                                    |
| Friction length (m)            | 1.59                                    |
|                                |   |
| <b>JUNCTION 3</b>              | (Connects blowdown pipe to wetwell)     |
| End elevation (m)              | 1.087                                   |
| Start elevation (m)            | 1.067                                   |
| Hydraulic diameter (m)         | 0.2                                     |
| Flow area (m <sup>2</sup> )    | 0.0314                                  |
| Inertia length (m)             | 1.59                                    |
| Friction length (m)            | 1.59                                    |
|                                |   |
| <b>CONDUCTOR 1</b>             | (Ceiling in the drywell)                |
| Thickness (cm)                 | 1                                       |
| Surface area (m <sup>2</sup> ) | 4.5                                     |
| Initial temperature (°C)       | 30                                      |
|                                |   |
| <b>CONDUCTOR 2</b>             | (Side wall of drywell )                 |
| Thickness (cm)                 | 1                                       |
| Surface area (m <sup>2</sup> ) | 23.98                                   |
| Initial temperature (°C)       | 30                                      |
|                                |   |
| <b>CONDUCTOR 3</b>             | (Floor between the drywell and wetwell) |
| Thickness (cm)                 | 1                                       |
| Surface area (m <sup>2</sup> ) | 4.5                                     |
| Initial temperature (°C)       | 30                                      |
|                                |   |
| <b>CONDUCTOR 4</b>             | (Blowdown tube model)                   |
| Thickness (cm)                 | 0.25                                    |
| Surface area (m <sup>2</sup> ) | 2.0                                     |

|                                |                         |
|--------------------------------|-------------------------|
| Initial temperature (°C)       | 30                      |
|                                |                         |
| <b>CONDUCTOR 5</b>             | (Wetwell side wall)     |
| Thickness (cm)                 | 1                       |
| Surface area (m <sup>2</sup> ) | 32.2                    |
| Initial temperature (°C)       | 30                      |
|                                |                         |
| <b>CONDUCTOR 6</b>             | (Bottom of the wetwell) |
| Thickness (cm)                 | 1                       |
| Surface area (m <sup>2</sup> ) | 4.5                     |
| Initial temperature (°C)       | 30                      |

| For pressure boundary | Time (sec) | Pressure (kPa) | Temperature (°C) |
|-----------------------|------------|----------------|------------------|
|                       | 0          | 110            | 114              |
|                       | 10000      | 340            | 147              |
|                       | 160000     | 340            | 147              |

### Appendix 3

#### PPOOLEX pre-test lumped parameter simulations with pressure boundary/flow boundary

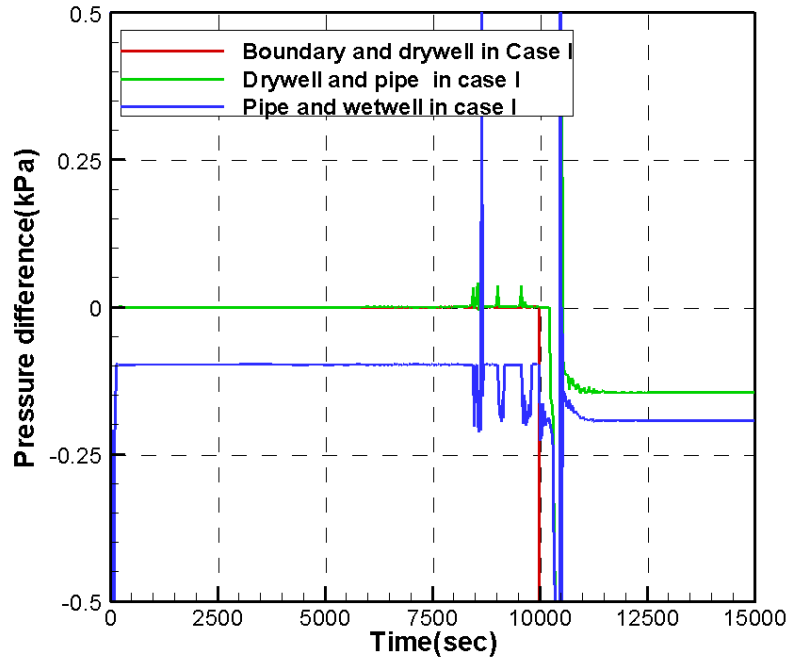


Figure 61: Pressure difference in Case I in PPOOLEX simulation with pressure boundary

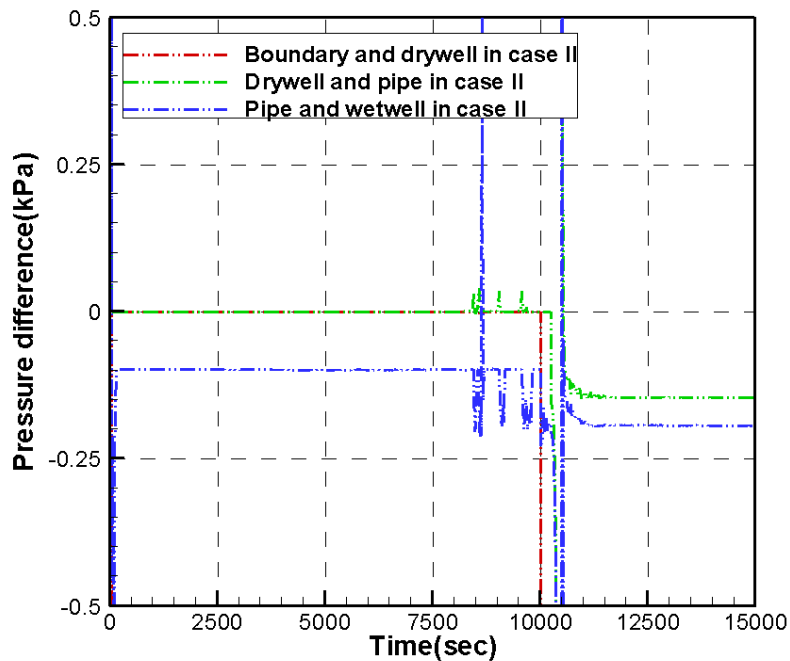


Figure 62: Pressure difference in Case II in PPOOLEX simulation with pressure boundary

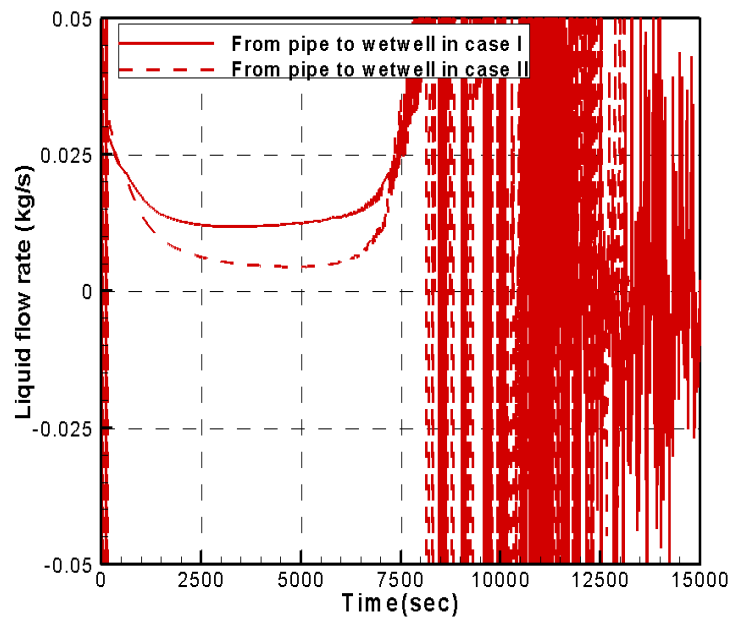


Figure 63: Liquid flow rate from tube to wetwell in PPOOLEX simulation with pressure boundary

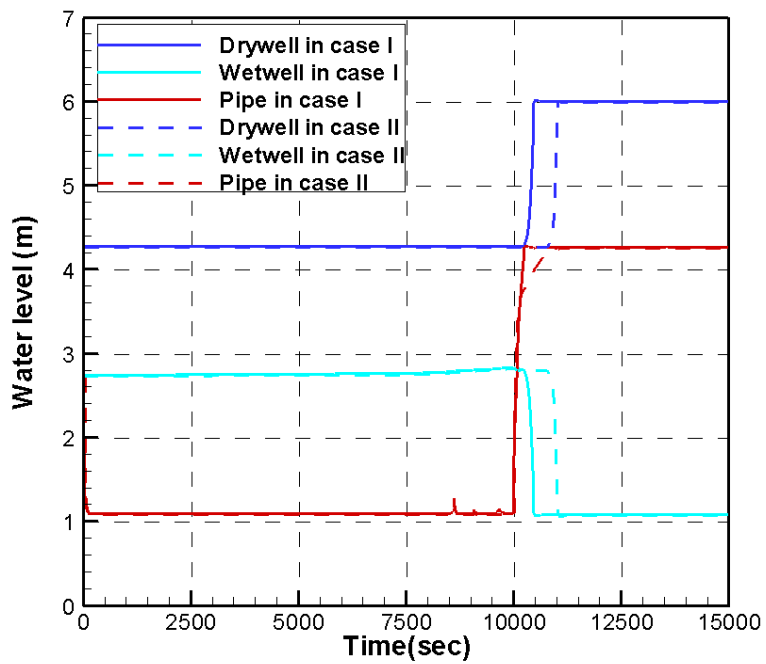


Figure 64: Liquid level in PPOOLEX simulation with pressure boundary

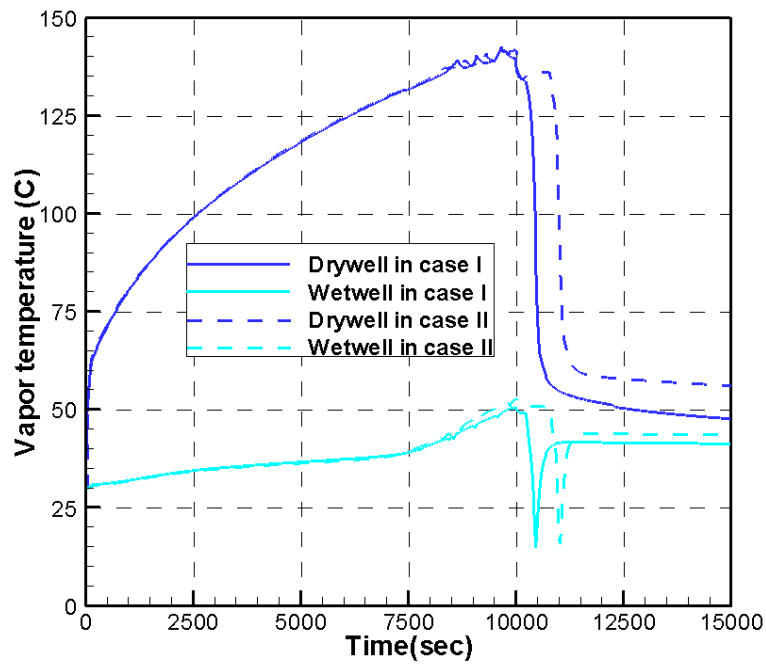


Figure 65: Vapor temperature trend in PPOOLEX simulation with pressure boundary

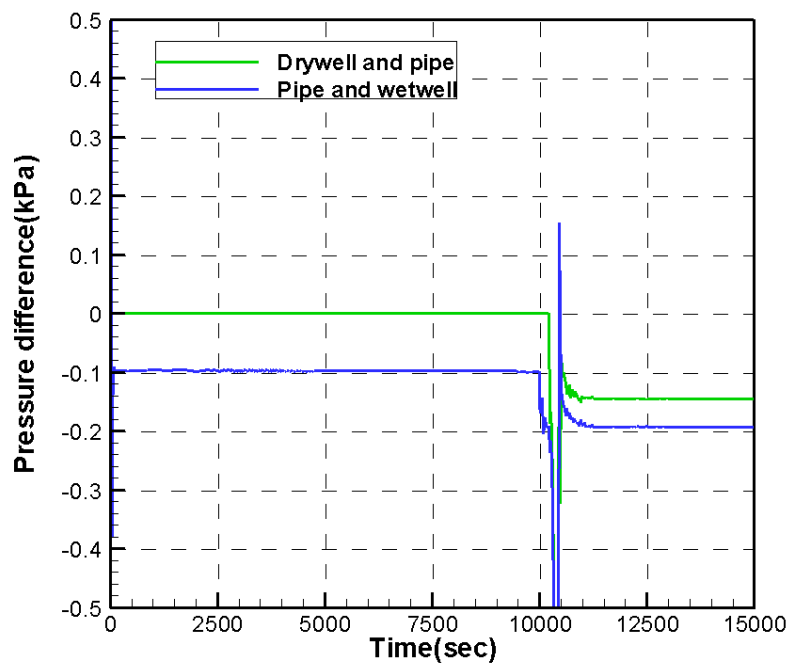


Figure 66: Pressure difference history in PPOOLEX simulation with flow boundary



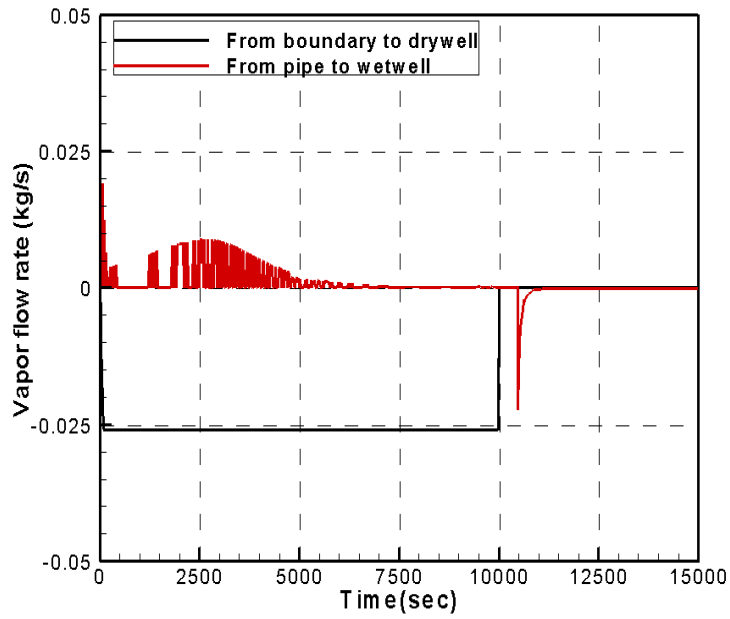


Figure 67: Vapor flow rate in PPOOLEX simulation with flow boundary

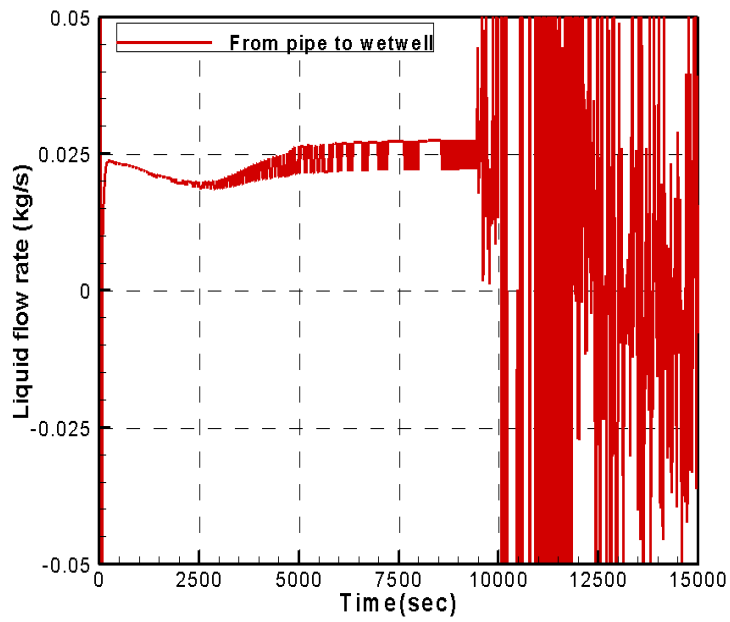


Figure 68: Liquid flow rate from tube to wetwell in PPOOLEX simulation with flow boundary

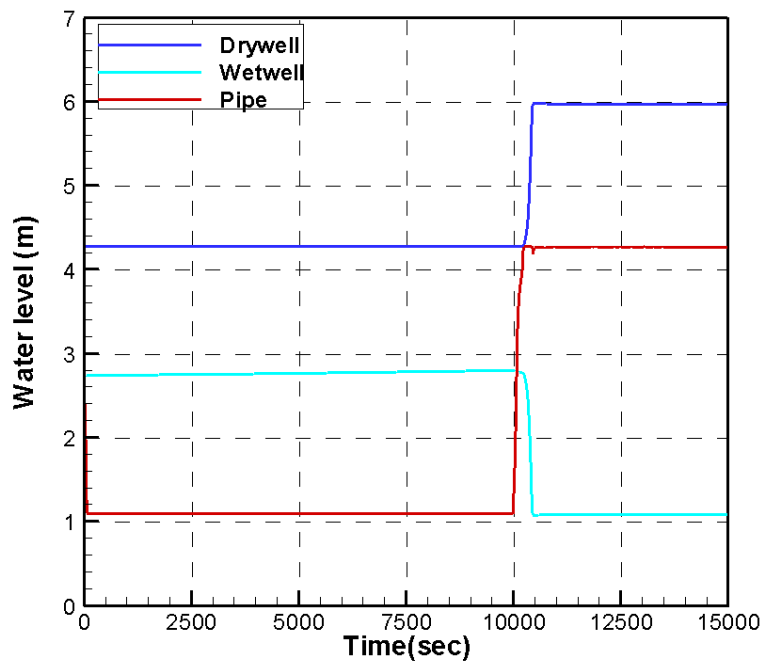


Figure 69: Liquid level in PPOOLEX simulation with flow boundary

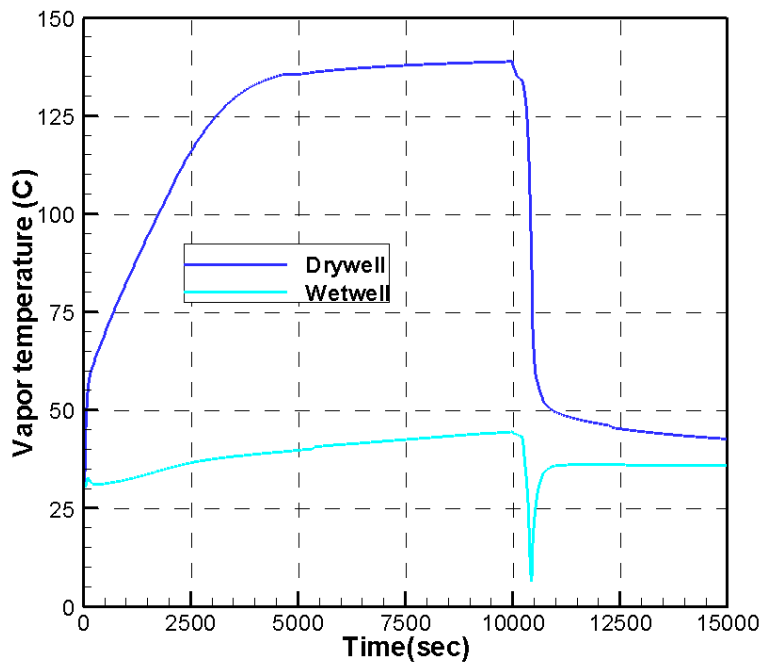


Figure 70: Vapor temperature trend in PPOOLEX simulation with flow boundary

**Figures of PPOOLEX post-test lumped parameter simulation with improved pressure for flow boundary**

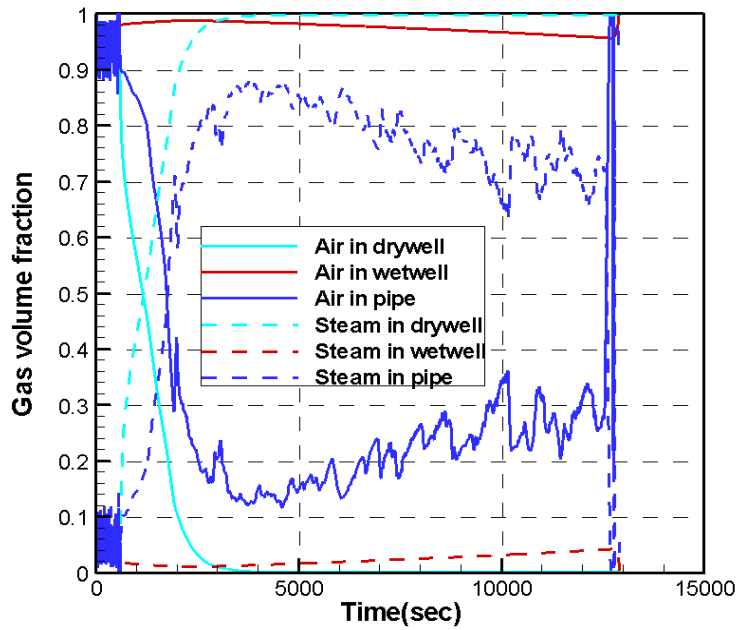


Figure 71: Gas volume fraction in PPOOLEX simulation with improved pressure for flow boundary

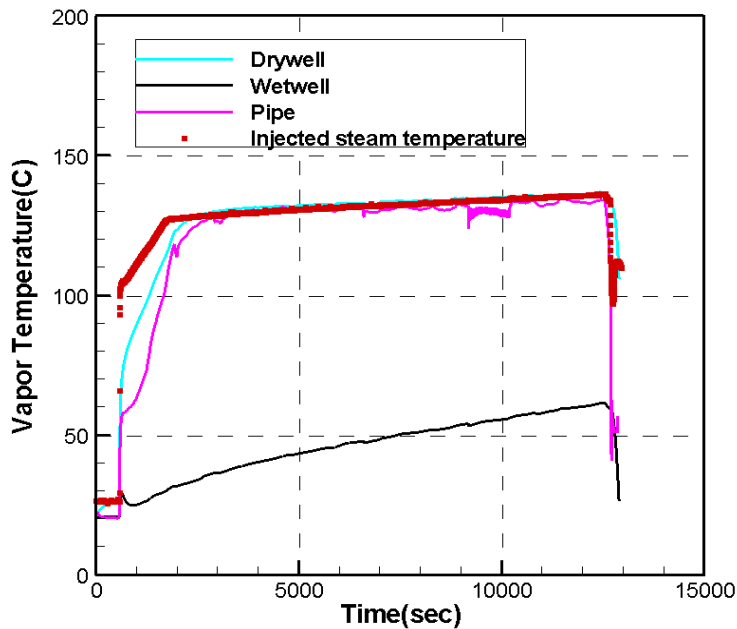


Figure 72: Vapor temperature in PPOOLEX simulation with improved pressure for flow boundary

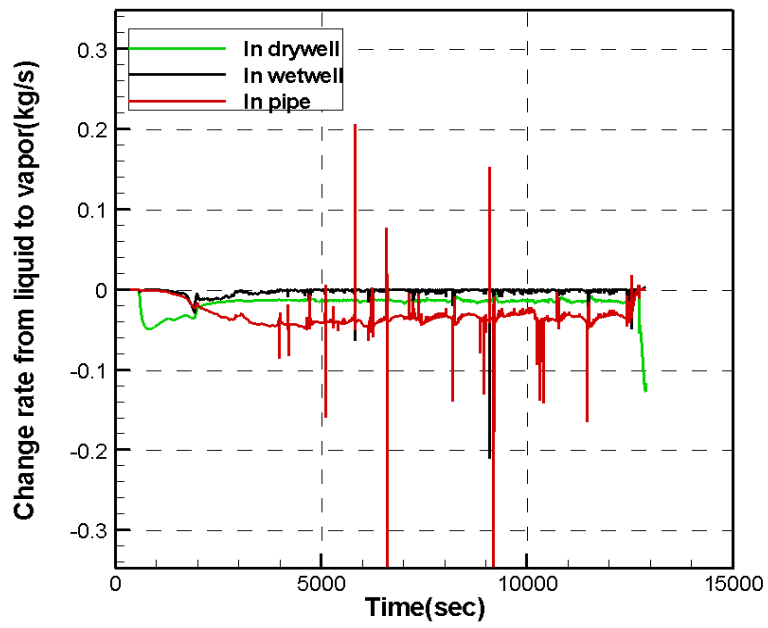


Figure 73: Condensation rate in PPOOLEX simulation with improved pressure for flow boundary

|                      |  |
|----------------------|--|
| Title                | Modeling of Condensation, Stratification, and Mixing Phenomena in a Pool of Water  |
| Author(s)            | H. Li, P. Kudinov, W. Villanueva   |
| Affiliation(s)       | Division of Nuclear Power Safety, Royal Institute of Technology, KTH, Sweden   |
| ISBN                 | 978-87-7893-295-2  |
| Date                 | December 2010  |
| Project              | NKS-R / POOL   |
| No. of pages         | 90   |
| No. of tables        | 4  |
| No. of illustrations | 73   |
| No. of references    | 57   |
| Abstract             | <p>This work pertains to the research program on Containment Thermal-Hydraulics at KTH. The objective is to evaluate and improve performance of methods, which are used to analyze thermal-hydraulics of steam suppression pools in a BWR plant under different abnormal transient and accident conditions. As a passive safety system, the function of steam pressure suppression pools is paramount to the containment performance. In the present work, the focus is on apparently-benign but intricate and potentially risk-significant scenarios in which thermal stratification could significantly impede the pool's pressure suppression capacity. For the case of small flow rates of steam influx, the steam condenses rapidly in the pool and the hot condensate rises in a narrow plume above the steam injection plane and spreads into a thin layer at the pool's free surface. When the steam flow rate increases significantly, momentum introduced by the steam injection and/or periodic expansion and shrink of large steam bubbles due to direct contact condensation can cause breakdown of the stratified layers and lead to mixing of the pool water. Accurate prediction of the pool thermal-hydraulics in such scenarios presents a computational challenge. Lumped-parameter models have no capability to predict temperature distribution of water pool during thermal stratification development. While high-order-accurate CFD (RANS, LES) methods are not practical due to excessive computing power needed to calculate 3D high-Rayleigh-number natural circulation flow in long transients. In the present work, a middle-ground approach is used, namely CFD-like model of the general purpose thermal-hydraulic code GOTHIC. Each cell of 3D GOTHIC grid uses lumped parameter volume type closures for modeling of various heat and mass transfer processes at subgrid scale. We use GOTHIC to simulate POOLEX/PPOOLEX experiment, in order to (a) quantify errors due to GOTHIC's physical models and numerical schemes, and (b) propose necessary improvements in GOTHIC sub-grid scale modeling. The study performed on thermal stratification in a water pool indicates that GOTHIC CFD-like model is fit for reactor applications in complex fluid-physics scenarios that avoids both over-simplification (as in single lumped-parameter model) and over-complication (as in CFD models). However, simulation of direct steam injection into a subcooled pool cannot be predicted reliably with the existing models. Thus we develop "effective heat source" and "effective momentum" approaches, and provide feasibility study for the prediction of thermal stratification and mixing in a BWR pressure suppression pool. The results are encouraging and further activity on the development and implementation of the proposed models in GOTHIC is currently underway.</p> |
| Key words            | BWR pressure suppression pool, thermal stratification, mixing, effective models, GOTHIC  |